A MODEL STUDY ON WAVE TRANSMISSION THROUGH PILE BREAKWATERS

A THESIS SUBMITTED TO
THE GRADUATE SCHOOL OF NATURAL AND APPLIED SCIENCES
OF
MIDDLE EAST TECHNICAL UNIVERSITY

BY

ÇAĞDAŞ BİLİCİ

IN PARTIAL FULFILLMENT OF THE REQUIREMENTS
FOR
THE DEGREE OF MASTER OF SCIENCE
IN
CIVIL ENGINEERING

JANUARY 2014

Approval of the thesis:

A MODEL STUDY ON WAVE TRANSMISSION THROUGH PILE BREAKWATERS

submitted by **ÇAĞDAŞ BİLİCİ** in partial fulfillment of the requirements for the degree of **Master of Science in Civil Engineering Department, Middle East Technical University** by,

Prof. Dr. Canan Özgen
Dean, Graduate School of **Natural and Applied Sciences** _____

Prof. Dr. Ahmet Cevdet Yalçıner
Head of Department, **Civil Engineering** _____

Prof. Dr. Ahmet Cevdet Yalçıner
Supervisor, **Civil Engineering Department, METU** _____

Prof. Dr. Ayşen Ergin
Co-Supervisor, **Civil Engineering Department, METU** _____

Examining Committee Members:

Prof. Dr. Ayşen Ergin
Civil Eng. Dept., METU _____

Prof. Dr. Ahmet Cevdet Yalçıner
Civil Eng. Dept., METU _____

Asst. Prof. Dr. Gülizar Özyurt Tarakcıoğlu
Civil Eng. Dept., METU _____

Dr. Işıkhan Güler
Civil Eng. Dept., METU _____

Dr. Hülya Karakuş Cihan
Yüksel Proje Uluslararası A.Ş. _____

Date: **21.01.2014**

I hereby declare that all information in this document has been obtained and presented in accordance with academic rules and ethical conduct. I also declare that, as required by these rules and conduct, I have fully cited and referenced all material and results that are not original to this work.

Name, Last name: Çağdaş BİLİCİ

Signature :

ABSTRACT

A MODEL STUDY ON WAVE TRANSMISSION THROUGH PILE BREAKWATERS

Bilici, Çağdaş

M.Sc., Department of Civil Engineering

Supervisor: Prof. Dr. Ahmet Cevdet Yalçıner

Co-Supervisor: Prof. Dr. Ayşen Ergin

January 2014, 122 pages

In the present study, wave transmission through pile breakwaters is examined experimentally. The experiments consist of eight model cases of set-up placed in three different wave flumes in Ocean Engineering Research Centre, Civil Engineering Department, Middle East Technical University with a model scale of 12.857. These experiments mainly focused on understanding how wave transmission changes under the influence of regular incident wave characteristics with different breakwater cross sections. Results are presented in graphical forms with incident wave steepness (H_i/L_i) versus transmission coefficient (K_t) and discussed with respect to spacing between piles (b), incident wave approach angle (α_i) and distance between rows of piles (B).

According to the results of the experimental studies, transmission coefficient decreases with increasing incident wave steepness. For lower wave steepness range ($H_i/L_i<0.030$), the transmission coefficients increase consistently with increasing pile spacing (b). However, in higher wave steepness range ($H_i/L_i>0.030$), influence of

pile spacing (b) on transmission coefficients diminishes for larger pile spacing values. Within the same wave steepness range (0.01-0.025), for the cases with relative pile spacing of b/D=0.11 and b/D=0.17, decreasing incident wave approach angles (α=90° to α=45°) do not affect transmission coefficients significantly. For the relative pile spacing of b/D=0.22, decrease in transmission coefficients reaches up to 25%. In a wave steepness range of $0.025<H_i/L_i<0.045$, decreasing distance between rows (B) results in increasing transmission through the breakwater.

Hayashi's (1968) solution for single row pile breakwaters is revised for double row breakwaters. Experimental results for both single and double row breakwaters shows similar trend with the theoretical results calculated using both numerical formulas for higher steepness ranges ($H_i/L_i>0.03$).

Keywords: Pile Breakwater, Wave transmission, Model

ÖZ

KAZIK TİPİ DALGAKIRAN YAPISININ DALGA GEÇİRİMLİLİĞİ ÜZERİNE MODEL ÇALIŞMASI

Bilici, Çağdaş

Yüksek Lisans, İnşaat Mühendisliği Bölümü
Tez Yöneticisi: Prof. Dr. Ahmet Cevdet Yalçıner
Ortak Tez Yöneticisi: Prof. Dr. Ayşen Ergin

Ocak 2014, 122 sayfa

Bu çalışmada, kazık tipi dalgakıran yapısının dalga geçirimliliği deneysel olarak incelenmiştir. Deneyler, Orta Doğu Teknik Üniversitesi, Kıyı ve Okyanus Mühendisliği Araştırma Merkezinde, üç ayrı dalga kanalında, 12.857 model ölçeği ile belirlenmiş sekiz farklı modelden oluşmaktadır. Model çalışmaları, düzenli dalgalar altında, farklı dalgakıran kesitlerindeki değişimin, dalga geçirimliliğini nasıl etkilediğini anlamayı amaçlamıştır. Sonuçlar, dalga dikliğine (H_i/L_i) karşı dalga geçirim katsayıları (K_t) formunda grafiksel olarak sunulmuş ve farklı kazık aralıkları (b), farklı dalga yaklaşım açıları (α_i) ve farklı kazık sıraları arası mesafeler (B) bakımından tartışılmıştır.

Model çalışmalarının sonuçlarına göre, gelen dalga dikliği arttıkça, dalga geçirim katsayıları azalmıştır. Düşük dalga dikliği değerleri için ($H_i/L_i<0.030$), dalga geçirim katsayıları, kazık aralığı (b) arttıkça istikrarlı bir şekilde artmıştır. Ancak, yüksek dalga dikliği değerleri için ($H_i/L_i>0.030$), kazık aralığı değişiminin, geniş kazık aralıklarında, dalga geçirim katsayıları üzerindeki etkisi azalmaktadır. Aynı dalga

dikliği aralığında (0.01-0.025), b/D=0.11 ve b/D=0.17 bağıntılı kazık aralığına sahip olan modellerde, gelen dalga yaklaşım açısının azalması (α=90° to α=45°), dalga geçirim katsayıları üzerinde önemli bir etki oluşturmamıştır. Bağıntılı kazık aralığının b/D=0.22 olduğu durumda, dalga geçirim katsayılarındaki düşüş %25 lere kadar çıkmıştır. Dalga dikliği aralığının $0.025<H_i/L_i<0.045$ olduğu durumlarda, kazık sıraları arasındaki mesafenin (B) azalması, dalgakıranın dalga geçirimliliğini arttırmıştır.

Hayashi'nin (1968) tek sıra kazık tipi dalgakıranların dalga geçirimliliği için önerilen çözümü, iki sıra kazık tipi dalgakıranlar için uyarlanmıştır. Tek ve iki sıra kazık tipi dalgakıranlar için elde edilen deney sonuçları, yüksek dalga dikliği durumunda ($H_i/L_i>0.03$), numerik formulleri kullanarak hesaplanan teorik sonuçlarla benzerlik göstermiştir.

Anahtar Kelimeler: Kazik Tipi Dalgakiran, Dalga Geçirimliliği, Model

To My Family…

ACKNOWLEDGEMENTS

I would like to thank my advisor Prof. Dr. Ahmet Cevdet Yalçıner who has supported me since the beginning of my graduate studies.

I would like to thank my advisor Prof. Dr. Ayşen Ergin for not only sharing her wealth of knowledge, but also giving me the opportunity to be a part of the Coastal and Ocean Engineering Laboratory's precious family. She always inspired me in all aspect of life.

I would like to thank Dr. Işıkhan Güler who helped me to develop my research and opened up my horizon in my graduate studies.

A special thanks to Dr. Gülizar Özyurt Tarakçıoğlu who helped me and supported me to achieve the finish line.

I would like to thank my family and Nilay. They are the meaning of my life. Words cannot express how grateful I am to them for all of the sacrifices that they have made on my behalf. They are the only reason what gets me thus far.

I would like to thank Cüneyt Baykal, Mustafa Esen and Hülya Karakuş for sharing the moments during my life in K5. I would also like to thank Arif Kayışlı and Yusuf Korkut for always helping for the experiments.

I would like to present my special thanks to Gökhan Güler, the best roommate in the world. He always believed in me.

I would like to thank Önder Ersen, Selin Güven, Betül Aytöre, Cem Sonat, Deniz Köksoy, Gülay and Halil Ünay couple, Dr. Asuman Aybey, Okan Aygün, Cemal İlhan and Ozan Gözcü couple and little Tolgahan for sharing joyful moments with me throughout my thesis period.

TABLE OF CONTENTS

LIST OF FIGURES

FIGURES

LIST OF TABLES

TABLES

LIST OF SYMBOLS

K_t	Transmission coefficient
b	Spacing between piles (cm)
D	Pile diameter (m)
B	Distance between pile rows (m)
d	Water depth (m)
H_i	Incident wave height (m)
H_t	Transmitted wave height (m)
L_i	Incident wave length (m)
T	Wave period (sec)
F_r	Froude number
λ_L	Length scale
λ_T	Time scale
α	Incident wave approach angle (°)
f	Wave frequency (1/sec)
S_0	Stroke amplitude of wave board
l	Vertical distance from hinge of the wave board to the flume bed (m)
k	Wave number

CHAPTER 1

INTRODUCTION

Throughout the history, coastal areas are always accepted as invaluable due to their strategic location near the seas and oceans. Knowing that the earth is covered with water with a percentage of 70%, the social and the economical potentials of these areas cannot be ignored. Therefore, to benefit from these resources by recreational, commercial and industrial activities, majority of the human population have always chosen coastal areas to inhabit. At first, the necessary sheltered calm seas were provided by the natural harbours. However, since the needs of humanity grew enormously at the last century, the required harbours are begun to be constructed artificially. Accordingly, the need to understand the natural processes enhanced. To understand the dynamics of the coastal regions, engineering became an essential part of these activities. The primitive structures were replaced with more complex and detailed structures. Correspondingly, breakwaters evolved with the developing technology.

Breakwaters are the structures constructed to protect facilities at the coastal regions. For the challenging climate conditions, these structures play a vital role to overcome the tremendous power of sea waves. In order to maintain the feasibility and to understand their behaviour while interacting with the nature, breakwaters are examined in terms of stability and energy dissipation capacity.

Suitable breakwater choice is one of the main aspects of the design of a harbour. There are several factors that affect the choice of the breakwater type such as wave

height, wave period, the depth of water, sea bottom soil foundation conditions, material which is available at or near the site, and equipment for the construction. According to their structural features, breakwaters can be classified into four which are; (Takahashi, 1996)

- Sloping (mound) type breakwaters
- Vertical breakwaters
- Composite type breakwaters
- Special (non-gravity) types of breakwaters

Mound type breakwaters are identified by the construction materials namely natural rock, concrete block, a combination of rock and concrete block, and concrete structures like tetrapods, dolos and others. Vertical type of breakwaters classification involves concrete-block gravity walls, concrete caissons and rock-filled sheet pile walls. Composite breakwater is a combination of a mound and a vertical superstructure. Special type breakwaters consist of non-gravity type ones. Common special type breakwaters are pile breakwaters, floating breakwaters, pneumatic breakwaters.

There are many advantages and disadvantages associated with each type of breakwater. Widely used gravity-type breakwaters such as rubble-mound and vertical caissons are effective against high wave heights and fast-moving waves. They offer considerable amount of protection in heavy storms. Maintenance is relatively easy such that dislocated or damaged stone or rubble can easily be replaced or repaired. On the other hand, they require great amount of construction material especially when they are planned to be constructed in deep water. They restrain water flow, and prevention of water circulation degrades water quality within the harbour. They also block the movement of the sediment and cause beach erosion In addition, these heavy structures are needed to be supported by solid soil sea bottom foundation.(Sundar & Subbarao, 2003)

Consequently, porous structures are introduced as an alternative against gravity-type breakwaters and a resolution to the mentioned problems. A pile breakwater is a

permeable structure which is a non-gravity type consisting of an array of vertical piles driven into seabed. As oppose to gravity-type breakwaters, pile breakwaters are constructed preferably in calm seas having poor soil conditions. Since pile breakwaters do not obstruct the passage of sediments, they eliminate the risk of potential coastal erosion which is a possible result of the construction of gravity-type breakwaters. (Kyung-Duck Suh, Shin, & Cox, 2006)

The behaviour of the flow through the pile gaps and the interaction between the wave and the structure is quite complex that requires techniques like field measurements and mathematical calculations for prediction. Besides any other method, researchers have focused on experimental studies to comprehend and predict the flow behaviour as precise and detailed as possible.

In this study, the wave transmission performance of pile breakwaters are examined with eight cases of model setup constructed at Coastal and Ocean Engineering Laboratory, Middle East Technical University (METU). The main aspect of the study is to understand how wave transmission changes under the influence of regular incident wave characteristics with different breakwater cross sections.

In Chapter 2, related studies in literature are briefly summarized in chronological order. In Chapter 3, aim of the model studies, model scale, wave flume and experiment set-up specifications and data analysis procedure are described in detail. In Chapter 4, results of the experiments are presented and discussed in detail. Moreover, the experimental results are compared to the theoretical results which are calculated by Hayashi's (1968) formulas. In Chapter 5, conclusions and future recommendations are given.

CHAPTER 2

LITERATURE SURVEY

The studies in the literature which are relevant to the subject of wave transmission through pile breakwaters are presented chronologically in this chapter.

Studies of pile breakwaters date back to the Wiegel (1960) who conducted his research on single row pile breakwater. He first explained the wave transmission through pile breakwater with permeability of the breakwater geometry. In his research, the spacing between piles was considered as the only parameter which affects the wave transmission and derived the Equation 2.1.

$$K_t = \frac{b}{D+b} \tag{3.1}$$

where:
K_t: Transmission coefficient
b: Spacing between piles
D: Pile Diameter

Later, Wiegel (1961) concluded that his theory overpredicts the transmission results. (as cited in Herbich, 1989)

Hayashi and Kano (1966) studied single row pile breakwaters focussing on moment distributions on piles and the wave transmission through the breakwater. In their research, they developed a theory considering the effect of contraction due to water jets passing through the pile breakwater. Furthermore, they conducted experiments to verify the solution. Then, they concluded that there is a slight difference between the

experimental results and the results predicted by the solution. They reasoned that this difference can be due to energy dissipation in front of the pile arrays which is ignored in their solution.

Furthermore, Hayashi (1968) developed his research and suggested the pile breakwaters to protect the shoreline from beach erosion. He revised his solution with shallow water wave theory and compared to the model studies. Accordingly, he reached a good agreement with the theory and experiments. He also stated that as the spacing between pile increases, the transmission will increase to a certain level. Later, Hayashi (1968) revised his solution. His revised solution is explained in the subsection 3.4 in detail. Moreover suggested formulas in his research are applied to the data obtained in this study and compared to the results of experiments in subsection 4.5.

Truit and Herbich (1987) also performed model studies for the wave transmission through pile breakwaters. In their studies, they conducted several cases with respect to different pile spacing and pile diameter. Furthermore, they improved the previous studies by utilizing the irregular waves instead of regular waves. They also used Hayashi's (1968) formulas to predict the transmission for model study and reached a good agreement with experimental results. They implied that Hayashi's solution gave viable results for irregular waves too. Moreover, Truit and Herbich (1987) investigated the influence of wave height and water depth on wave transmission. They stated that the model wave parameters are important variables on wave transmission but breakwater geometry have more essential role on transmission phenomenon. Then, they implied that more research was required on transmission through pile breakwaters in order to understand the influence of wave transmission.

Herbich and Douglas (1989) extended the previous research to a new level by utilizing the double row pile breakwaters instead of single row. Then, they compared the results for double row pile breakwaters with single row pile breakwaters. The comparison showed that utilizing second row reduced the wave transmission up to 15% for relative pile spacing of b/D=0.2 (where b: spacing between piles; D=pile

diameter) and up to 10 % for relative pile spacing of b/D=0.1. Moreover, they also investigated the effect of wave period, wave height and water depth on wave transmission. They concluded that wave transmission increases for increasing water depth to wave height ratio (d/H) and increasing wave period (T) and wave transmission decreases with increasing wave steepness (H/L).

Kakuno and Liu (1993) studied the dispersion of the waves passing through single row vertical cylinders. They developed a theoretical method to solve the scattering effect of piles on water waves by modelling the flows near the piles. They considered the energy dissipation between piles. In addition, they used rectangular and circular piles in their study. They concluded that their research is reliable to limited cases and requires further investigation on different cross section and wave characteristics.

Mani (1995) studied the wave transmission for single row suspended pipe breakwater which was a new approach to the vertical barrier type breakwaters. The studied breakwater consists of one row of closely spaced pipes connected to a horizontal frame above still water level. The research was conducted with the spacing to diameter ratio of b/D=0.22 and incident wave steepness of $H_i/gT^2>0.008$ for regular waves. The results of this research show that for single row suspended pipe breakwaters with the given parameters, wave transmission reduces to 50% of the incident waves. He also predicted his results with Hayashi's (1968) solution and concluded that the experimental results and the predicted results are in good agreement.

Isaacson (1998) also studied on the single row vertical suspended breakwaters. He utilized a numerical solution (which is based on eigenfunction expansion) to understand the wave interactions on piles and energy dissipation due to vertical suspended pile system. He also conducted model studies with regular and irregular wave trains and concluded that the numerical model can be applied to both regular and irregular waves. He also accepted that this method overestimates the wave transmission for higher wave steepness ranges.

Rao and Sathyanarayana (1999) conducted model studies focussing on wave transmission through two rows of perforated hollow piles. Utilizing the perforated piles for such breakwaters was first suggested by them. In model studies, their intention was to understand influence of water depth, incident wave steepness, pile spacing and distance between rows on wave transmission. They compared the perforated and non-perforated pile breakwaters. As a result of model studies, they reached the following conclusions:

- Effect of water depth on wave transmission can be ignored for both perforated and non-perforated cases.
- As wave steepness increases, wave transmission decreases.
- As pile spacing increases, wave transmission increases to a certain level.
- Utilizing the second row for perforated pile breakwater results in decreasing wave transmission while for the non-perforated pile breakwaters, the effect of second row is negligible.
- For both perforated and non-perforated piles, as the distance between rows increases, the wave transmission decreases at a certain level.
- Perforated piles shows negligible decrease for the wave transmission compared to the non-perforated piles.

They also stated that to search for the effect of wave period alone is not viable.

Suh et al. (2011) proposed a new solution developed by Kim (1998) for single row vertical slotted barriers with square piles. They stated that the suggested solutions in literature to predict the wave transmission underestimate the wave transmission for lower wave steepness ranges. This new solution consists of both fundamental fluid mechanics and empirical formulas in a hybrid form. They suggest that the new approach gives better results and empirical formulas should be combined with the basic principles in fluid mechanics. They stated that the hybrid method can also be applied to the circular pile breakwaters.

The most recent research is conducted by Koraim et al. (2014). They conducted model studies to appraise the performance of double rows of piles with suspended horizontal c-shaped bars with regular waves. They searched for the influence of water depth ratio to wave length (d/L), pile diameter ratio to water depth (D/d), row distance ratio to water depth (B/d). It is concluded that as d/L, D/d or B/d increases, wave transmission decreases.

CHAPTER 3

MODEL STUDIES

3.1 Introduction

Physical models are the reproduced scaled models of the designed structures which helps engineers to put forward an idea about a physical system. In coastal engineering, hydraulic modelling of a real-life phenomenon is rather difficult. Diversified amount of environmental conditions should be replicated and tested in the models. However, there can be some advantages and disadvantages of this process.

As Dalrymple (1985) stated, physical model environment in laboratories are cost efficient and practical compared to the data collection in field and can integrate the necessary equations related to the processes evading to make impractical assumptions. Besides Dalrymple, Kamphuis (1991) pointed out the fact that to observe a physical model experiment provides insight to the engineers for their design. Le Mehaute (1972) summarizes the advantages of physical models as follows (as cited in Hughes, 1993):

- Model studies are needed to optimize the costs of large-scale coastal projects.
- Due to the fact that there will always be limits for fluid mechanics due to turbulence, physical model studies are one of the most efficient techniques in coastal engineering.
- With the developing technology, new techniques have emerged and will emerge in time. With these techniques more variables can be observed in the

laboratory environment which will enable us to understand the process of complex phenomenon coastal engineering phenomenon in more detail.

- Unlike mathematical models, physical models give engineers chance to observe physics in laboratory environment which makes easier to predict the physics of real-life situations.
- Physical models, unlike the computer solutions and existing theories, offers imaginative solutions for engineers enabling heuristic senses.

On the other hand, there are also some serious handicaps of physical hydraulic models as Hughes summarizes in different aspects. Firstly, to include all the correct relationship of all of the variables is not practical for the physical models. Existing scaling criteria cannot replicate all the forces and their relationship with each other. Therefore, scale effects like the viscous forces being larger in the model than in the prototype can occur. Furthermore, exact imitation of the nature in laboratory environment is impossible due to the limita

tions of the laboratory resources. For example, all the boundary conditions acting in the nature and all the forces like winds shear stresses on the water surface cannot be created in the mechanical models. Moreover, for the most of the cases, physical models are more expensive and time consuming than the numerical models. That is why if the numerical models can give reasonable results for a specific case, numerical models can be the first choice (Hughes, 1993).

3.1.1 Aim of the Model Studies

As mentioned in the Chapter 1, there are several types of breakwaters which vary according to their field of application. Knowing the fact that the coastal structures are expensive, the most appropriate and economic solution must be determined carefully. In this thesis, performance of pile breakwaters are studied as an alternative to conventional breakwaters considering the disadvantages of conventional type breakwaters in deep bathymetric conditions.

The structural stability of conventional type of breakwaters is maintained by a specific slope. For the gravity type breakwaters like rubble mound breakwaters, if the water depth is higher than the usual cases, width of the breakwaters increases to maintain the slope stability. Accordingly, the section area of the breakwaters becomes wider increasing the expenses and the weight of the structure. In this respect, heavier structures would need sound foundation. Moreover, there would be other negative consequences like erosion and accretion for the beaches at the same coastline and decreasing water quality in the area due to structures' blocking the water circulation. (Suh et al., 2011)

Considering all the drawbacks of the traditional type of breakwaters in deep water, pile breakwaters, being a permeable and porous structure, comes forward as an alternative design approach. However, since this design approach is not common in the field, it requires further investigation in order to understand how this structure will behave under real life conditions. Accordingly, in this study, wave transmission through pile breakwaters is chosen as a major design consideration.

Wave transmission is a phenomenon which occurs when the sea defence structure is designed as a permeable and porous breakwater. When the waves encounter the permeable structure, a great amount of its energy dissipates and reflects from the structure. Remaining portion of the wave energy is transmitted through the structure into the harbour side which is defined as wave transmission. This transmitted energy disturbs the protected tranquil zone of the harbour causing agitation. Therefore, it is important to understand the level of agitation under real life conditions for a design of a coastal structure. (Coastal Engineering Manual, 2003)

For a pile breakwater system as in this case, the existing model experiments and empiric equations are not sufficient to explain the transmission through complex breakwater structure. There are few experiments in the literature examining transmission through single row piled system and few and general discussions about how it would be if double row systems are used. Thus performing physical model

studies has become mandatory to analyse and understand the performance of the designed pile breakwater system focusing on transmission.

The model studies were basically implemented to comprehend how the transmission coefficient changes under regular wave conditions with respect to:

- Incident wave approach angles,
- Spacing between piles,
- Incident wave steepness,
- Distances between rows.

The model studies were performed following the procedure given in the flowchart. (Figure 3.1)

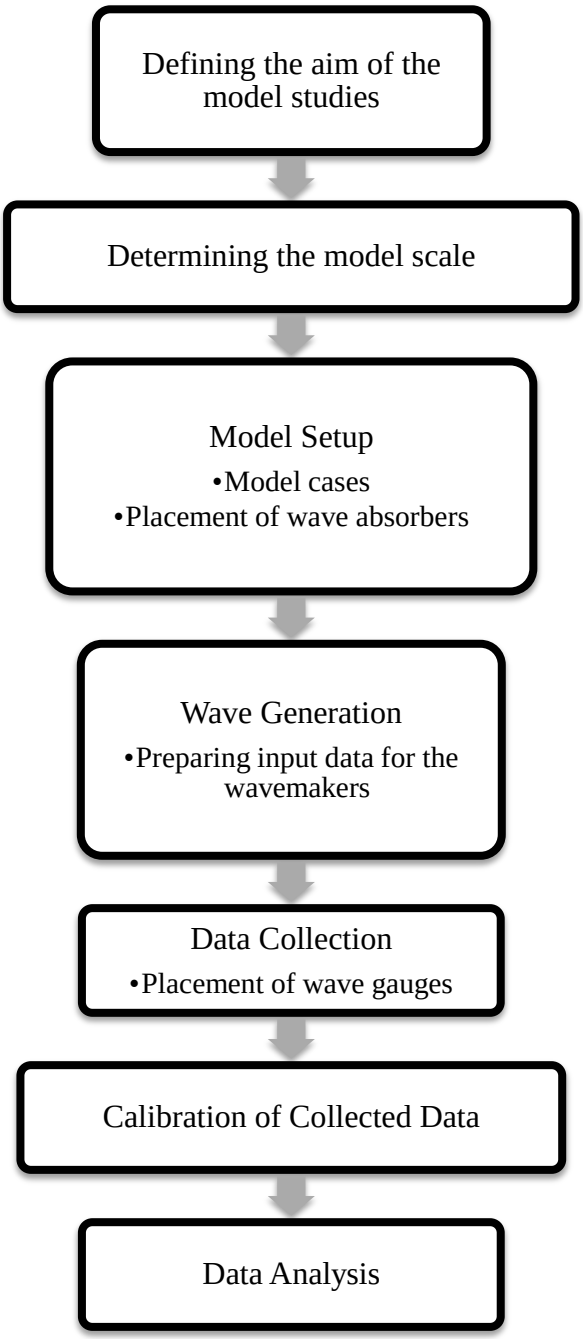

Figure 3.1: Flowchart of the model studies

3.2 Model Scale

All physical model experiments are based on the idea that the model and prototype should behave in a similar way under predefined conditions. Accordingly, to achieve the similitude concept in experiments, significant factors in the physical model processes should be defined as proportional to the prototype. (Hughes, 1993)

In most of the hydrodynamic physical model studies of coastal and ocean engineering, since the influence of surface tension and elastic compression is rather small, it is necessary to define whether gravity (Froude Theorem) or viscous terms (Reynolds Theorem) are more effective in the study. In this study, Froude Theorem is implemented as a law. The underlying reason is that the wave motion and their effects on structures are mainly resulted from the gravity and inertial terms, rather than viscosity. Thus, Froude theorem is implemented with the geometric similarity for hydrodynamic similitude in the model studies (Hughes, 1993). As a dimensionless number, Froude number (F_r) is determined as the square of particle velocity of water over multiplication of acceleration of gravity (g) and water depth (d). Accordingly in the model studies of pile breakwater, Froude numbers in model and prototype are equalled.

$$F_r = \frac{u^2}{gd} \qquad (F_r)_p = (F_r)_m \tag{3.1}$$

Parameters, which define the model and prototype, are coordinated by a ratio. This ratio is defined as model scale. The model scale is determined with dividing a specific parameter of the model by its match in prototype which can be shown as:

$$\lambda_X = \frac{X_m}{X_p} \tag{3.2}$$

Where "λ" is scale ratio of model to prototype, "X" is a specific parameter, "m" is the subscript for model values, and "p" is subscript for prototype values.

Geometric similitude in the model is defined by the variables which have length as a dimension. In other words, to maintain the geometric similitude, the ratio of the values of these variables in the model (L_m) to the actual values in the prototype (L_p) is equalized with the model length scale (λ_L).

$$\lambda_L = \frac{L_m}{L_p} \tag{3.3}$$

Additionally, time scale (λ_T) is defined as the square root of the length scale (λ_L).

$$\lambda_T = \sqrt{(\lambda_L)} \tag{3.4}$$

Furthermore, as Hughes (1993) stated that it is impossible to find exact similitude in model studies. For large scale models, the model will be more similar to the prototype eliminating the scale effects and the deficiencies resulted from the inaccurately scaled parameters like fluid density and viscosity. However, the importance of the economic advantages of small scale models cannot be ignored and in some cases laboratory environment can be insufficient for large scale models. For example, there may not be enough space in the flumes for the equipment such as wave generator. Accordingly, small scale models are selected to accommodate with the laboratory conditions. Therefore, for the selection of the most convenient mode scale, advantages and disadvantages of both large and small scale models are considered.

In the application of the Froude and geometric similarity in the model studies of pile breakwater, model scale is defined according to the following criteria due to restrictions of laboratory environment:

- Water depth limits that can be studied in the experiment channel, ($0.3\ m < d < 0.7\ m$),
- The breaking conditions of the waves created in the flume, ($H_s/d < 0.6$; where the significant wave height is denoted as H_s, water depth is denoted as d),

- Minimum diameter of the piles used in experiments, (pile diameter ≥ 14 cm)
- Operation limits of the wave generator,
  (0.05 Hz < Frequency < 2.0 Hz; -290 mm < piston amplitude < 290 mm),
- Prototype value of depth which will be studied in the flume is taken as -8.75m in front of the structure.

These criteria were investigated with the Table 3.1. As it can be observed, the critical parameters were chosen as water depth and pile diameter which restrict the model scale in a range of max: 1/12.5 and min: 1/12.857.

Table 3.1: Selection of the model scale

Parameters	In Prototype	Laboratory Restriction	Model Scale
Water Depth (d)	8.75 m (constant)	Max: 70cm	1/12.50
Wave Height (H)	Max: 3.2m	Max: 25cm	1/12.00
Pile Diameter (D)	1.80 m (constant)	Min: 14 cm	1/12.86

After considering all the restrictions in the laboratory, the model scale was chosen as 1:12.857 which gives integer values for diameters of piles used in model construction. Length and time scale are given in Table 3.2.

Table 3.2: Length (λ_L) and time (λ_T) scales used in the model studies

	Model Scale
Length (L)	λ_L = 1:12.857
Time (T)	λ_T = 1:3.586

3.3 Wave Flume and Experiment Set-up Specifications

3.3.1 Wave Flumes

Experiments were conducted in three flumes at METU, Coastal and Ocean Engineering Laboratory. Two of the flumes are located in a large basin (Basin-1) with a flap-type wave generator (Figure 3.2). The third one is located in the relatively small basin (basin-2) with a piston-type wave generator (Figure 3.4). Larger basin's dimensions are 30 meter in length and 20 meter in width. Smaller basin's dimensions are 26 meter in length and 6 meter in width.

In basin-1, first flume (Flume-1) has dimensions of 16 meter in length and1.72m in width. The second one (Flume-2) has dimensions of 16 meter in length and 4.25 m in width. In Figure 3.3, Flume-1 and Flume-2 is shown. Third flume located in Basin-2 has width of 1.8 m and length of 16 m as shown in Figure 3.4. These flumes have Plexiglas walls and they are built inside of the basins to eliminate the reflected waves from the basins borders.

Figure 3.2: Basin-1

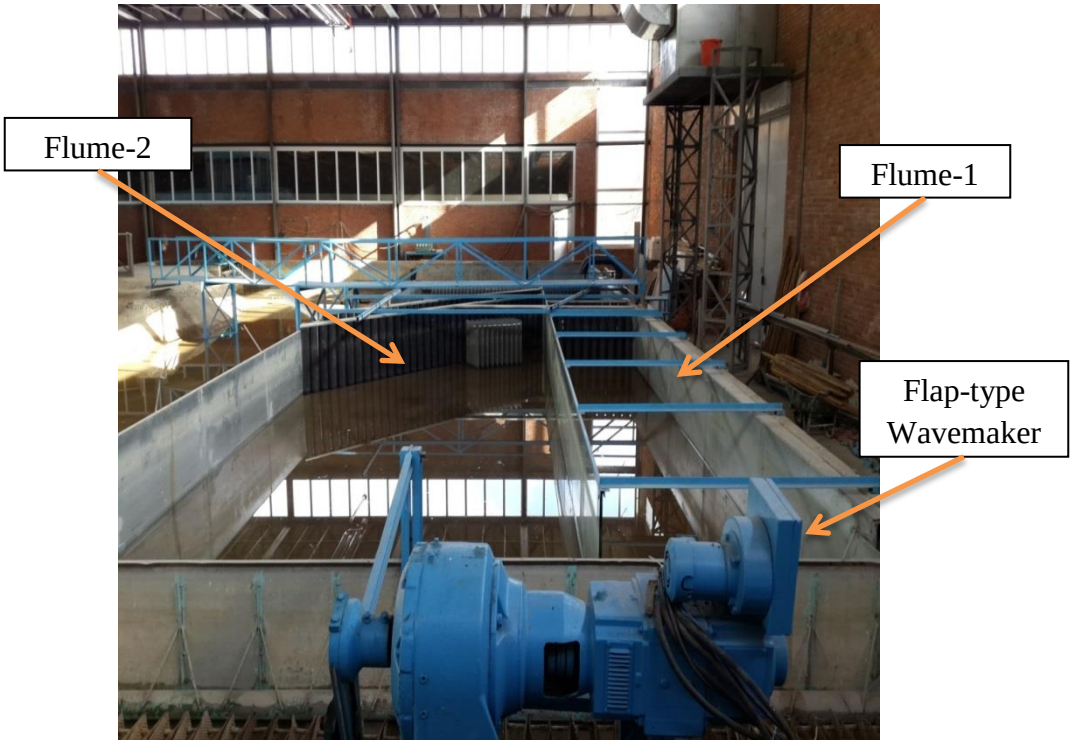

Figure 3.3: Flume-1 and Flume-2 in Basin-1

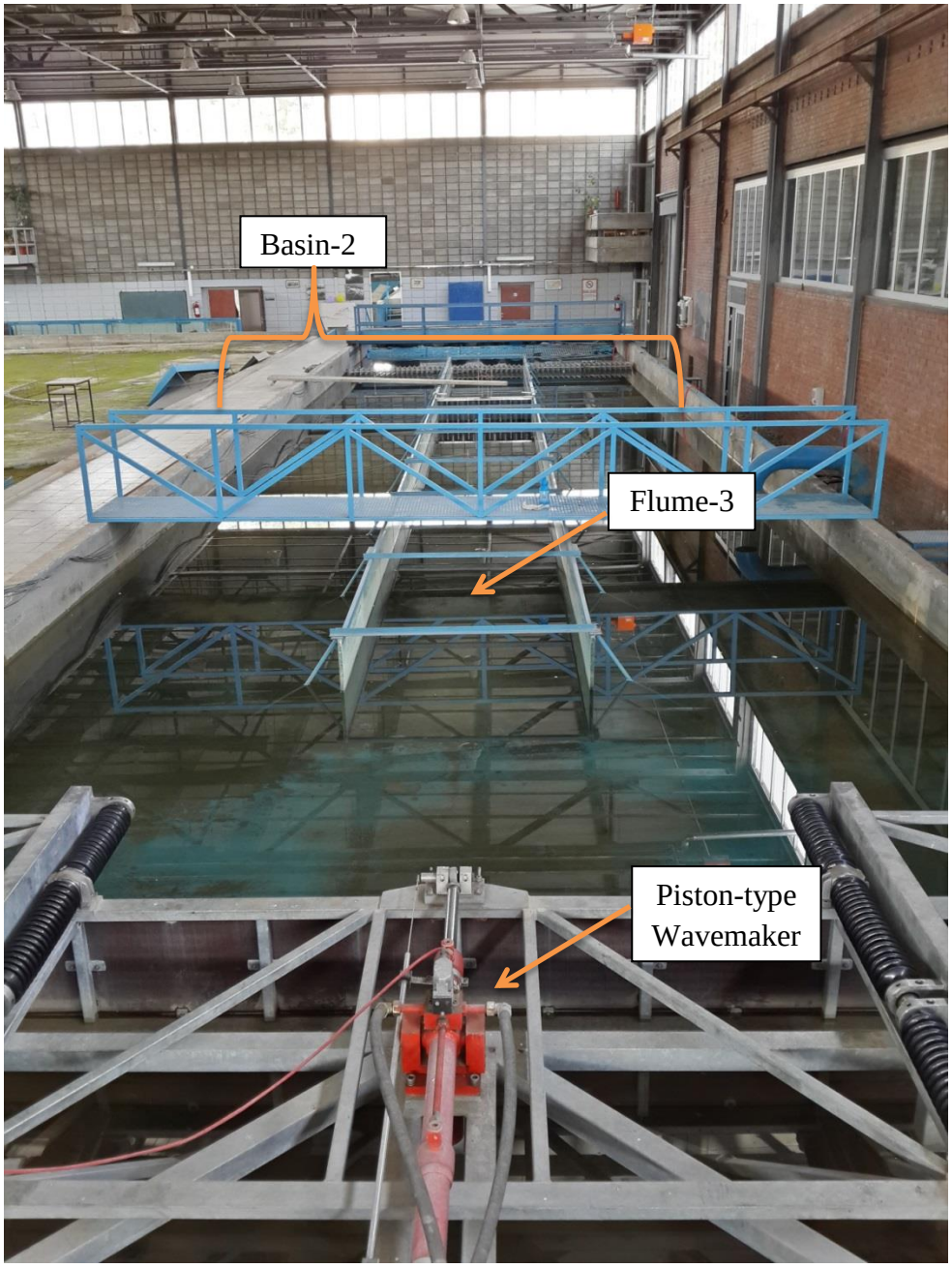

Figure 3.4: Flume-3 in Basin-2

3.3.2 Model Set-up

Piles used in the experiments had dimensions with height of 1m and diameter of 14 cm as shown in Figure 3.5.

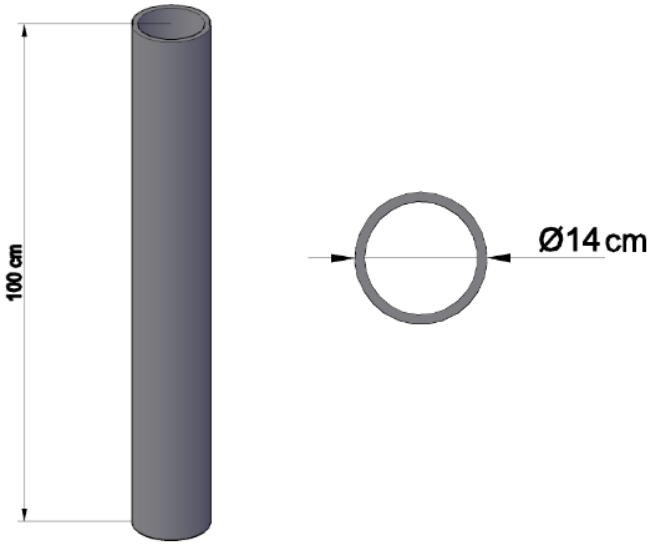

Figure 3.5: Piles used in the model studies

Experiments were conducted for eight cases of set-up. These cases were defined to understand how the structure will behave for different placement of piles. Case-1, Case-2 and Case-3 were built in flume-1 and flume-3, while Case-4, Case-5 and Case-6 were constructed in flume-2. After those six cases were completed, experiments were continued further with Case-7 and Case-8 in flume-3. (Table 3.3)

Table 3.3: Variables of the model cases

Flume #	Case #	Pile Spacing b (cm)	Distance between rows B (m)	Incident wave approach angle (α)
Flume 1&3	Case-1	20	12	90°
	Case-2	30	12	90°
	Case-3	40	12	90°
Flume 2	Case-4	20	12	45°
	Case-5	30	12	45°
	Case-6	40	12	45°
Flume 3	Case-7	30	7	90°
	Case-8	30	0 (single row)	90°

For Case-1, Case-2 and Case-3, the purpose was to observe how the structure will behave if the piles are placed perpendicular to the wave direction. Distance between rows (B) was kept constant at 12m in prototype (93.3 cm in model). To investigate the effect of gap between piles (b), for each case, the gap was increased with 10 cm in prototype (0.78 cm in model).

For Case-7 and Case-8, gap between piles was kept constant at 30 cm in prototype. While the piles were placed perpendicular to the wave direction as in first three cases, the distance between rows were decreased to investigate the effect of distance between rows. For Case-7, the distance between rows was decided to be 7 m in prototype (0.55 cm in model). For Case-8, one of the rows was removed and the experiments were done with single row pile breakwater which means that the distance between rows (B) equals to zero. Figure 3.6 illustrates the set-up for Case-1, 2, 3, 7 and 8 in flume-1 and flume-3.

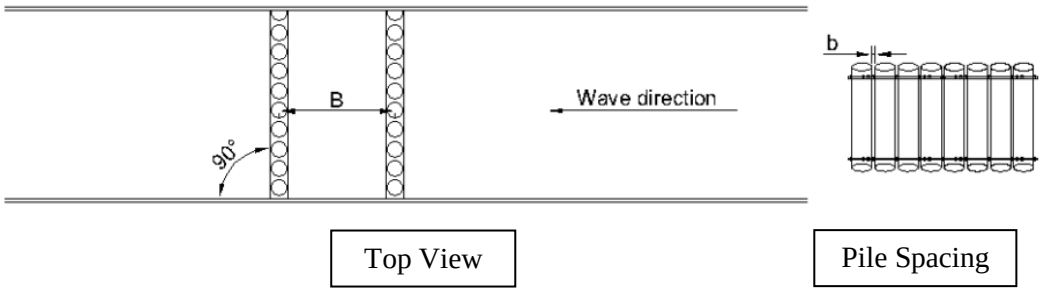

Figure 3.6: General layout of the model set-ups in Flume-1 and Flume-3

For Case-4, Case-5 and Case-6, the idea was to examine the changes when the piles are placed with a 45 degree angle to the wave direction. Once again, for each case, the gap is increased with 10 cm in prototype (0.78 cm in model). Accordingly, the gap between piles in case-4 is 20cm in prototype, the gap in case-5 is increased to 30 cm and the gap in case-6 is increased to 40cm. Figure 3.7 illustrates the set-up for case-4, 5 and 6 in flume-3.

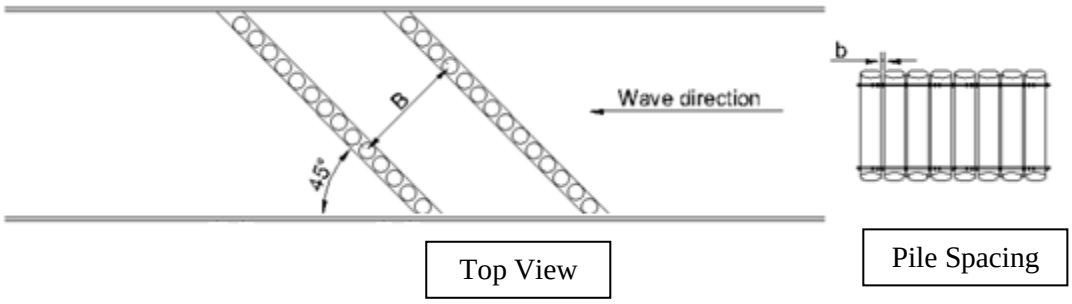

Figure 3.7: General layout of the model set-ups in Flume-2

3.3.3 Wave Absorbers:

One of the drawbacks of the laboratory model experiments is the wave reflection from the boundaries of the model channels. In that case, reliability of the experimental results decreases because the incident wave profile is affected by the reflected energy. Therefore, to increase the efficiency of the model experiments, wave absorbers are placed at the reflective boundaries. (Ouellet & Datta, 1986).

Hughes (1993) examines the wave absorber in two groups as passive and active absorbers. Active wave absorbing systems are mechanical devices that can respond according to the incoming wave conditions. However, these types of absorbing systems are complex and difficult to be implemented in the laboratory environment.

In this model experiments, passive absorbers are used. Passive absorbers simply damp the wave energy by different techniques. At the boundaries, mild slopes, porous materials or screens can be placed. The length, type and placement of these absorbers can be adapted to different condition to overcome the substantial amount of reflected wave energy. However, to reduce the reflection, passive absorbers requires quite large spaces in the model channels.

In literature, there are many studies performed on passive absorbers to determine the type, location and orientation of these absorbers for the most reliable results. Some guidelines for the use of passive absorbers can be given as follows;

- Straub, Bowers, and Herbich (1957) revealed that crushed rock absorber slopes must be less than 1:4 to keep reflections under 10%. (as cited in Hughes, 1993)
- Goda and Ippen (1963) make experiments on vertical mesh screens and come to conclusion that the screen absorbers should be placed at least at the same extent of the wave length of the incident wave. (as cited in Hughes, 1993)

- Lean (1967) revealed that if the absorber is placed over a sloping depth, the reflected energy will be smaller than placing the absorbers over a constant depth. Moreover, he proposed that the length of the absorbing system should be at least 75% of the wavelength of incident wave to reduce the reflection to 10%.
- Le Méhauté (1972) suggests that a composite system of wave absorbers with different porosity will work more effective. If the system is examined in sections with decreasing porosity of absorbers, the wave in each section will encounter different energy dissipation ratios. Accordingly the length of the absorption system will be less than a wavelength.
- Keulegan (1972) used screens made from aluminium wool with high porosity, rubberized horse-hair and polyurethane foam as an absorption system and reached fair results. (as cited in Hughes, 1993)

Also, Oullet and Datta (1986) reviewed the literature and reached the following conclusions;

- In the case of the impervious plane-sloped absorbers, with constant wave steepness, reflection decreases if the slope of the absorber decreases. With constant slope, reflection increases if the wave steepness decreases.
- Effect of stone size in permeable wave absorbers on reflection coefficient can be ignored
- For sloped absorbers, crushed rock and wire mesh gives similar results on wave reflection if the slope angle is smaller than 15 degrees. In other cases, wire mesh absorbers are more efficient.
- For most of the cases, in form of a parabola-sloped absorbers work better.

Jamieson and Mansard (1987) made further investigation of the wire mesh screen-type absorbers and came to the following conclusions (as cited in Hughes, 1993);

- Framework of the absorber should be as small as possible.
- Energy of high steepness waves can effectively be absorbed with high porosity absorbers, energy of low steepness waves can effectively be absorbed with low porosity absorbers.
- Porosity of mesh screen absorbers should be decreased gradually towards the back.
- Nodal locations of partial standing waves would be the best place for the location of the absorbers
- Optimum length of the wave absorber system changes between 0.35 and 1.0 of the maximum wave length.

Passive Absorption System of the Study:

Before the model studies, several experiments were performed to optimize the absorption system setup (Appendix A). The results of these experiments were discussed in various aspects. The main questions were which materials should be used and how the attenuators should be placed.

Since the experiments were simultaneously applied in 3 flumes in 2 basins, three different configurations of wave absorber system were used in the model studies. In the configurations, sloping steel frame, steel mesh boxes and plastic wire scrubbers were used to attenuate the wave energy. In flume-1 and flume-2, steel mesh boxes were used. In flume-3, all three attenuator types were used. (Figure 3.8)

Figure 3.8: Sloping steel frame, steel mesh boxes and plastic wire scrubbers

Since the flume-1 and flume-2 are in the same basin, the experiments were done together to improve the efficiency of the absorbers and tested configurations are given in the appendix. For the flume-3, the configuration which was developed by Kürüm (2008) was used. Moreover, following factors were considered for the absorption system:

- Sloping steel frames with plastic scrubbers were placed at the harbour side of the structure to eliminate the reflection of waves from the back wall. (Figure 3.9 and 3.10; Point A)
- Furthermore, steel mesh boxes were placed in front of the steel frames to improve the attenuation of the reflected waves from the back wall. (Figure 3.9 and 3.10; Point B)
- Steel mesh boxes were placed in front of the model units in Flume-2 to attenuate the agitation occurred due to jammed waves between the wall and model units. (Figure 3.9; Point C)
- Plexiglas wall was replaced with steel mesh boxes to eliminate the reflection from the wall indisposing the measurements. (Figure 3.9; Point D)

Resulted configurations of the passive absorption systems are given in Figure 3.7 and Figure 3.8.

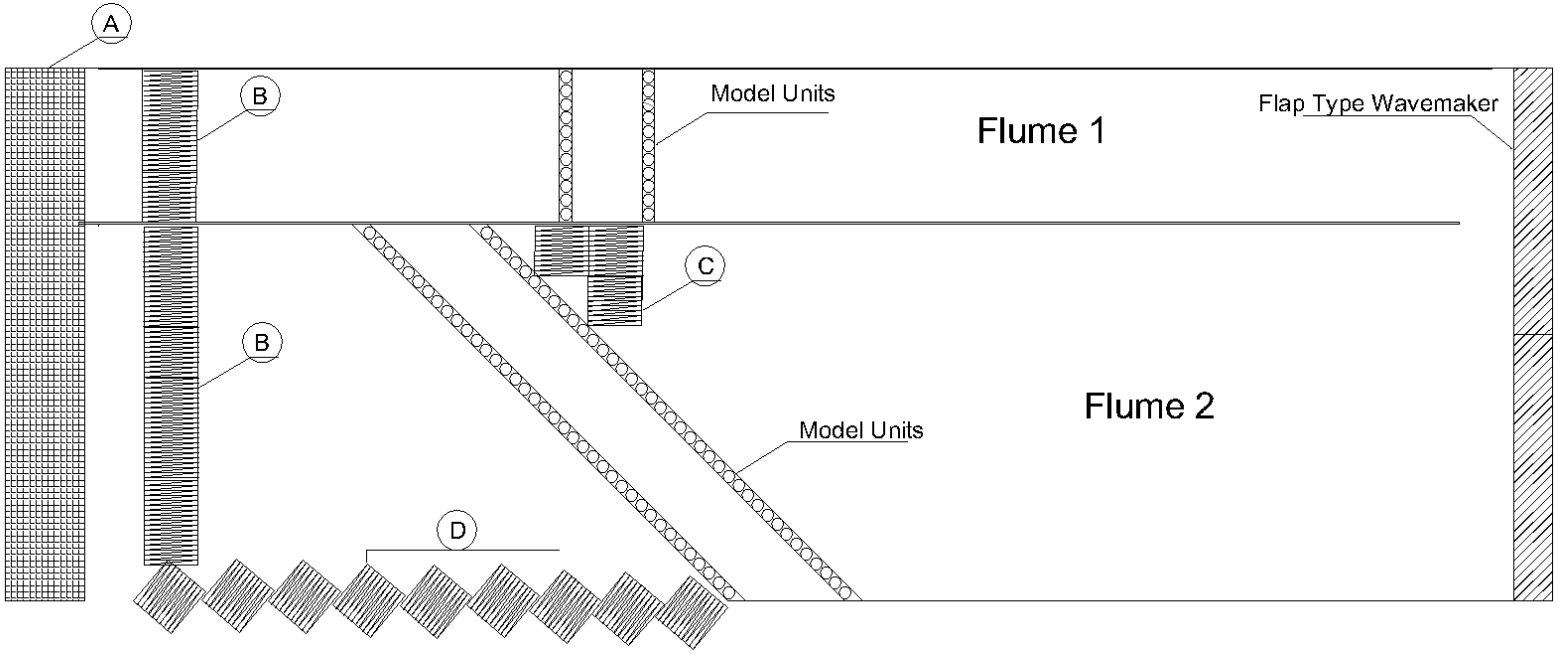

Figure 3.9: Absorption system of Basin-1

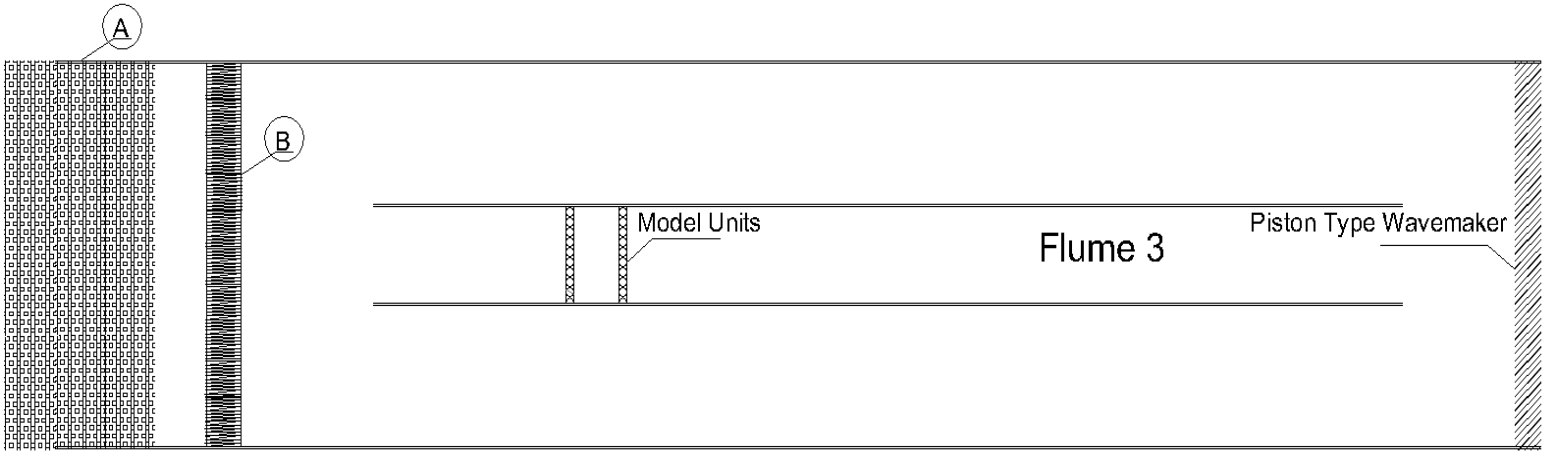

Figure 3.10: Absorption system of Basin-2

3.3.4 Model Wave Generation

Physical models would be ineffective if the waves in nature cannot be imitated in the laboratory conditions. In the modelling procedure of the wind waves, it is not practical to utilize large spaces for wind to generate waves. Therefore, mechanical devices are used to generate the waves for the coastal engineering laboratory models. Mechanical wave generators consist of a movable partition placed in the wave basins.

Formerly, waves were generated with a moving board in a sinusoidal motion with a specific amplitude and period of oscillation (regular waves). However, it was very basic and could not generate waves similar to the nature (irregular waves). Later, portable devices appeared to be an effective alternative by creation a train of unidirectional wave crests parallel to the board. These devices consisted of an electrical motor driving the board. In time with the developing technology, hydraulic servo-systems became widespread. These systems provided engineers more control over the wave generation systems. Imitation of irregular waves, sinusoidal waves and solitary waves in basins became possible. (Hughes, 1993)

Two kinds of wave generator were used in this study. First one is flat-type wavemaker that works with an electrical motor driving the wave board. It is used in the basin-1 to generate waves simultaneously in flume-1 and flume-2. Second one is piston-type hydraulic servo-system placed in the basin-2.

3.3.4.1 Wavemakers:

Basically, all wave generators work with the data which consists of amplitude and frequency of a motion. However, how the data is provided to the system vary for each wavemaker.

In principle, frequency input of the motion can be calculated from the model wave period. For each wave that is going to be generated in the basin, wave frequency can be calculated using the following formula:

$$f = \frac{1}{T_m} \tag{3.5}$$

where;

f: frequency of the wavemaker board (Hz)

T_m: Scaled wave period in model (sec)

In the model studies, for both wavemaker, input data for wave period was prepared using the Equation 3.5 to generate the required wave period in the model.

On the other hand, it is a rather complicated process to prepare the amplitude of the wave motion as input for the wavemakers. Considering the two-dimensional wave flume given in the Figure 3.11, Hughes (1993) discusses general theory of mechanical wave generation referring to the two-dimensional governing equations.

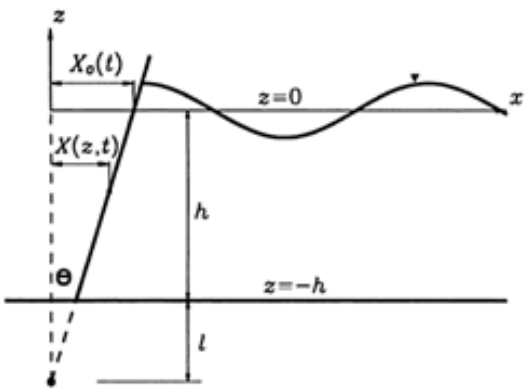

where;

x: Coordinate in x direction

z: Coordinate in z direction

h: Water depth (m)

Θ: Angle of displacement

l: Vertical distance from hinge of the wave board to the flume bed (m)

Figure 3.11: Two-Dimensional wave flume sketch

As seen from the schematic drawing above, two- dimensional wave flume consists of a rotation wave board on a flat bed. On the coordinate system in the figure above, Hughes (1993) solves two-dimensional Laplace equation with the assumptions of inviscid, irrotational fluid and the reasonable boundary conditions.

Accordingly, a general first-order wavemaker solution is;

$$\frac{H}{S_0} = \frac{4\sinh kh}{\sinh 2kh + 2kh}\left[\sinh kh + \frac{(1-\cosh kh)}{k(h+l)}\right] \tag{3.6}$$

where;

H: Wave Height (generated)

h: Water depth

S_0: Stroke amplitude of wave board

l : Vertical distance from hinge of the wave board to the flume bed (m)

k: Wave number

For the flap-type wavemaker which is used in Basin-1, wave board is hinged at the flume bed, so the l value is accepted as zero and the Equation 3.6 is revised as;

$$\frac{H}{S_0} = \frac{4\sinh kh}{\sinh 2kh + 2kh}\left[\sinh kh + \frac{(1-\cosh kh)}{kh}\right] \tag{3.7}$$

For piston-type wavemaker which is used in Basin-2, wave board is not hinged at the flume bed and will move perpendicular to the flume bed, so the l value is accepted as $l \to \infty$, and the Equation 3.6 is revised as;

$$\frac{H}{S_0} = \frac{4\sinh^2 kh}{\sinh 2kh + 2kh} \tag{3.8}$$

Then Equation 3.7 and 3.8 are used to calculate the proportion of wave heights to stroke amplitudes for each wavemaker. (Table 3.4)

Table 3.4: Variables of the model cases

Wave Period (T)		For Flap-Type Wavemaker	For Piston-Type Wavemaker
In Prototype	**In Model**	**H/S_0**	**H/S_0**
6	1.7	0.62	1.12
8	2.2	1.06	1.70
10	2.8	1.21	1.84

3.3.4.2 Process of Input Data:

Two different methods are used to provide input data for the wavemakers according to their types.

Input for the flap type wavemaker:

Flap-type wavemaker located in Basin-1 consists of three basic parts; a wave board, an electrical motor and a deck connected to the motor. The input data is provided to the system manually. For the wave period, frequency is calculated using the Equation 3.5 and provided to the system via a rotary switch on a deck connected directly to the electrical motor. (Figure 3.12)

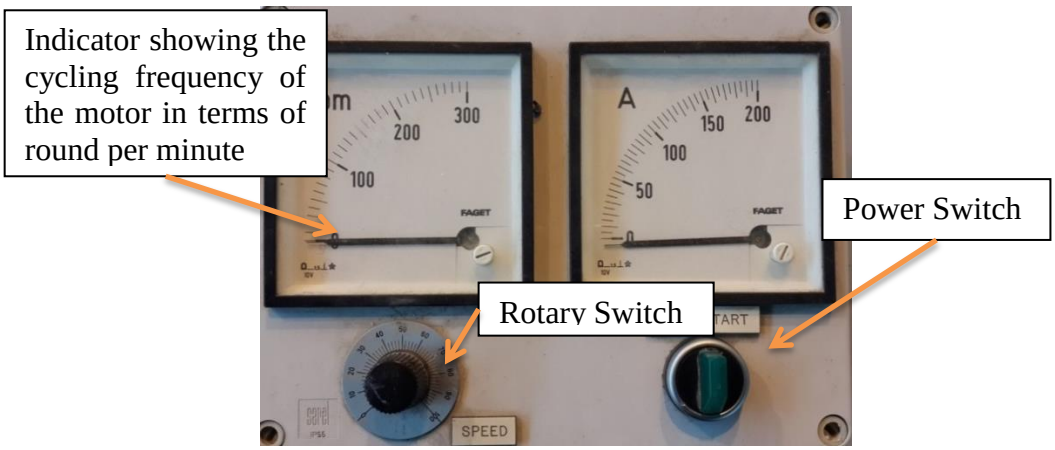

Figure 3.12: Control deck of the flap-type wavemaker

After starting the electrical motor with the requested frequency input, the wave board moves forward and backward. For each complete round of the motor, the wave board completes its single sinusoidal motion and comes to its original position again. This single motion acts like a stroke and create a single wave. For each stroke, a new wave is generated in the flume. (Figure 3.13)

Figure 3.13: Cycling motion of the motor of the flap-type wavemaker

The wave height data for the flap-type wavemaker is prepared with stroke amplitude data using the Equation 3.7 The stroke amplitude is the distance which the wave board will travel in one cycle of the motor. For this wavemaker, the stroke amplitude can only be adjusted manually. (Figure 3.14)

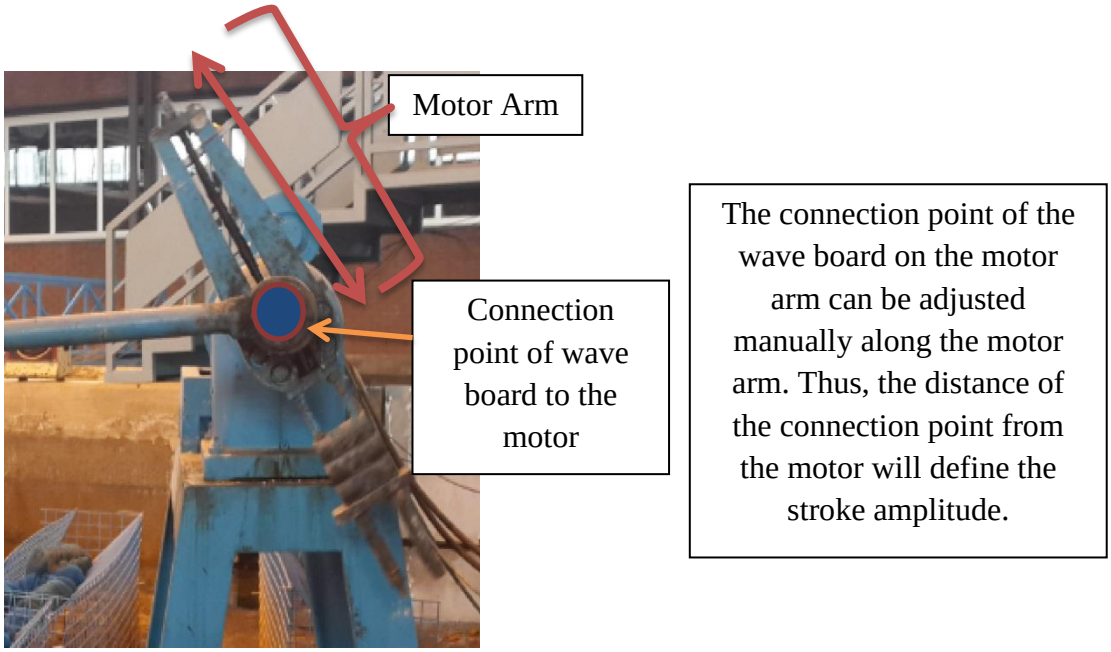

Figure 3.14: Control deck of the flap-type wavemaker

Input for the piston-type wavemaker:

Piston-type wavemaker consists of three basic parts: a wave board perpendicular to the flume bed, a piston connected to the wave board and a deck which connects the piston to the computer. Data can be input either by the computer or using the deck connected to the piston which allows the engineer full control of the data. In this study, wave input was prepared as a matrix of regular wave train of thirty seconds with twenty data for each second. Data is input into the computer via a program named “Waveform”. (Figure 3.15)

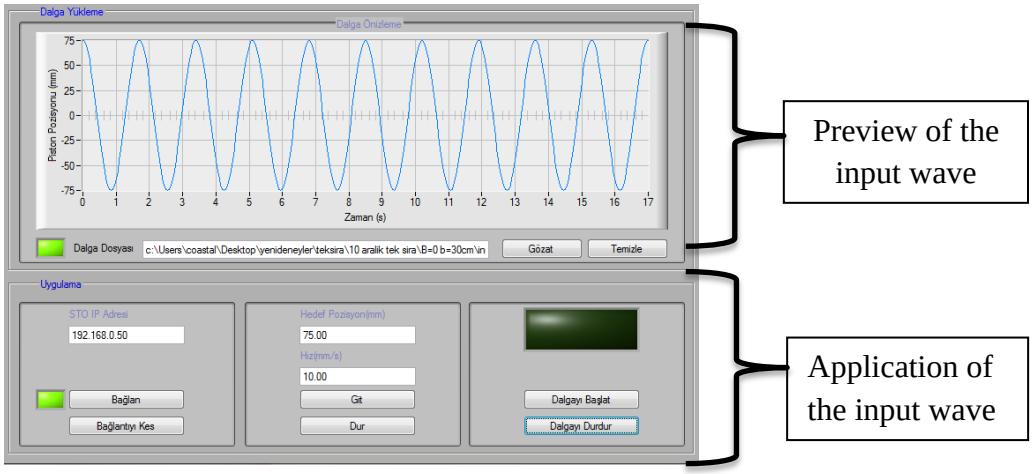

Figure 3.15: Interface of the Waveform

However, if it is required to work with irregular waves, the data can be prepared using an appropriate computer program like MATLAB. Another method to generate the regular waves directly is to use the deck named Moog SmarTest with no need of computer usage. (Figure 3.16)

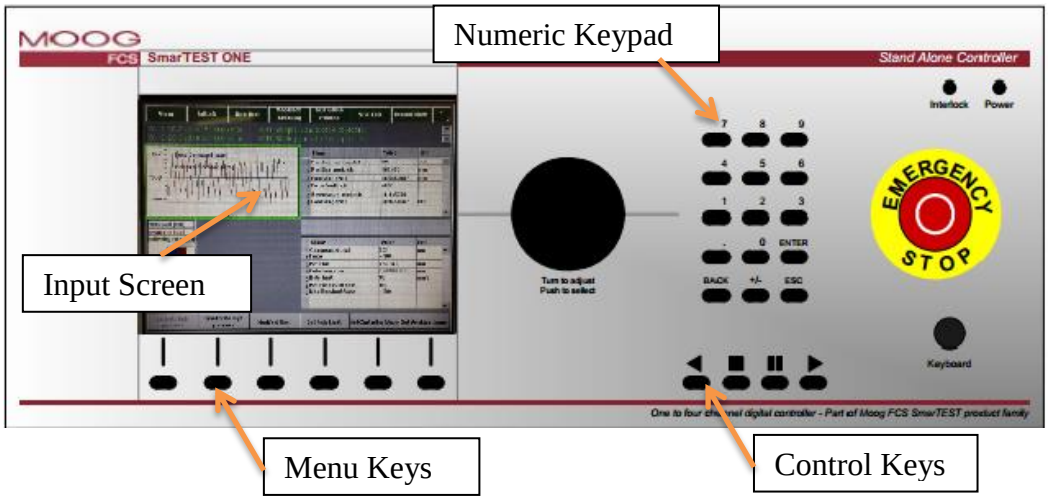

Figure 3.16: Front panel of Moog SmarTest

3.3.5 Data Collection:

In the model studies, data collection was implemented as sea surface elevation measurements which can be called as wave measurements. The wave measurements were done for incident waves and corresponding transmitted waves through the structure with appropriate instrumentation.

As Hughes (1993) stated, in data collection phases, accuracy of the model studies depends on the reliability of the instruments used. If adequate tools are not used, the data obtained will be uncertain and doubtful. Also, the investigator should have full control on the capabilities and limitations of the instrumentation. Furthermore, which instrumentation will be used in the experiments should be decided in the design stages. Thus, there should be enough time for testing the tools, calibration and servicing.

The instruments, which are used to collect data, consist of two parts. One of them is a sensor or transducer (wave gauge) which measures a physical quantity and converts it to a signal that can be recorded. The other part is a unit to record the signal. In these model studies, recording procedure of the signal data was implemented by the DHI (Danish Hydraulics Institute) Instrument System for hydraulic model tests (Figure 3.17). The DHI system establishes the connection between computer and wave gauges. Moreover, the DHI Instrument System works as a modular system with transducers, plug-in conditioning, amplifier modules and two cabinets which are DHI-Standard cabinet 101E and DHI- filter cabinet 153/IF. The DHI-Standard cabinet provides power to the modules with a power supply through a dashboard. BNC sockets located on the modules works for collection of signal outputs. Also, there are 8 signal outputs located on the back panel of the DHI-Standard cabinet which simplifies data sampling when connected to the DHI-input filter cabinet. The filter cabinet provides the data collection of the signals from the transducers and an easy connection between the transducers and the computer. This filter cabinet works for the combination of pc- computers and 16 channel A/D converter. (Kürüm, 2008)

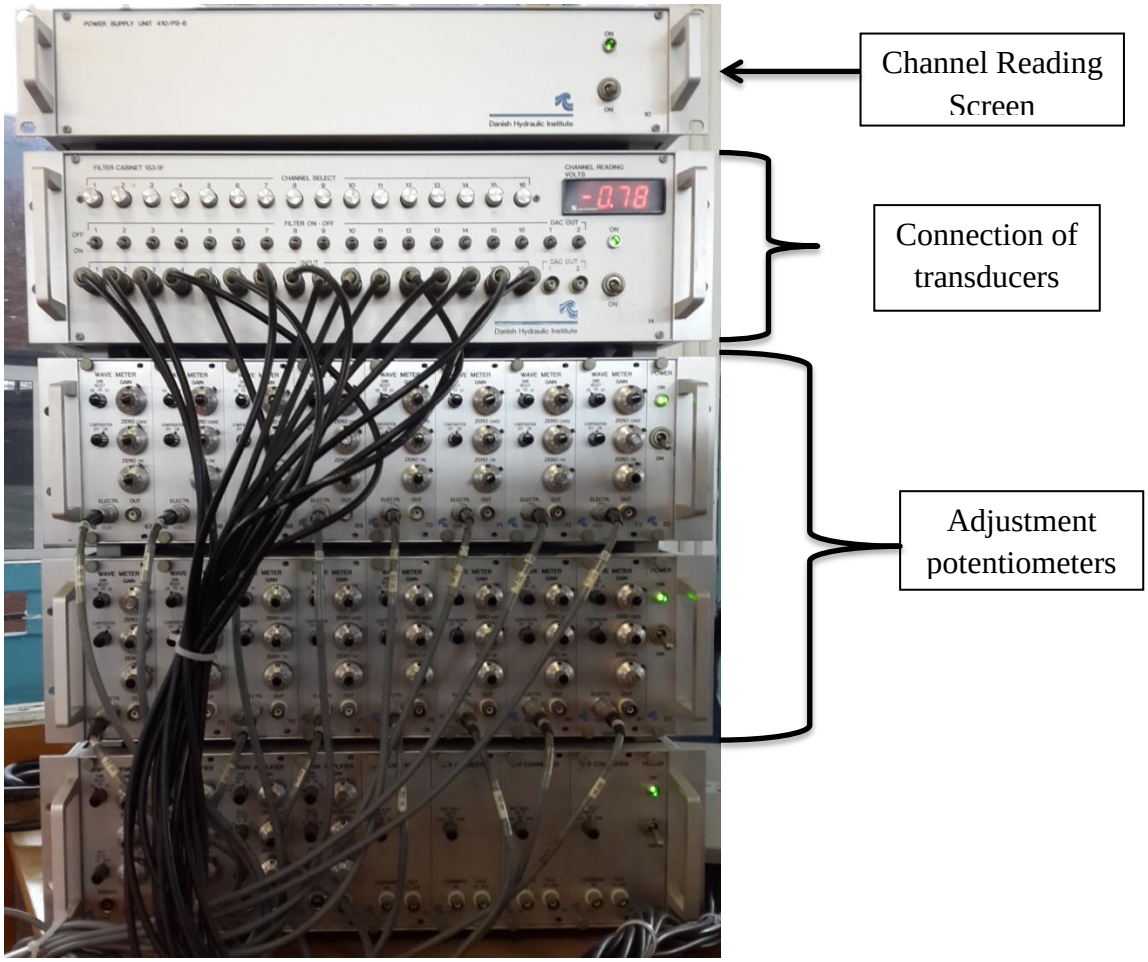

Figure 3.17: Front panel of recording unit

Wave Gauges

In the experiments, DHI-Wave Meter wave gauges were used as transducers (Figure 3.18). These wave gauges are conductive tools with two parallel stainless steel electrodes aligned perpendicular to wave direction. Also, the bottom part of the wave gauges is the compensation electrodes which eliminate the effect of salinity and temperature changes.

Figure 3.18: DHI-Wave Meter Wave Gauge

Wave gauges are the most essential parts of data collection system because they are used for the measurement of wave height and wave period. To acquire accurate measurements, wave gauges should be installed in the wave flumes in such a way that they would not move under the action of waves generated in the basin. The midpoint of the steel electrode parts of the gauges should be at the same level with the still water level. In any condition, the head parts of the gauges should be kept dry and stable. Moreover, the location of each gauge in the wave flume should be defined carefully. Exact locations of the wave gauges were defined after several experiments (Appendix A).

These experiments provided some guidelines to decide the location of the wave gauges in the laboratory basins. It was concluded that the following factors should be considered for the final setup of wave gauges:

- Wave gauges should be placed at least one wave length away from the wave generator. Thus, it will enable a full wave to be generated. (Figure 3.19 and 3.20, Point A)
- Wave gauges should be placed away from the reflective surfaces like side walls to collect accurate data without undesired fluctuation. (Figure 3.19 and 3.20, Point B)
- If the studies are conducted with the individual waves or regular waves purged from reflection as in this study, wave gauges should be located at least half of a wave length away from the structure. Therefore, at least one solitary wave profile would be recorded. (Figure 3.19 and 3.20, Point C)
- Wave gauges should be located in pairs side by side to validate accuracy of the measurements. (Figure 3.19 and 3.20, Point D)
- Since it is not efficient to use sea water, tap water is used. Thus, before each experiment, wave gauges should be cleaned to eliminate the inaccuracy due to lime and accumulated film which occurs due to the tap water.
- If the studies are to be conducted with the irregular waves, wave gauges should be placed in pairs in the direction of the wave orthogonal to observe the reflected waves. (Goda &Suziki, 1976)

Resulted location of the wave gauges in the laboratory basins are given in Figure 3.19 and 3.20.

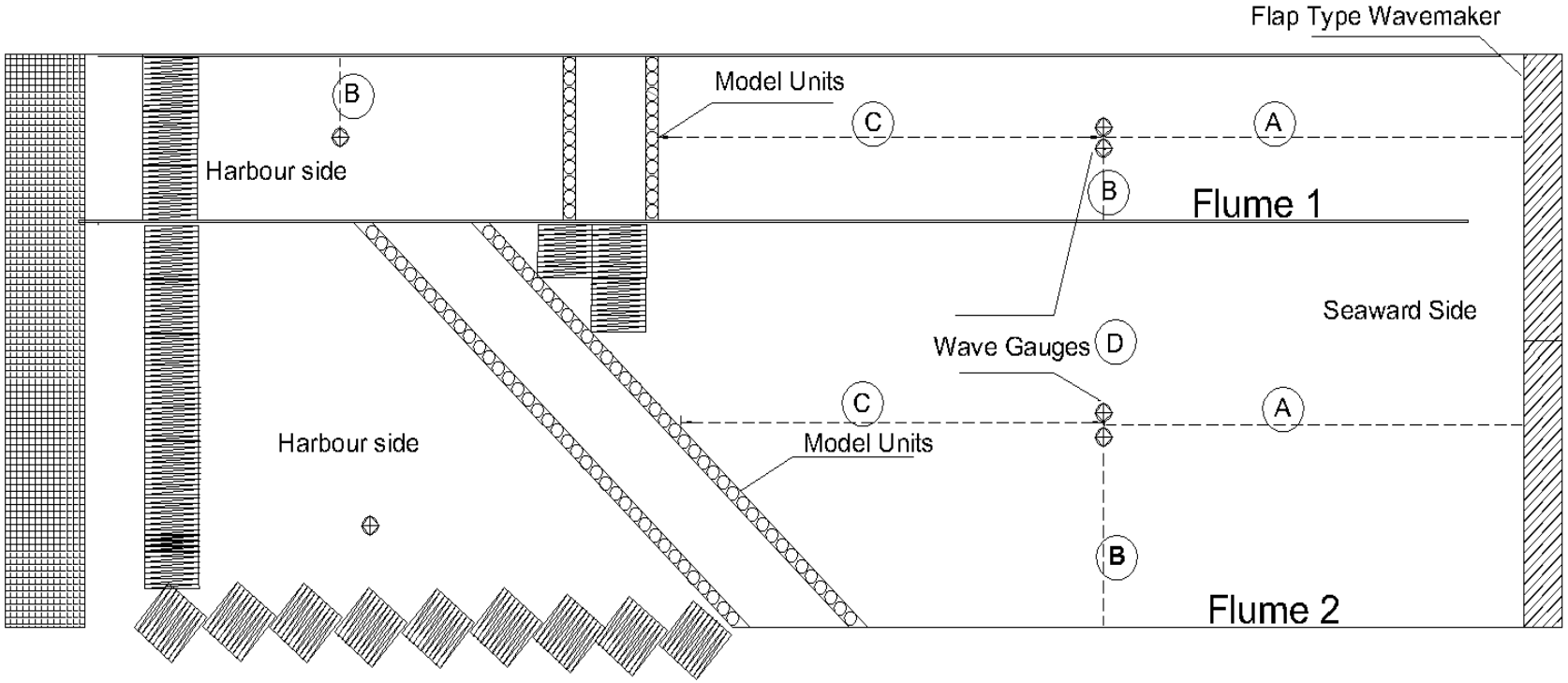

Figure 3.19: Location of the wave gauges in Basin-1

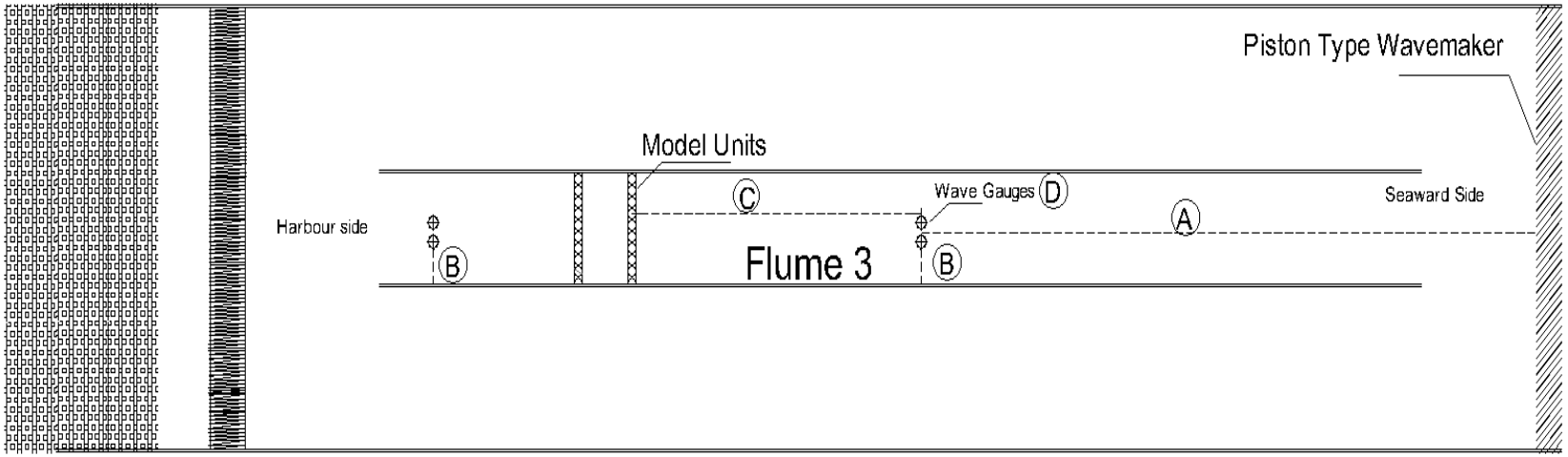

Figure 3.20: Location of the wave gauges in Basin-2

When the basin is filled, wave gauges will be immersed in the water and the conductivity difference between two electrodes of the wave gauge will be recorded instantaneously. The change in the voltage measured by the wave gauge is proportional to the change of water surface elevation. The voltage data is recorded via software developed by TDG with a rate of 20Hz. (Figure 3.21)

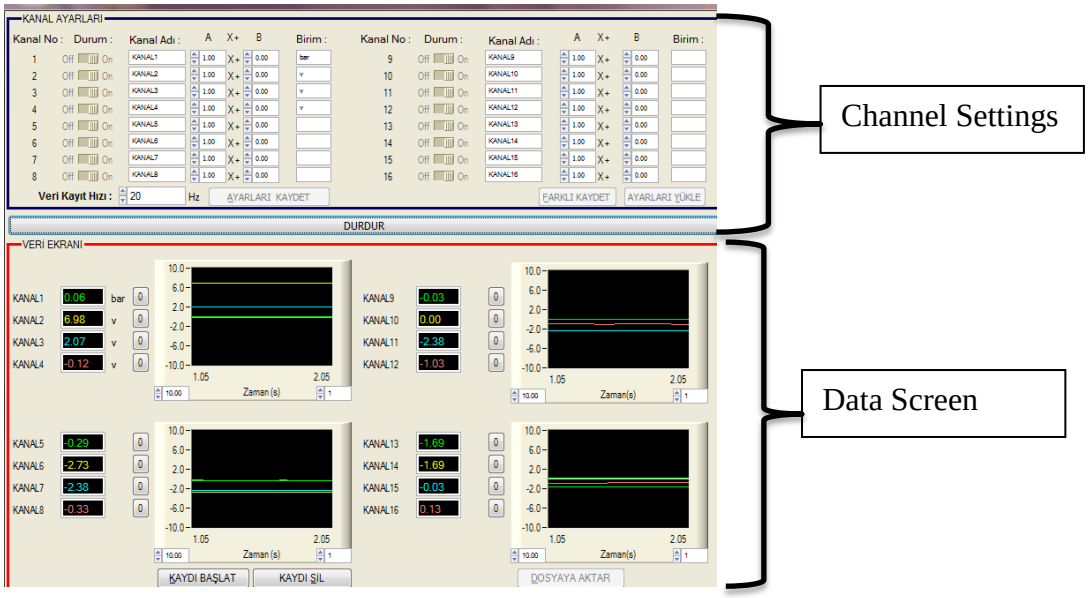

Figure 3.21: Data Recording Software developed by TDG

Recorded data is saved as comma-separated values file format (*.csv). This file format enables to record data simultaneously for 16 wave gauges. (Table 3.5)

Table 3.5: Sample Data Recorded in ".csv" format

Deney Başlangıcı: 12-06-2013 11:34:08 Delta t = 0.05															
Kanal1	Kanal2	Kanal3	Kanal4	Kanal5	Kanal6	Kanal7	Kanal8	Kanal9	Kanal10	Kanal11	Kanal12	Kanal13	Kanal14	Kanal15	Kanal16
1.411	-0.308	5.093	0.176	-0.293	-2.632	-2.319	-0.181	0.01	0	-2.339	-0.952	-1.25	0.01	0.2	-0.771
1.411	-0.308	5.093	0.171	-0.298	-2.632	-2.319	-0.176	0.01	0	-2.339	-0.957	-1.25	0.01	0.2	-0.771
1.411	-0.308	5.093	0.171	-0.293	-2.632	-2.319	-0.176	0.005	0	-2.339	-0.952	-1.245	0.01	0.2	-0.767
1.411	-0.308	5.093	0.176	-0.293	-2.632	-2.319	-0.181	0.01	0	-2.344	-0.957	-1.25	0.01	0.2	-0.771
1.411	-0.312	5.093	0.171	-0.298	-2.632	-2.319	-0.176	0.01	-0.01	-2.339	-0.952	-1.25	0.01	0.195	-0.771
1.411	-0.312	5.088	0.181	-0.293	-2.632	-2.319	-0.195	0.01	0	-2.339	-0.947	-1.25	0.01	0.2	-0.771
1.411	-0.312	5.093	0.171	-0.293	-2.632	-2.319	-0.181	0.01	0	-2.339	-0.952	-1.25	0.01	0.2	-0.762
1.411	-0.317	5.093	0.181	-0.293	-2.632	-2.354	-0.181	0.01	0	-2.339	-0.957	-1.25	0.01	0.2	-0.771
1.411	-0.312	5.093	0.171	-0.298	-2.632	-2.319	-0.176	0.01	0	-2.339	-0.952	-1.25	0.01	0.2	-0.776
1.411	-0.312	5.093	0.176	-0.293	-2.632	-2.319	-0.176	0.005	0	-2.339	-0.947	-1.25	0.01	0.2	-0.767
1.411	-0.312	5.093	0.171	-0.293	-2.637	-2.319	-0.176	0.01	0	-2.339	-0.952	-1.25	0.01	0.2	-0.767
1.411	-0.312	5.093	0.176	-0.298	-2.632	-2.319	-0.181	0.01	0	-2.339	-0.957	-1.25	0.01	0.2	-0.771
1.411	-0.312	5.093	0.176	-0.298	-2.632	-2.319	-0.176	0.005	0	-2.339	-0.952	-1.25	0.01	0.2	-0.771
.	.	.	.	.	.	.	.	.	.	.	.	.	.	.	.
.	.	.	.	.	.	.	.	.	.	.	.	.	.	.	.
.	.	.	.	.	.	.	.	.	.	.	.	.	.	.	.
.	.	.	.	.	.	.	.	.	.	.	.	.	.	.	.
.	.	.	.	.	.	.	.	.	.	.	.	.	.	.	.

Calibration:

Calibration is a mathematical relationship between the output of transducer and the water level elevation. The relationship between recorded raw voltage data and the observed physical quantity should be determined with calibration procedure before each experiment. In the model studies, calibration procedure is required to be repeated each day before experiments due to the fact that used wave gauges can easily be affected by the temperature changes and salt effects in the water. (Kürüm, 2008)

For the calibration, the wave gauges are fixed at the same height; the still water level is lowered or raised to known heights. After the stillness of the water level is ensured, at each predetermined water level height, the sensor output is recorded. At this point, it is essential to stabilize the water level, since slightest water level fluctuation would invalidate the calibration procedure. The recorded sensor outputs in unit volt and the corresponding water level heights in unit lengths are used to plot calibration lines.

In the model studies, after it was ensured that the wave gauges worked properly, calibration procedure was applied at three predefined water level elevation. To save

time, calibration was done at the beginning of each experiment day and the water level was decreased from +10cm to -10cm of still water level with 10 cm intervals or from +0cm to -10cm with 5 cm intervals. The resulting plots for gauge 5, 8, 12 and 16 are given as examples to show the consistent linear relationship between voltage data and water level distance relative to still water level. For each gauges, linear regression gave the R^2 value equal to one as perfect fit. (Figure 3.22)

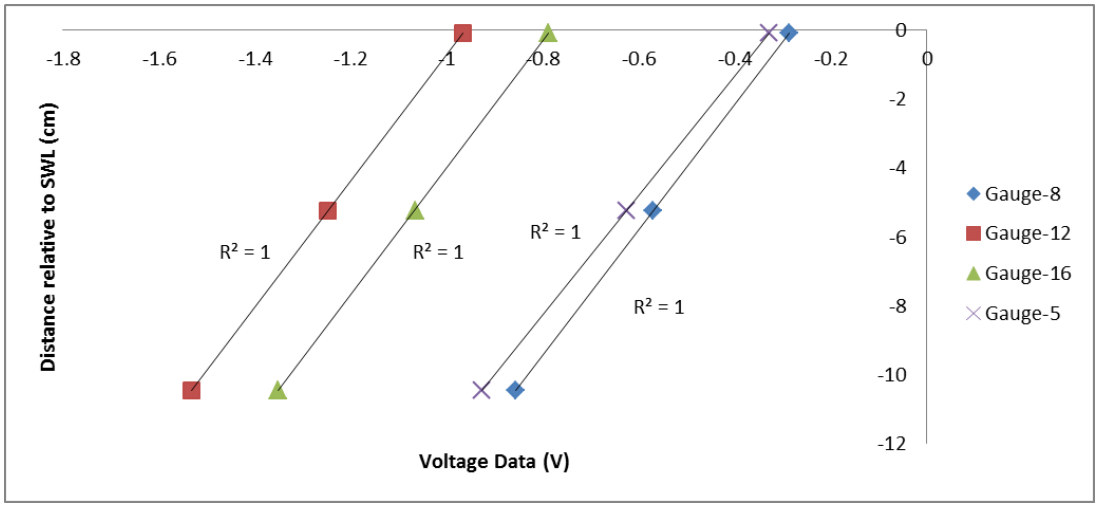

Figure 3.22: Linear regression for Gauge-5, 8, 12 and 16 (3 point calibration)

The calibration procedure is used to obtain calibration coefficients. These coefficients enabled to convert the recorded voltage data to the water level elevation data for each experiment conducted in the model studies. The calculation of calibration coefficients was done automatically using the MATLAB code, "calib.m" written by Baykal (2009).

3.4 Data Analysis

Laboratory experiments consist of a certain systematic work-flow as given in the Figure 3.1. First, the laboratory set-up was decided. Then, input data and the wave generation method were identified. Later, the output data were collected with the data collection instruments. These procedures were explained in the former subsections in detail. After the data collection procedure was completed for each experiment, the output data should be analysed to understand how the system behaves under the experiment conditions. All the stages in the data analysis part of the model studies were performed using the MATLAB Codes written by Baykal (2012). In this subsection, basic principles followed in the data analysis stages of the studies will be explained in detail using the flowchart given in Figure 3.23.

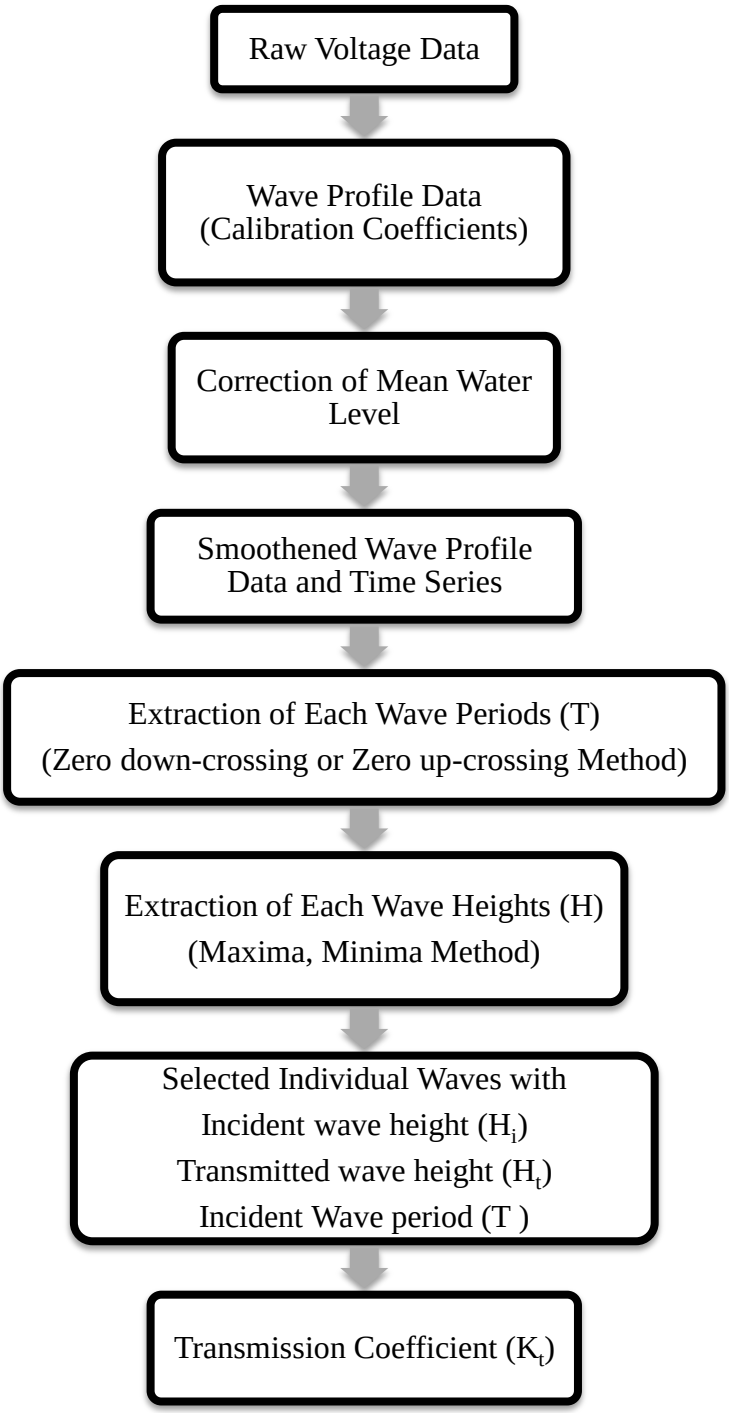

Figure 3.23: Flowchart of the data analysis stages

At the first stage, the data were collected via the wave gauges as voltage data which is explained in the former subsection. Using the calibration functions, the voltage data was converted into the water level elevation data.

Later, the arithmetic mean of all data was subtracted from all the time series recorded for each gauge to set the arithmetic mean to zero. Thus, the raw data was converted into distances from the mean water level.

Then, the recorded data was smoothed in order to eliminate the errors like glitches and spikes caused by the laboratory environment. Each data recorded by the gauges was corrected using the two former and two latter successive data points.

After the data is corrected, each individual wave in a time series was defined using zero up-crossing and zero down-crossing method which is a common tool to define the wave characteristics in time series. Furthermore, minima-maxima method is employed to define wave height of each wave in a time series.

In these experiments, only the individual waves selected from the wave profile were employed to omit reflection from readings. For example, for the experiment case given in Figure 3.24 and 3.25, first and second individual waves are chosen and recorded as the desired experimental data. The first troughs were not considered because the desired wave profile could not be reached in the still water. Thus, for this experiment case, analysis was made with zero up-crossing method. The waves after second and third wave encountered the reflection from surfaces and thus were not taken into consideration.

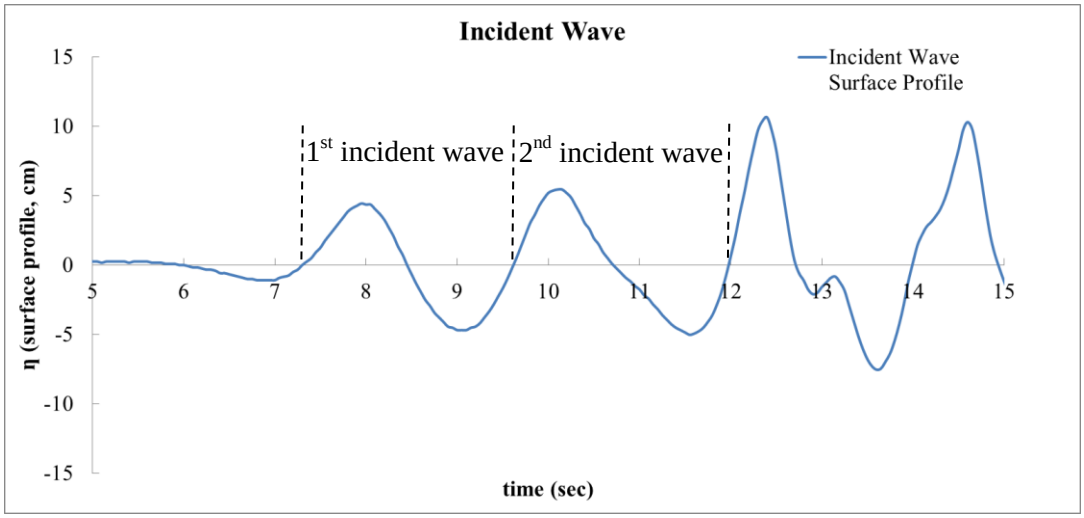

Figure 3.24: Sample surface profile for incident wave

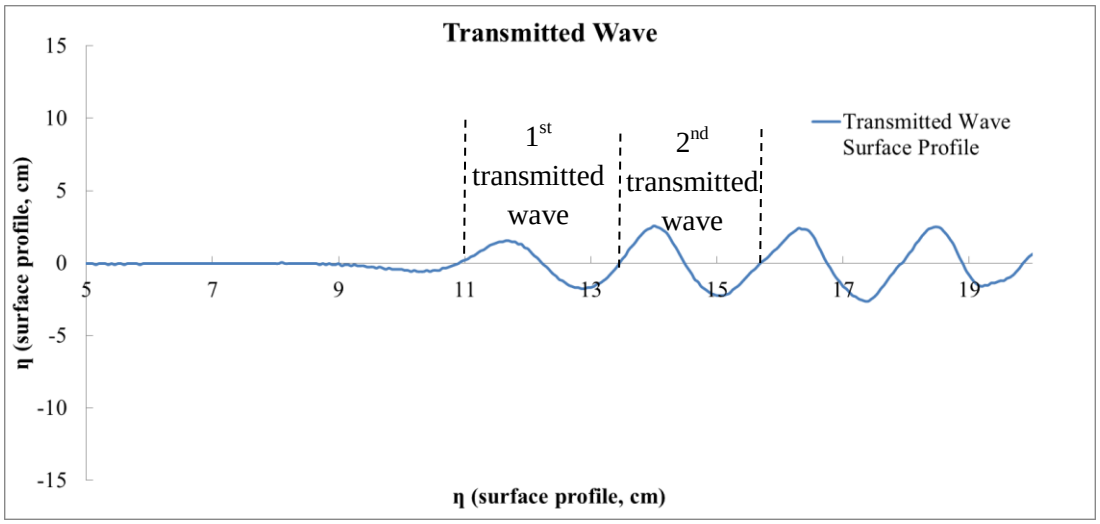

Figure 3.25: Sample surface profile for corresponding transmitted wave

Transmission Coefficient:

After incident and transmitted individual waves were defined, the wave transmission phenomenon can be investigated in terms of transmission coefficient "K_t";

$$K_t = \frac{H_t}{H_i} \tag{3.9}$$

Where;

H_i: Incident wave height (m)

H_t: Transmitted wave height (m)

For the cases of full transmission, K_t equals to 1 and for the cases of no transmission, K_t equals to 0. (Kürüm, 2008)

Measured:

In this study, incident wave heights (H_i) which were used to calculate the transmission coefficients were calculated as the mean of the data recorded by the wave gauges in front of the structures. On the other hand, corresponding wave heights were calculated as the mean of the data recorded by the wave gauges behind the structure.

Predicted:

As mentioned in Chapter 2, there exist very few studies on wave transmission through pile breakwaters. In the most resembling study to this thesis, Hayashi (1968) has proposed a solution to predict the wave transmission through single-row pile structure. (Figure 3.26)

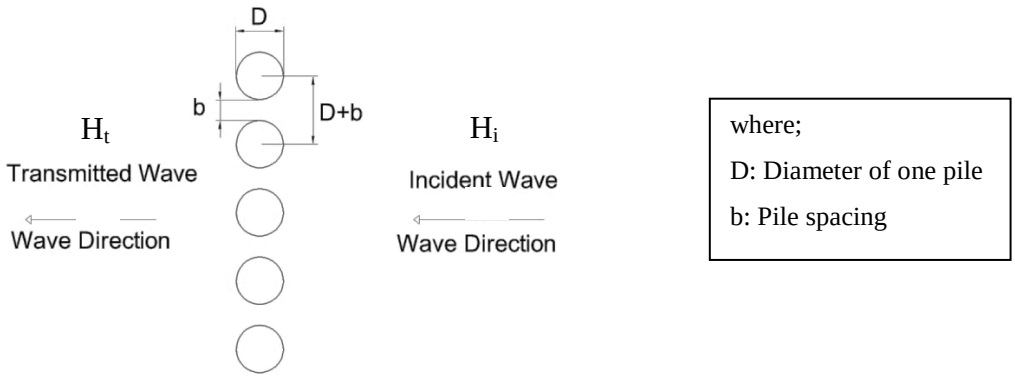

Figure 3.26: Single row pile breakwater

He emphasized the effect of the velocity of the water jets passing through the pile spaces and reached to solution given in Equation 3.10 and 3.11 (Hayashi, 1968);

$$\frac{H_t}{H_i} = 4\left(\frac{d}{H_i}\right)E\left[-E+\sqrt{E^2+\frac{H_i}{2d}}\right] \tag{3.10}$$

$$E = \frac{C\left(\frac{b}{D+b}\right)}{\sqrt{1-\left(\frac{b}{D+b}\right)^2}} \tag{3.11}$$

where;

D: Pile diameter

b: Pile spacing

d: Water depth

H_i: Incident wave height

H_t: Transmitted wave height

C: Constant

In this solution, C parameter consists of the effect of jet contraction and velocity in Bernoulli's theorem and similar to discharge coefficient. The value of C is defined

by the characteristic of the piles. Truitt (2011) recommended the C value as equal to 0.9 for closely spaced piled structures.

In this study, due to the fact that the experiments were mainly conducted on double-row pile breakwater except for Case-8, Hayashi's (1968) equations were revised and implemented twice to predict the results. As shown in the Figure 3.27, the transmitted wave from the first row was accepted as the incident wave for the second row and the solution was repeated for the second row to reach the transmitted wave from the second row.

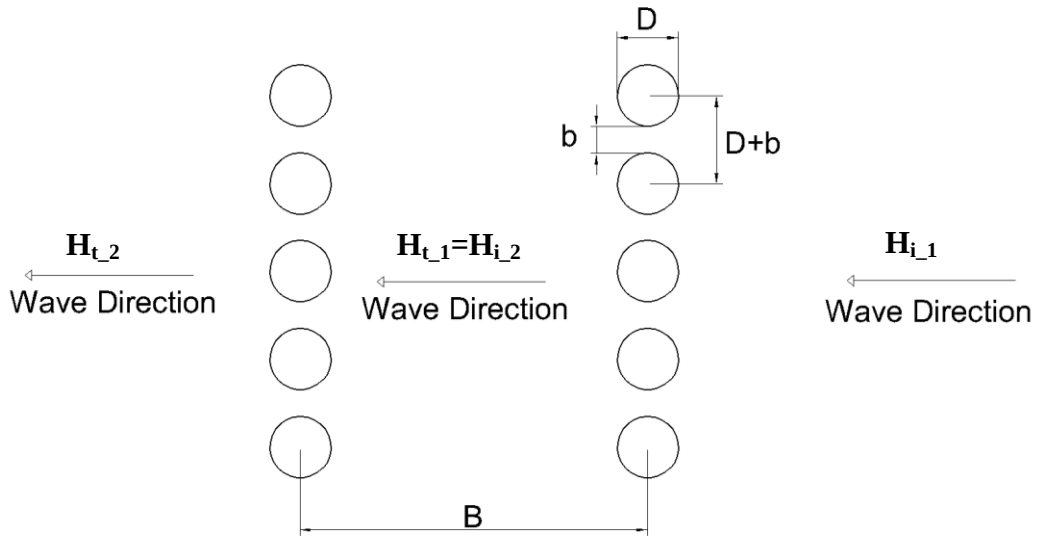

Figure 3.27: Double row pile breakwater

Accordingly the results were predicted with the following formulas (Hayashi, 1968):

$$\frac{H_{t\_1}}{H_{i\_1}} = 4\left(\frac{d}{H_{i\_1}}\right)E\left[-E+\sqrt{E^2+\frac{H_{i\_1}}{2d}}\right] \tag{3.12}$$

$$H_{t\_1} = H_{i\_2} \tag{3.13}$$

$$\frac{H_{t\_2}}{H_{i\_2}} = 4\left(\frac{d}{H_{i\_2}}\right)E\left[-E+\sqrt{E^2+\frac{H_{i\_2}}{2d}}\right] \tag{3.14}$$

$$E = \frac{C\left(\frac{b}{D+b}\right)}{\sqrt{1-\left(\frac{b}{D+b}\right)^2}} \tag{3.15}$$

$$K_t = \frac{H_{t\_2}}{H_{i\_1}} \tag{3.16}$$

where;

H_{i_1}: Height of the wave incident to the 1st row

H_{i_2}: Height of the wave incident to the 2nd row

H_{t_1}: Height of the wave transmitted from the 1st row

H_{t_2}: Height of the wave transmitted from the 2nd row

D: Pile diameter

b: Pile spacing

d: Water depth

C: Constant

CHAPTER 4

EXPERIMENTS AND DISCUSSION OF RESULTS

4.1 Introduction

Aim of the model studies and the model setup specifications are explained in the Chapter 3. In this chapter, the results of physical model experiments of one-row and two-row piled breakwater cross-sections are explained in detail. Then, the results obtained from different experiment setups are compared to each other. Furthermore, the results of the physical model experiments are compared to the values calculated by theoretical Hayashi's (1968) formula.

4.2 Model Waves

As stated in the Section 3.3.2, the experiments were conducted in three different wave flumes with eight cases of model setups. The dimensions of model setup were selected appropriately to investigate the dependency of wave transmission through piled breakwaters to breakwater dimensions. In total, 390 experiments were conducted to understand the influence of breakwater dimensions on wave transmission phenomenon.

During the experiments, water depth was kept constant at d=8.75m (d=68cm in the model). Waves were generated via both piston type and flap type wavemakers (Section 3.3.4). Model wave periods were decided to range from 6 to 10 sec (1.7 to 2.8 sec in model). Because of the limitations of the wave makers, wave steepness of the input waves differed in each flume. In Flume-1, the wave steepness ranging from

0.009 to 0.024 were used while the wave steepness ranging from 0.008 to 0.020 were used in Flume-2. In Flume-3, experiments were conducted to obtain higher steepness rates and accordingly, generation of waves with wave steepness ranging from 0.024 to 0.049 were achieved. Following these wave steepness ranges, wave heights from 0.8 to 1.5m, 0.7 to 1.2m and 1.3 to 3.2m were used in Flume-1, Flume-2 and Flume-3, respectively. The prototype wave parameters for each flume are given in Table 4.1.

Table 4.1: Prototype wave characteristics in Flume-1, 2 and 3

Flume #	Case #	Incident Wave Height (H_i) Range(m)	Incident Wave Period (H_t) Range (sec)	Incident Wave Steepness range
Flume-1	Case-1,2,3	0.8-1.5	6-10	0.009-0.024
Flume-2	Case-4,5,6	0.7-1.2	6-10	0.008-0.020
Flume-3	Case-1,2,3,7,8	1.3-3.2	6-10	0.024-0.049

4.3 Model Cases

Out of the eight different cases that were studied, physical model was constructed in both Flume-1 and 3 for Cases-1, 2 and 3. On the other hand, for Cases-4, 5 and 6, the models were constructed only in Flume-2 and for Cases-7 and 8, the models were constructed only in Flume-3. For each case, experimental results are presented with corresponding prototype values.

The schematic drawing with the dimensions of the prototype and the physical model are defined in Figure 4.1.

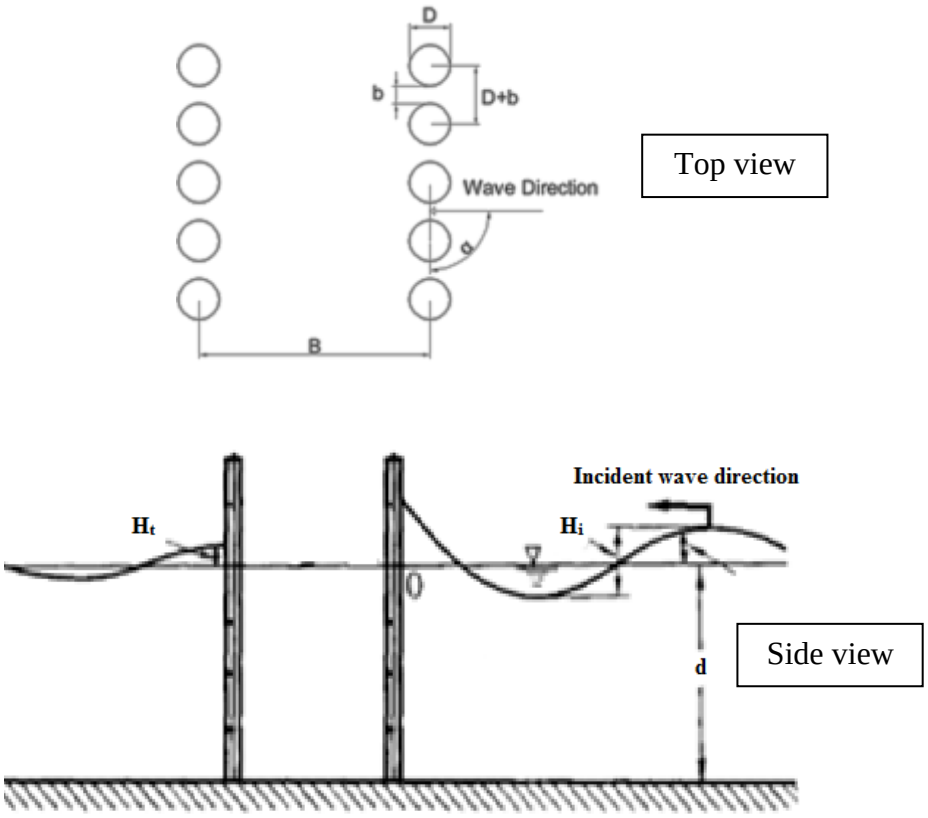

Figure 4.1: Double row pile breakwater dimensions

Where;

D: Pile diameter

b: Pile spacing

d: Water depth

B: Distance between rows

α : Incident wave approach angle

H_i: Incident wave height

H_t: Transmitted wave height

The selected dimensions for each case are given in Table 4.2 with prototype values for each case.

Table 4.2: Dimensional parameter of model cases (In prototype)

	Water depth d (m)	Pile diameter D (m)	Pile spacing b (cm)	Distance between pile rows B (m)	Incident wave approach angle (α)
Case-1	8.75	1.8	20	12	90°
Case-2	8.75	1.8	30	12	90°
Case-3	8.75	1.8	40	12	90°
Case-4	8.75	1.8	20	12	45°
Case-5	8.75	1.8	30	12	45°
Case-6	8.75	1.8	40	12	45°
Case-7	8.75	1.8	30	7	90°
Case-8	8.75	1.8	30	0 (single row)	90°

4.4 Experimental Results and Discussion:

For each experiment, incident wave heights, wave periods and transmitted wave heights were measured. Wave lengths, wave steepness and transmission coefficients were calculated accordingly, and tabulated. The data for Case-1 is illustrated as an example in the Table 4.2.

Table 4.3: Measured and calculated sampled data for Case-1

Measured			Calculated		
Wave Period (T_m) (sec)	Incident Wave Height (H_i) (m)	Transmitted Wave Height (H_t) (m)	Incident Wave Length (L_i) (m)	Incident Wave Steepness (H_i/L_i)	Transmission Coefficient (K_t)
7	1.4	0.4	62.0	0.023	0.28
8	1.4	0.4	62.4	0.022	0.29
8	1.2	0.4	69.2	0.017	0.37
8	1.1	0.4	69.4	0.017	0.37
10	0.9	0.4	85.8	0.010	0.48
10	0.9	0.4	85.8	0.010	0.47
7	1.4	0.4	61.7	0.022	0.30
6	1.6	0.3	46.2	0.034	0.22
6	1.6	0.3	46.2	0.034	0.18
6	2.0	0.4	46.2	0.044	0.17
6	2.0	0.4	42.8	0.048	0.17
6	2.0	0.4	42.9	0.048	0.17
8	3.6	0.5	62.6	0.057	0.14
8	3.6	0.5	63.3	0.056	0.14
10	3.6	0.7	85.8	0.042	0.20
10	3.6	0.7	85.9	0.042	0.20
6	2.2	0.4	42.8	0.050	0.17
.	.	.	.	.	.
.	.	.	.	.	.
.	.	.	.	.	.
.	.	.	.	.	.
.	.	.	.	.	.

The experimental results are presented in graphical forms to reflect the effect of the incident wave steepness (H_i/L_i) versus transmission coefficient (K_t). Additionally, these results are discussed with respect to spacing between piles (b), incident wave approach angle (α_i) and distance between rows of piles (B).

In following subsections, influence of chosen parameters on transmission coefficients are presented and further discussed to shed light on the complex mechanism of transmission phenomenon.

4.4.1 Incident Wave Steepness:

In Figures 4.2, 4.3 and 4.4, calculated transmission coefficients (K_t) and corresponding incident wave steepness values (H_i/L_i) are plotted for Cases-1, 2 and 3 respectively. Plotting the charts using (H_i/L_i) enables to observe the effects of both wave height and wave period on transmission phenomenon. Also, for the similar piled breakwater cross sections, transmission coefficients can be predicted from charts if the incident wave characteristics are known.

As it can be observed from Figures 4.2, 4.3 and 4.4, transmission coefficient decreases with increasing incident wave steepness. This trend is in agreement with the studies of Hayashi (1968), Herbich (1993), Suh (2011).

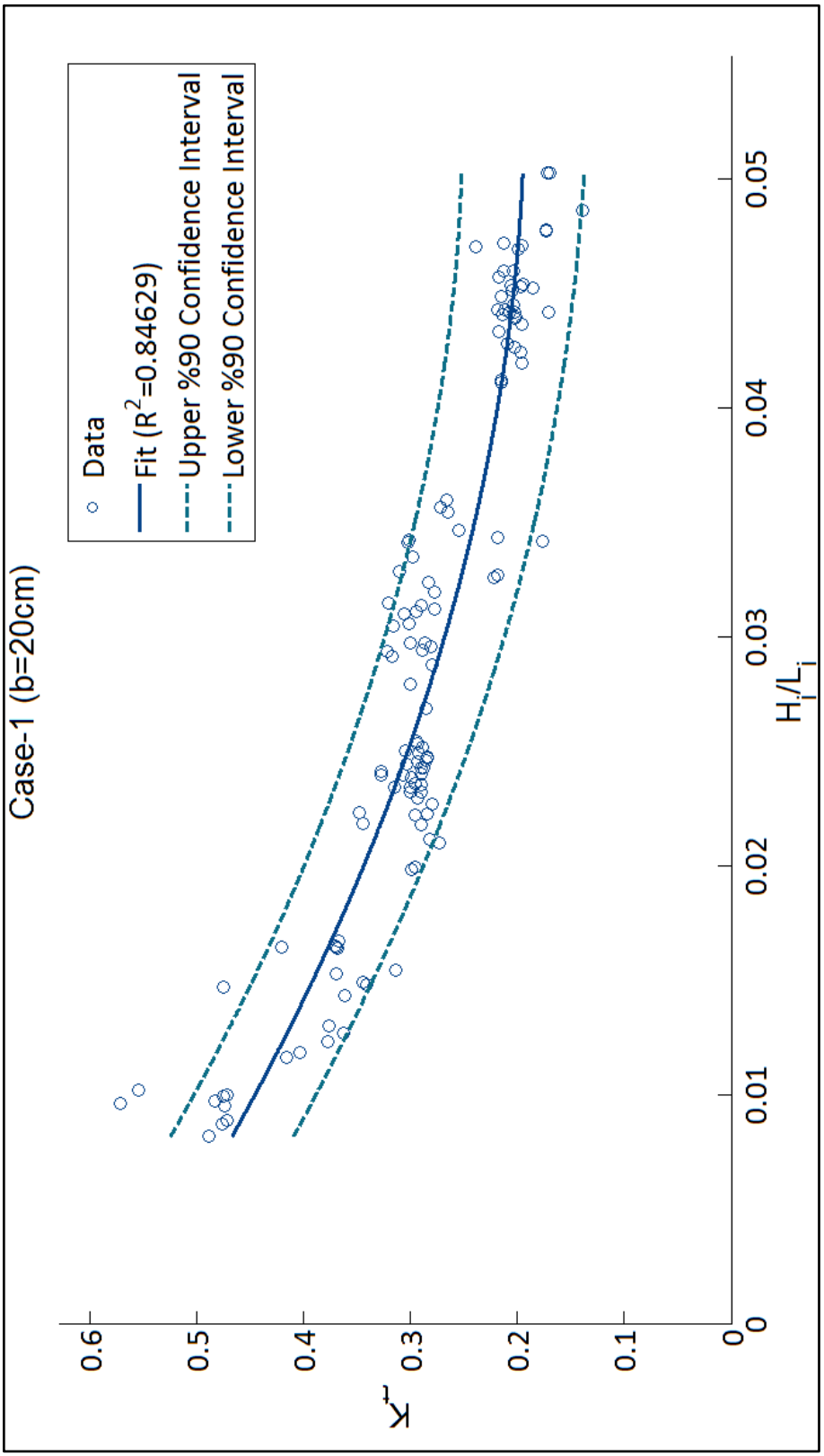

Figure 4.2: K_t vs H_i/L_i for Case-1

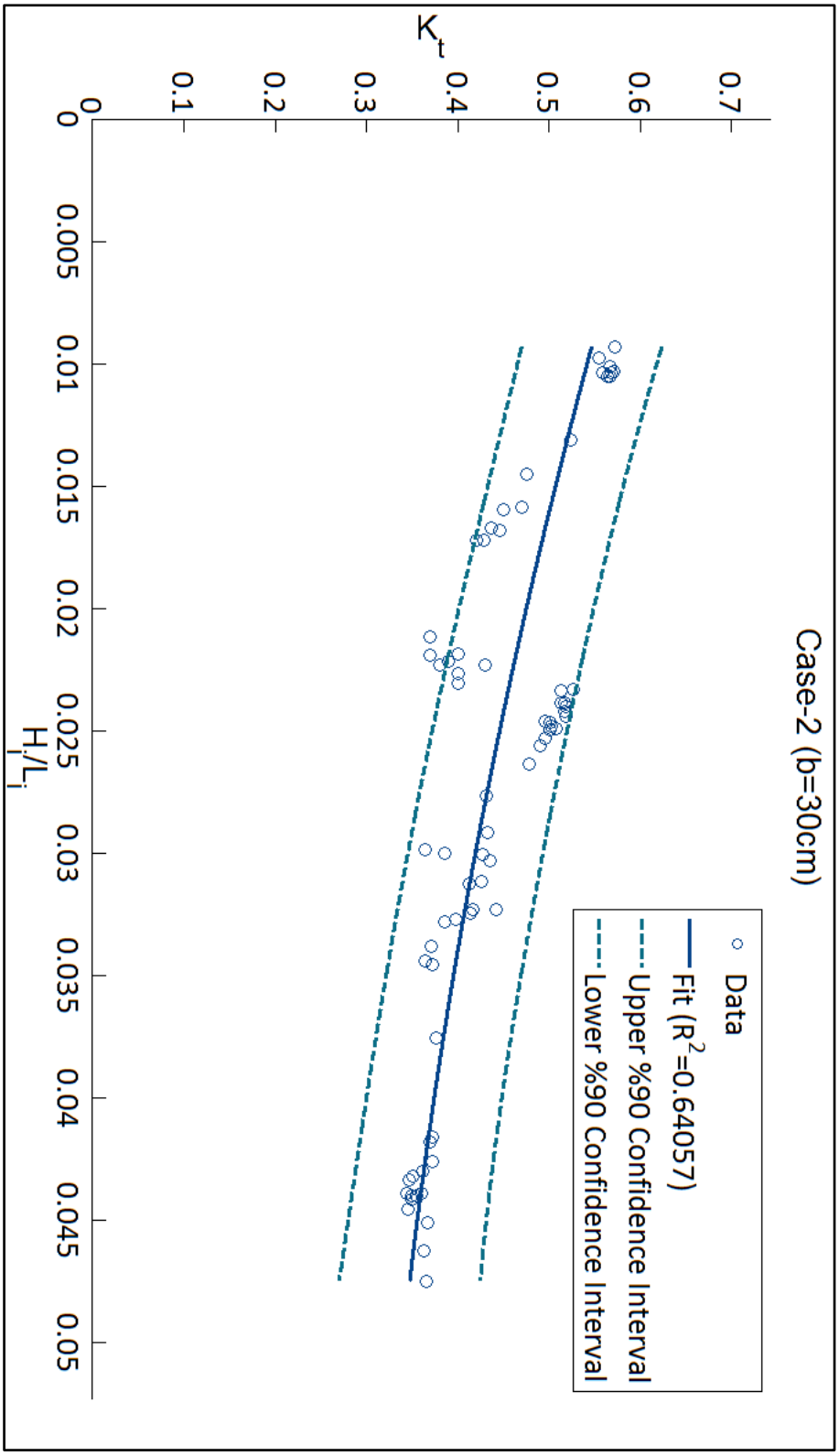

Figure 4.3: K_t vs H_i/L_i for Case-2

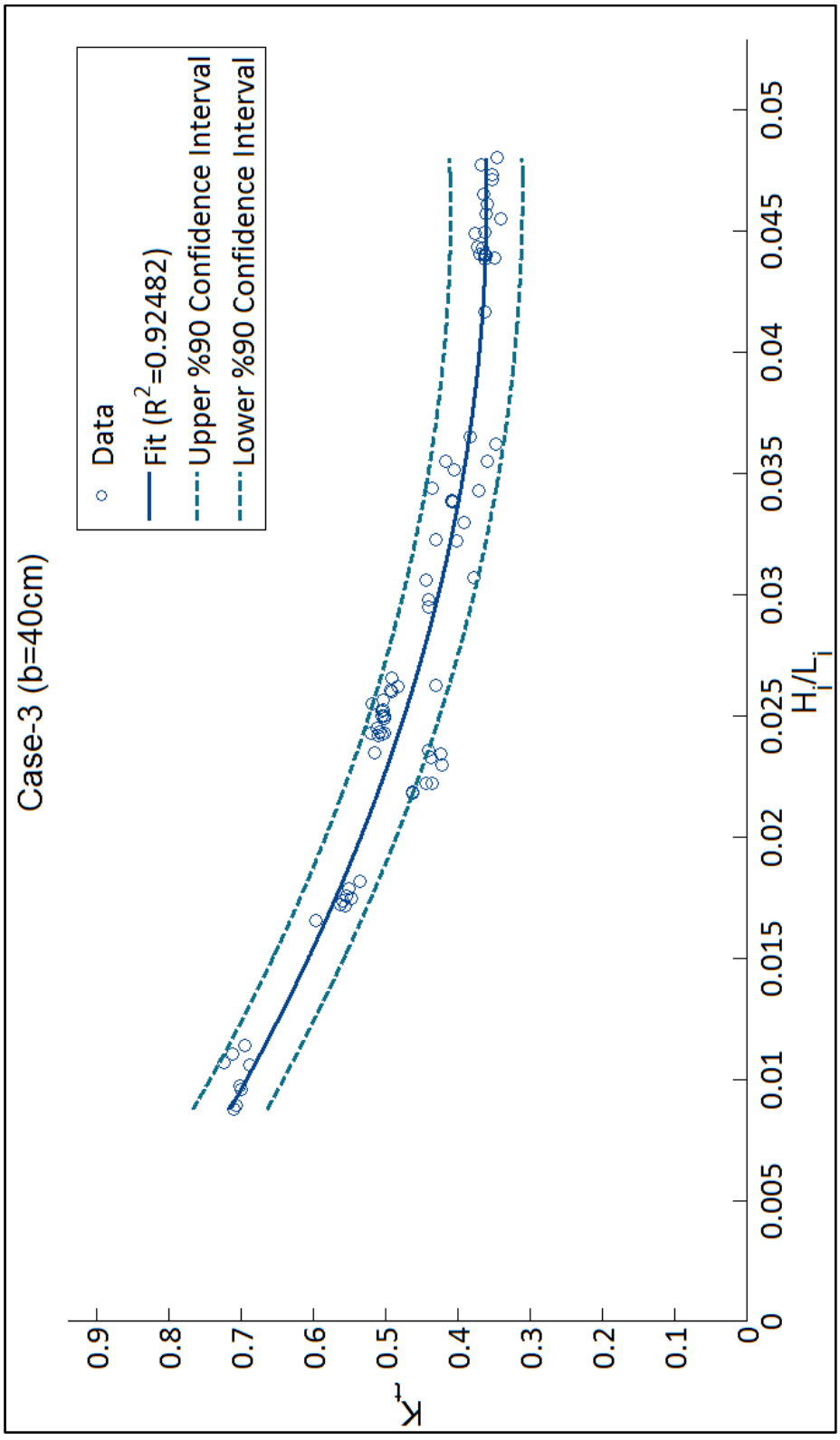

Figure 4.4: K_t vs H_i/L_i for Case-3

Furthermore, the decreasing rate of transmission coefficient is higher for lower steepness values whereas it is lower for higher steepness values. Table 4.4 gives transmission coefficient ranges for corresponding wave steepness ranges for Case-1, 2 and 3.

Table 4.4: Wave steepness ranges and corresponding transmission coefficient ranges for Case-1, 2 and 3

	Case-1	**Case-2**	**Case-3**
Incident Wave steepness range (H_i/L_i)	**Transmission Coefficient range (Kt)**	**Transmission Coefficient range (Kt)**	**Transmission Coefficient range (Kt)**
0.010-0.030	0.45-0.27	0.54-0.42	0.69-0.43
0.030-0.040	0.27-0.22	0.42-0.37	0.43-0.37

Therefore, it can be concluded that the influence of incident wave steepness on wave transmission reduces for the higher wave steepness values (H_i/L_i>0.030).

Results of the experiments also coincides with the idea suggested by Suh (2011) which indicates that for lower wave steepness values, pile breakwaters become ineffective to block waves resulting in larger wave transmission.

Rao et al. (1999) states that this reduction trend of K_t with increasing H_i/L_i as seen in this study, can be explained with the water particle motions. When wave steepness increases, velocity and the acceleration of a particle increase. Accordingly, an obstacle like piled type breakwater can cause a dramatic change in velocity and acceleration. This rapid change results in energy dissipation due to turbulence. Due to dissipated energy, transmission through the breakwater (K_t) decreases.

Also, the range of data is shown with upper and lower confidence interval lines on the charts. Accordingly, the studies of Rao et al. (1999) are given in (Appendix C) to show the scattering of data in similar experimental researches.

The results of Case-1, 2 and 3 were also tabulated and plotted as transmission coefficient (K_t) vs deep water wave steepness (H_0/L_0) and given (Appendix D). Similarly, the trend of decreasing K_t with increasing H_i/L_i is observed for the deep water wave steepness values.

4.4.2 Spacing between the piles (b):

To investigate the influence of spacing between piles, for the Cases-1, 2 and 3, where the pile spacing were changed as 20cm, 30cm and 40cm respectively, H_i/L_i vs K_t were presented in Table 4.5 and plotted in Figure 4.5 with relative spacing between piles as design parameter (b/D; where D: pile diameter).

Table 4.5: Wave steepness and corresponding transmission coefficients for Case-1, 2 and 3

	Case-1 b=20cm	**Case-2 b=30cm**	**Case-3 b=40cm**
(H_i/L_i)	**K_t**	**K_t**	**K_t**
0.010	0.45	0.54	0.69
0.015	0.39	0.51	0.61
0.020	0.34	0.48	0.53
0.025	0.30	0.45	0.47
0.030	0.27	0.42	0.43
0.035	0.24	0.40	0.39
0.040	0.22	0.37	0.37
0.045	0.20	0.36	0.36
0.050	0.20	0.34	0.36

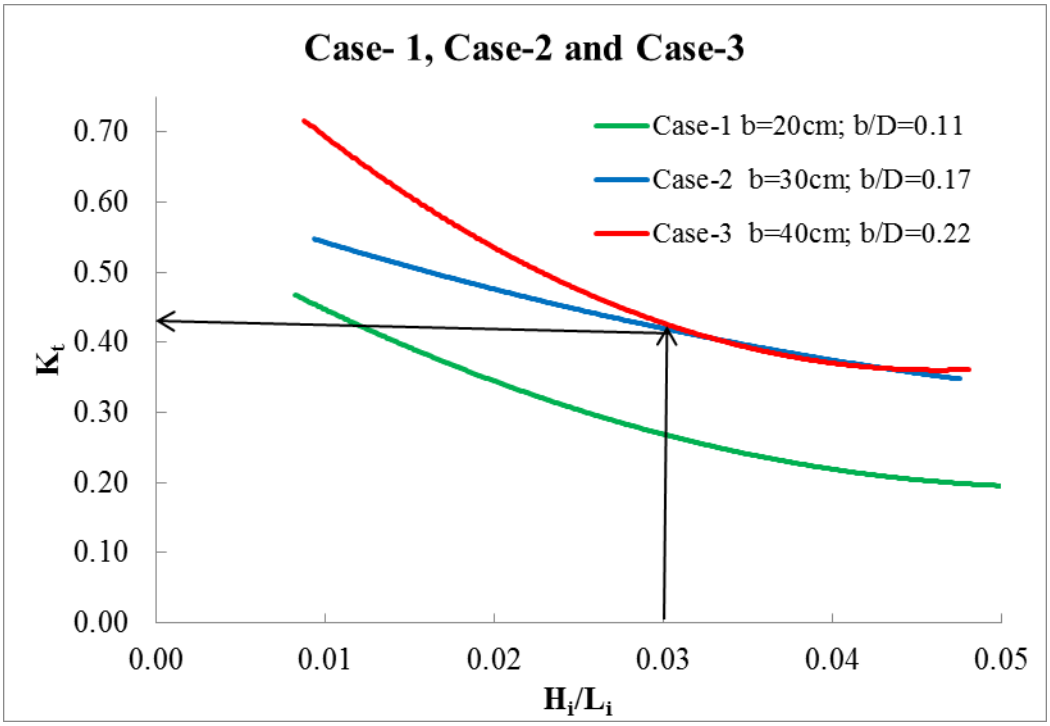

Figure 4.5 Comparison of Case 1, 2 and 3 with K_t vs H_i/L_i

As can be seen from the Figure 4.5, if the wave steepness is smaller than 0.03, the transmission coefficient values would increase consistently with increasing pile spacing (b). For example, when the H_i/L_i equals to 0.02, for Case-1 (b/D=0.11), Case-2 (b/D=0.17) and Case-3 (b/D=0.22), K_t is 0.34, 0.48 and 0.53 respectively reflecting the effect of pile spacing. Thus, it can be concluded that decreasing pile spacing results in decrease in wave transmission coefficients for lower wave steepness range (H_i/L_i<0.03) which is as expected that the smaller pile spacing means larger wave dissipation.

For the wave steepness range of 0.050>H_i/L_i>0.030, difference between the wave transmission coefficient values of Case-1 and Case-2 increase up to 40%, but transmission coefficient values of Case-2 and Case-3 overlap. The latter results can be stated as influence of pile spacing (b) reduces for larger pile spacing values in higher wave steepness range. This reasoning can be supported by the study of Hayashi (1968) which was focused on wave transmission through one-row piled

breakwater. For different d/L values, he presented his experimental results on charts as b/D vs K_t and plotted trendlines for specific incident wave steepness values (H_i/L_i). As given in the Figure 4.6 and 4.7, the closest parameter ranges in this research which can be used to support the results of present research are $0.1<d/L_i<0.2$; b/D=0.11-0.17-0.22 and $H_i/L_i=0.03$.

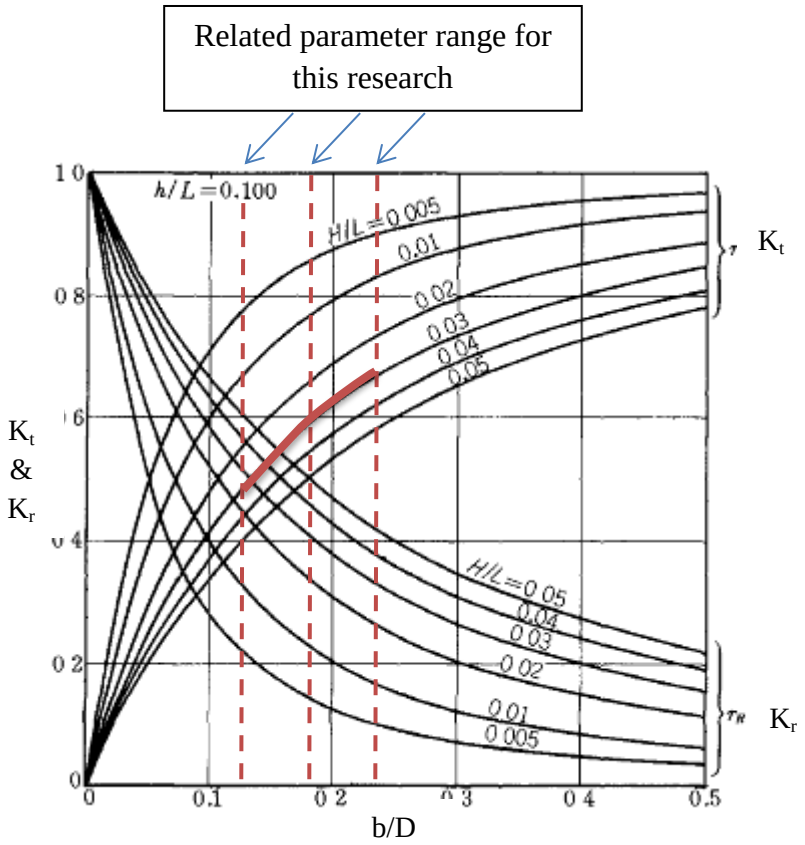

Figure 4.6 Coefficients of wave transmission vs relative pile spacing (K_t vs b/D) for d/L=0.1 Hayashi (1968)

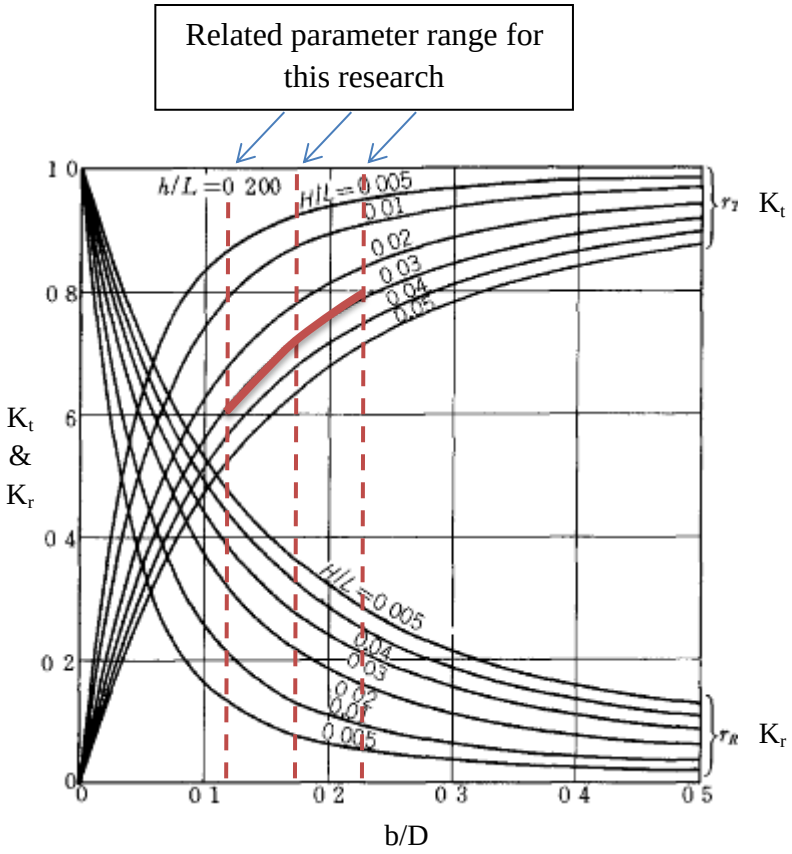

Figure 4.7 Coefficients of wave transmission vs relative pile spacing (K_t vs b/D) for d/L=0.2 Hayashi (1968)

As can be observed from the dashed lines on figures, for a constant incident wave steepness of H_i/L_i=0.03, as b/D value increases, the influence of b/D on K_t decreases. Although, Hayashi's (1968) study was implemented for one-row piled breakwater, the same trend can support the results of two-row piled breakwaters studies as in present study.

4.4.3 Wave approach angle (α):

Case 4, Case-5 and Case-6 were carried out to investigate the effect of wave approach angle on transmission coefficient where the wave approach angle is set to α=45° degree using the experimental setup of Case-1, 2 and 3 respectively. The results of the experiments are presented for approach angles, α equals to 45° and 90° using the cases that have same pile spacing (b). (Figures 4.8, 4.9 and 4.10)

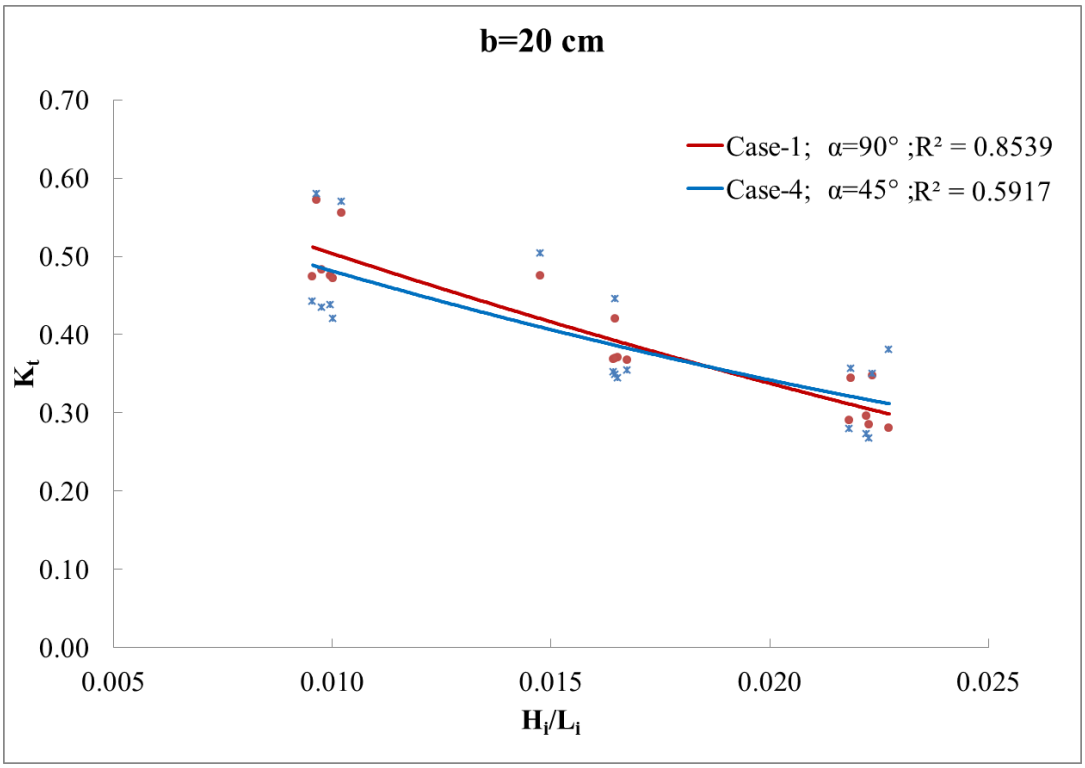

Figure 4.8 Comparison of Case-1 and Case-4 (b=20 cm, constant)

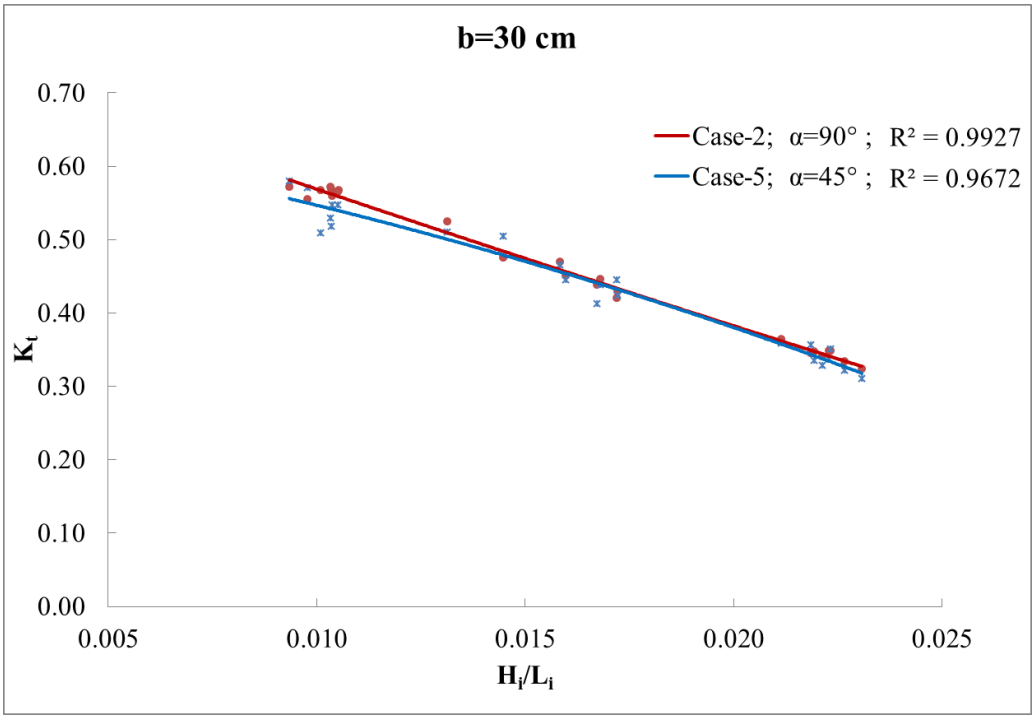

Figure 4.9 Comparison of Case-2 and Case-5 (b=30 cm, constant)

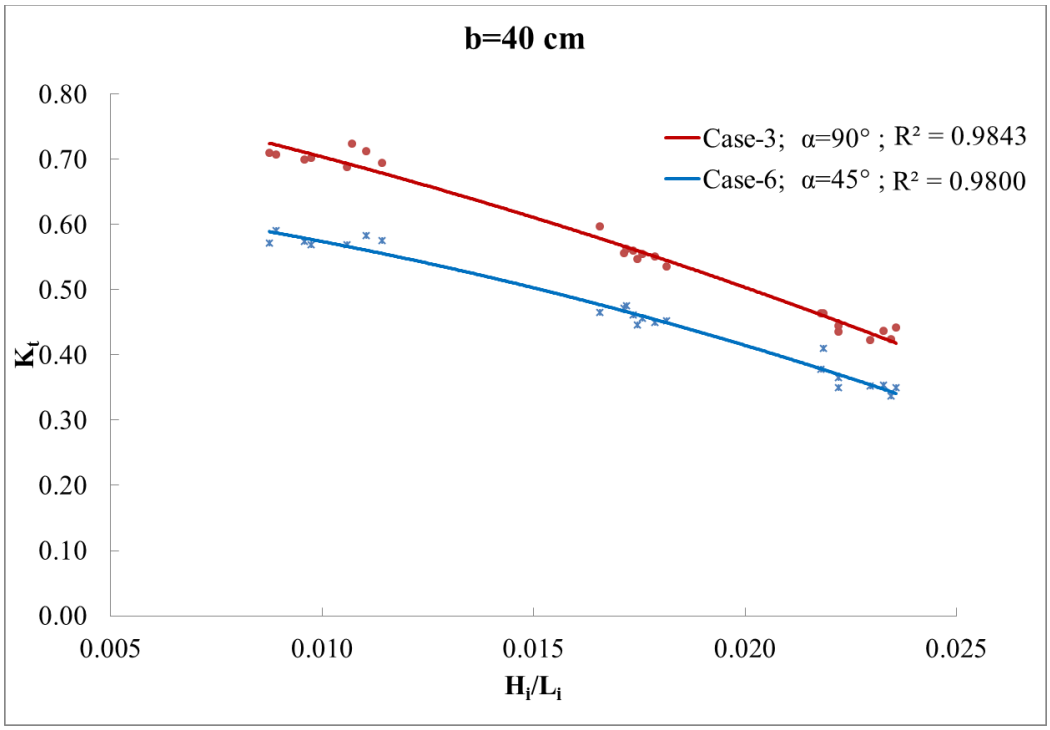

Figure 4.10 Comparison of Case-3 and Case-6 (b=constant)

As it is seen from Figures 4.8, 4.9 and 4.10, increasing wave steepness results in decreasing transmission coefficient for Case-4, 5 and 6 which is similar to the trend for Case-1, 2 and 3. Moreover, within the same wave steepness range (0.01-0.025), transmission coefficients for Case-1 (α=90°) and Case-4 (α=45°) and transmission coefficients of Case-2 (α=90°) and Case-5 (α=45°) almost overlap. In other words, when spacing between piles is 20 cm and 30 cm, different incident wave approach angles do not affect transmission coefficients significantly. On the other hand, transmission coefficients for Case-6 (α=45°) decreases by up to 25 % compared to Case-3 (α=90°).

For Case-4 (b=20cm) and Case-5 (b=30cm), decrease of wave approach angle to 45° does not reveal a remarkable change for the transmission phenomenon. The results for these two cases can be associated with the early studies of Wiegel (1969). Wiegel suggests that transmission coefficient is only related to a simple formula based on geometry of piles which is gap ratio. The formula is derived from the sketch given in Figure 4.11 and by Equation 4.1. (as cited in Herbich et al., 1990)

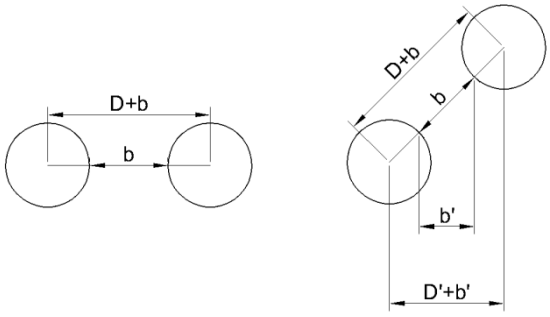

Figure 4.11 Wiegel's approach to the wave transmission phenemenna (Wiegel, 1969)

$$\frac{H_t}{H_i} = K_t \cong \frac{b}{D+b} \approx \frac{b'}{D'+b'} \tag{4.1}$$

where;

H_i: Incident wave height

H_t: Transmitted wave height

K_t: Transmission coefficient

D: Pile diameter

b: Pile spacing

Since the projection of the gap ratios did not change dramatically with the wave approach angle, the transmission coefficient would slightly change or does not change for different wave approach angles. Nevertheless, as seen from the comparison of Case-6 and Case-3 (b=40cm), decrease in transmission coefficients reaching up to 25 % can be reasoned with the argument that when the gap ratio is increased to a certain level, decreasing the wave approach angle would cause decrease in transmission coefficient in the same manner.

4.4.4 Distance between pile rows (B):

Case-7 (B=7m) and Case-8 (B=0m, single-row) were studied to investigate the effect of distance between two rows of piles on transmission coefficient. The results for both cases are presented including the results of Case-2 (B=12m) which have same pile spacing, b=30 cm and same wave approach angle, α=90°. The results are given in the Table 4.6 and plotted in Figure 4.12 as H_i/L_i vs K_t with corresponding distances between pile rows (B).

Table 4.6: Wave steepness and corresponding transmission coefficients for Case-2, 7 and 8

Wave Steepness (H_i/L_i)	Case-2 B=12m K_t	Case-7 B=7m K_t	Case-8 B=0m (single row) K_t
0.025	0.50	0.55	0.66
0.030	0.42	0.48	0.57
0.035	0.38	0.44	0.51
0.040	0.36	0.42	0.48
0.045	0.36	0.43	0.48

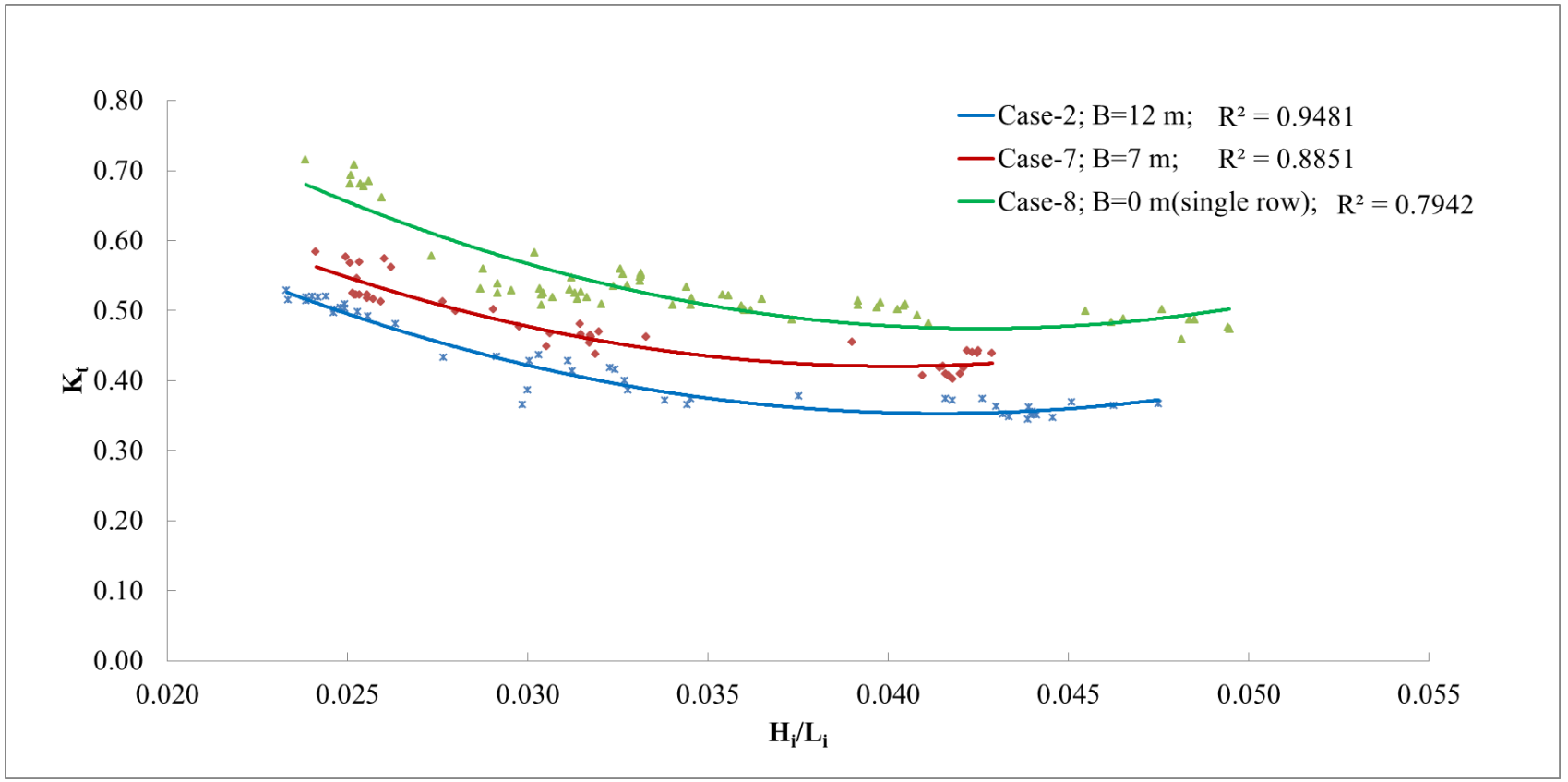

Figure 4.12: K_t vs H_i/L_i for Case-2, 7 and 8

As seen from Table 4.6, decreasing distance between rows results in increasing transmission through the breakwater up to 21% for B=7m, and 33% for B=0m (single row) with respect to B=12m. Also it can be concluded from the results that with double row piled breakwater, Case-7 (b/D=0.17 and B=7m=3.9D), wave transmission was decreased by up to 17% with respect to Case-8 (b/D=0.17 and B=0m) as single-row piled breakwater. These results are in agreement with the research of Herbich (1990). Herbich (1990) suggested that with the two row breakwater (with B=2D and b/D=0.20), wave transmission was reduced by 15% with respect to single row breakwater.

Furthermore, Figure 4.12 pointed out the fact that, transmission through piled breakwater increases with decreasing distance between rows. It can be explained by the fact that increasing distance between pile rows leads to more energy dissipation between rows and consequently lower transmission coefficient values. Rao et al. (1999) explains this phenomenon with energy dissipation due to eddy loses between piles. Waves facing with the obstruction losses a part of their energy by reflecting, remaining energy will partially dissipate due to eddy losses, and then transmitted through the protected area. He stated that "for two rows of piled breakwaters with lower B, before eddies due to first row completely formed, the second row of piles interferes and consequently less energy dissipation and large transmission occurs." As B increases, turbulence between the pile rows increases and transmission reduces. This discussion strongly supports the results of the present study.

4.5 Comparison of Theoretical and Experimental Results:

Experimental results are explained in the previous subsections. In this subsection, theoretical results and the experimental results are compared for cases of double-row pile breakwater (Case-1, 2 and 3) and the case of single-row pile breakwater (Case-8).

Single-Row Pile Breakwater:

Since the current theoretical approach was derived for the single row piled breakwater, theoretical values of transmission coefficient for single row case (Case-8) are predicted using the Hayashi's (1968) solution to investigate the agreement of the experimental results with the literature.

$$\frac{H_t}{H_i} = 4\left(\frac{d}{H_i}\right)E\left[-E+\sqrt{E^2+\frac{H_i}{2d}}\right] \tag{4.2}$$

$$E = \frac{C\left(\frac{b}{D+b}\right)}{\sqrt{1-\left(\frac{b}{D+b}\right)^2}} \tag{4.3}$$

where;

D: Pile diameter

b: Pile spacing

d: Water depth

H_i: Incident wave height

H_t: Transmitted wave height

C: Constant

Hayashi's (1968) approach to the wave transmission phenomenon is explained in the previous chapter. Following Hayashi's solution to predict transmission coefficients, the calculated and the predicted values of Kt are presented in the Figure 4.13, for single row piled breakwater (Case-8).

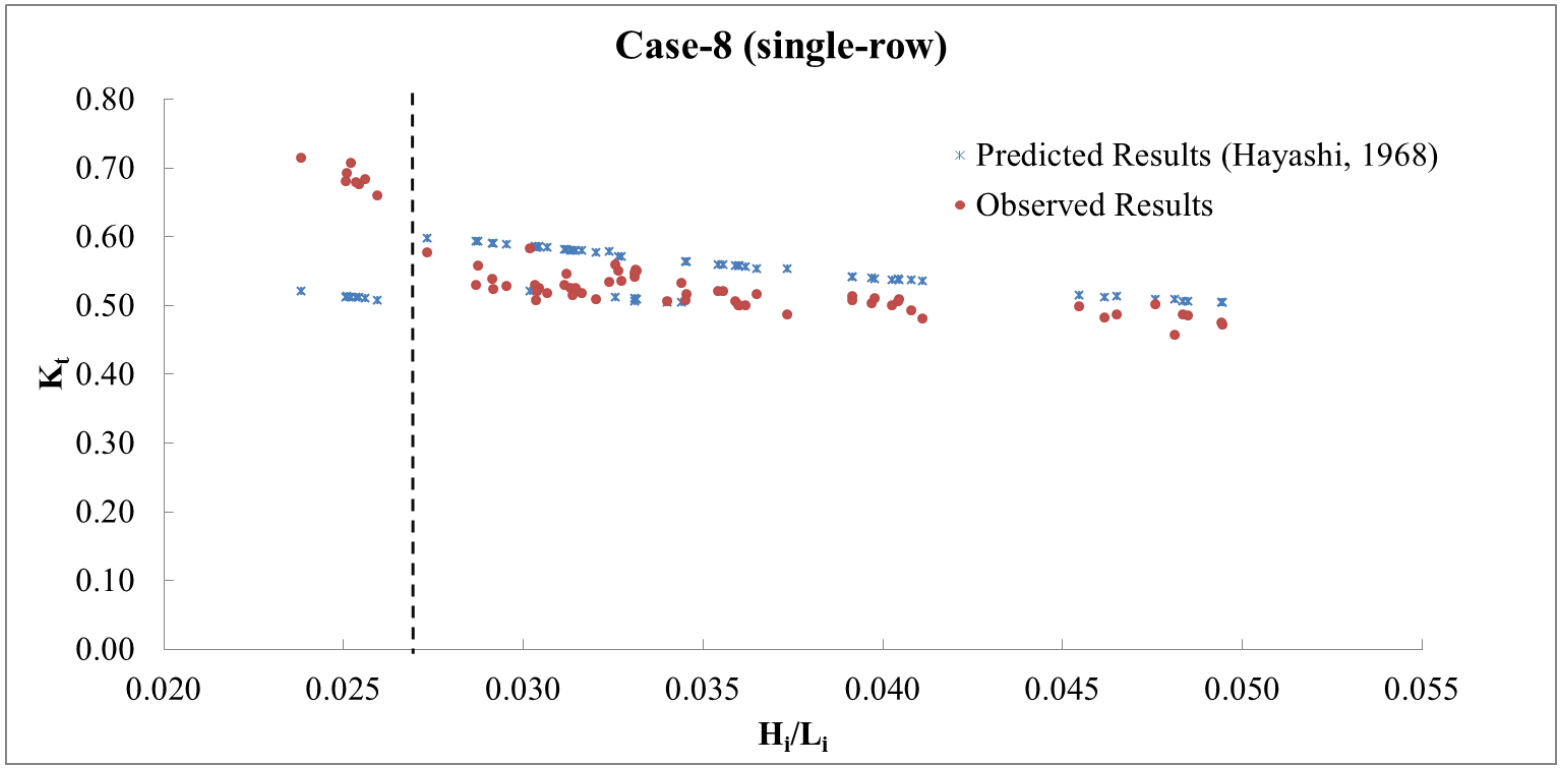

Figure 4.13: Observed and Predicted K_t values vs H_i/L_i (Case-8 single-row)

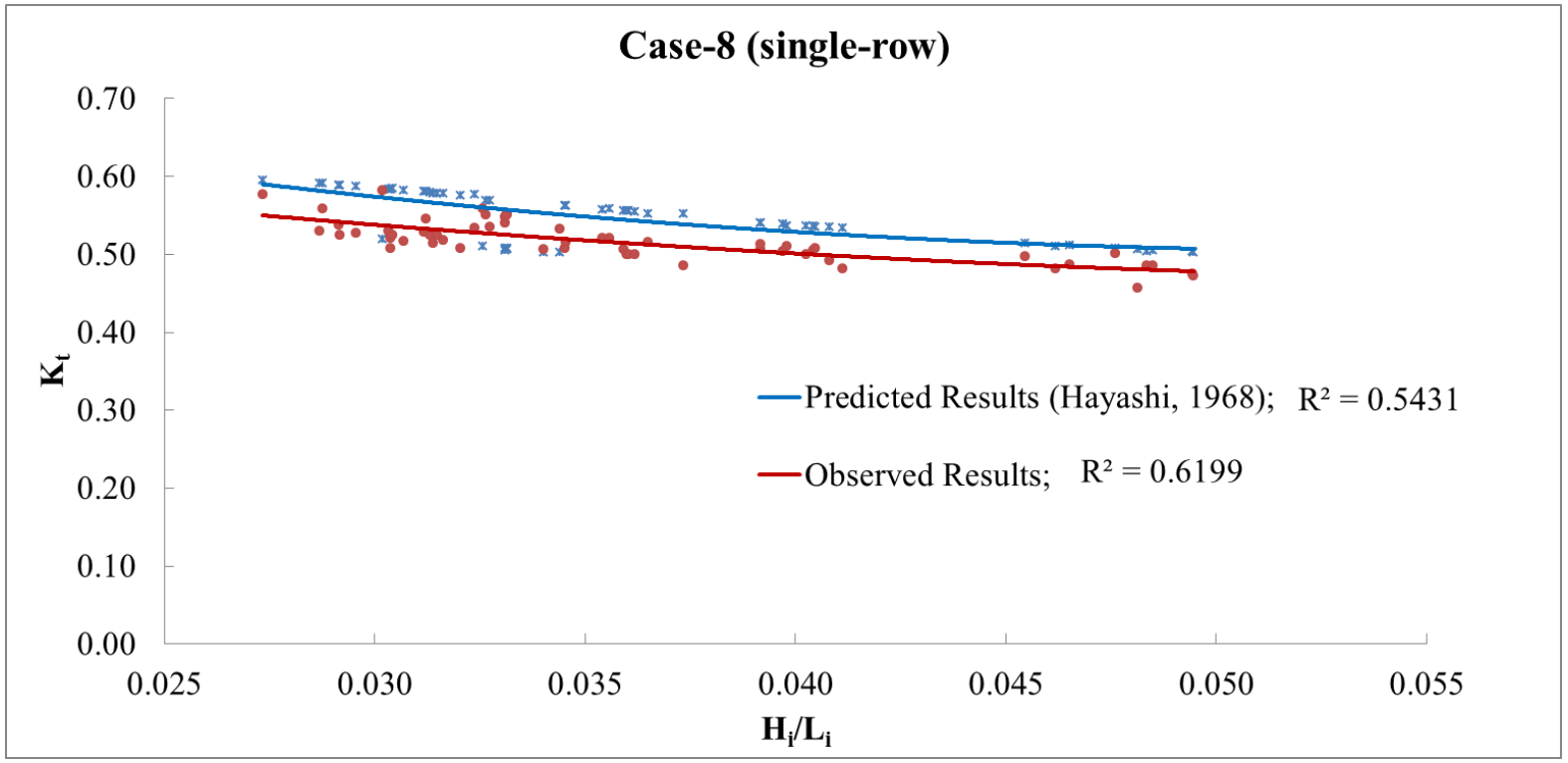

Figure 4.14: Observed and Predicted K_t values vs H_i/L_i with trendline

(Case-8 single-row)

For lower wave steepness ranges (H_i/L_i<0.027; left side of the dashed line on Figure 4.13), observed and predicted values of K_t differ up to 25%. Suh et al. (2010) explains this argument with the fact that in literature, not all numerical solutions for wave transmission studies are successful for lower wave steepness. The solutions predict large reflection and small transmission coefficients compared to the experimental results. Therefore, the trends for the higher steepness rates cannot be extended to the lower wave steepness ranges, where in the present study, this range is partially covered. Thus lower steepness ranges require further investigation. Accordingly, Figure 4.14 is plotted with trendline for higher steepness. For the incident wave steepness higher than 0.027, it can be interpreted from the Figure 4.14 that the test results for Case-8 and the predicted results with Hayashi's (1968) formula are in agreement.

Double-Row Pile Breakwater:

Furthermore, as explained in the Chapter-3, for Case-1, 2 and 3, transmission coefficients were predicted with the formulas derived for two-row piled breakwater and comparison of calculated and predicted K_t values are presented in Figures 4.16, 4.17 and 4.18. As shown in the following sketch, the transmitted wave from the first row was accepted as the incident wave for the second row and the solution was repeated for the second row to reach the transmitted wave from the second row.

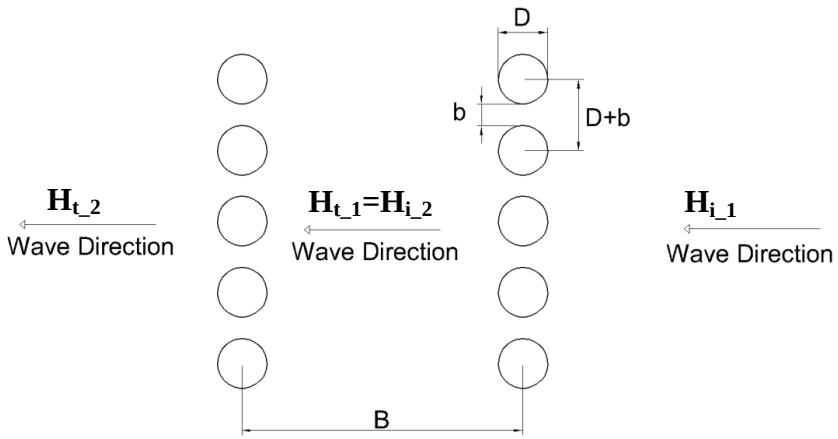

Figure 4.15: Double row pile breakwater

Accordingly the results were predicted with the following formulas:

$$\frac{H_{t\_1}}{H_{i\_1}} = 4\left(\frac{d}{H_{i\_1}}\right)E\left[-E+\sqrt{E^2+\frac{H_{i\_1}}{2d}}\right] \tag{3.12}$$

$$H_{t\_1} = H_{i\_2} \tag{3.13}$$

$$\frac{H_{t\_2}}{H_{i\_2}} = 4\left(\frac{d}{H_{i\_2}}\right)E\left[-E+\sqrt{E^2+\frac{H_{i\_2}}{2d}}\right] \tag{3.14}$$

$$E = \frac{C\left(\frac{b}{D+b}\right)}{\sqrt{1-\left(\frac{b}{D+b}\right)^2}} \tag{3.15}$$

$$K_t = \frac{H_{t\_2}}{H_{i\_1}} \tag{3.16}$$

where;

H_{i_1}: Height of the wave incident to the 1st row

H_{i_2}: Height of the wave incident to the 2nd row

H_{t_1}: Height of the wave transmitted from the 1st row

H_{t_2}: Height of the wave transmitted from the 2nd row

D: Pile diameter

b: Pile spacing

d: Water depth

C: Constant

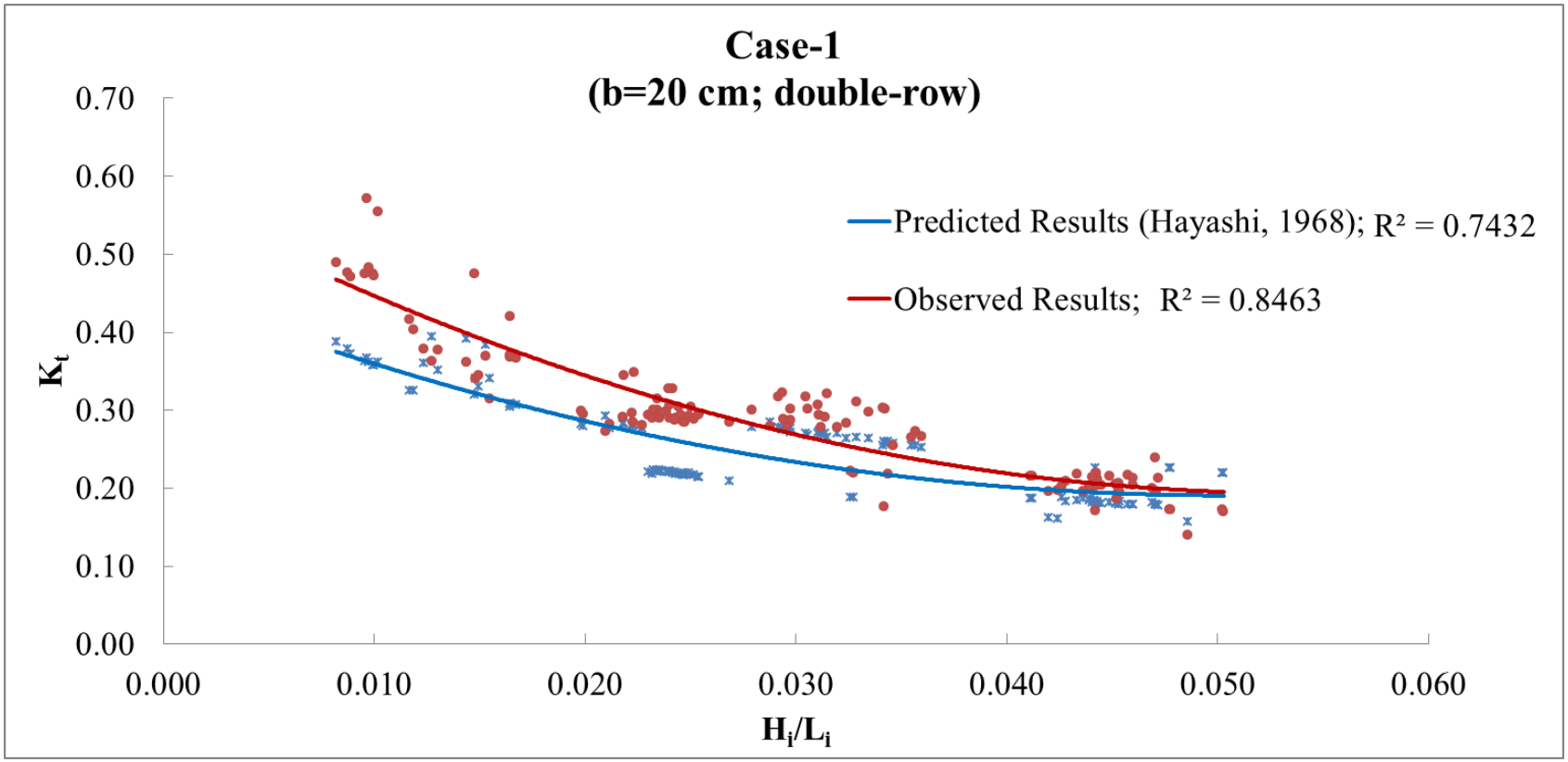

Figure 4.16: Observed and Predicted K_t values vs H_i/L_i (Case-1;b=20cm; double-row)

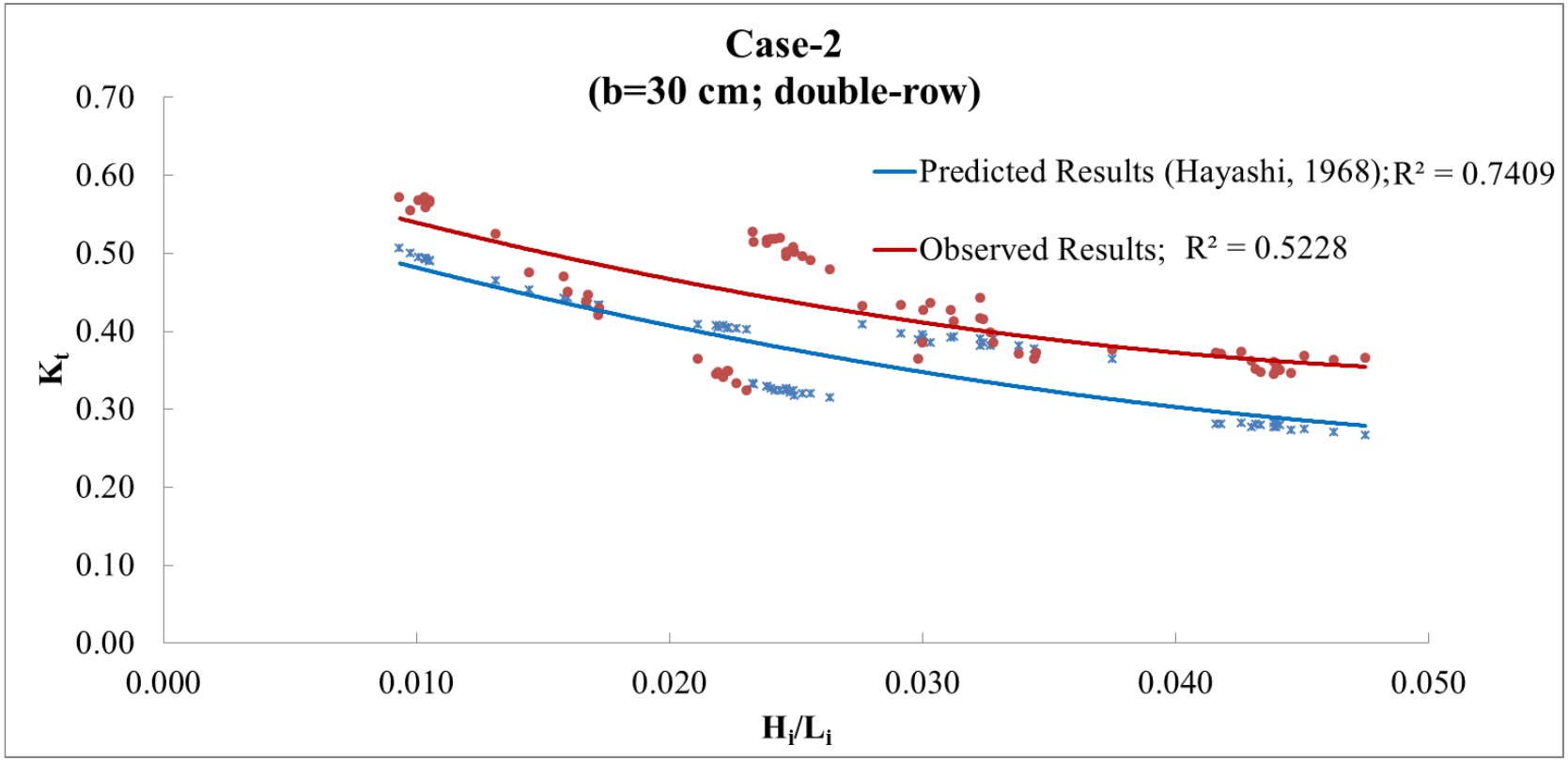

Figure 4.17: Observed and Predicted K_t values vs H_i/L_i (Case-2; b=30cm; double-row)

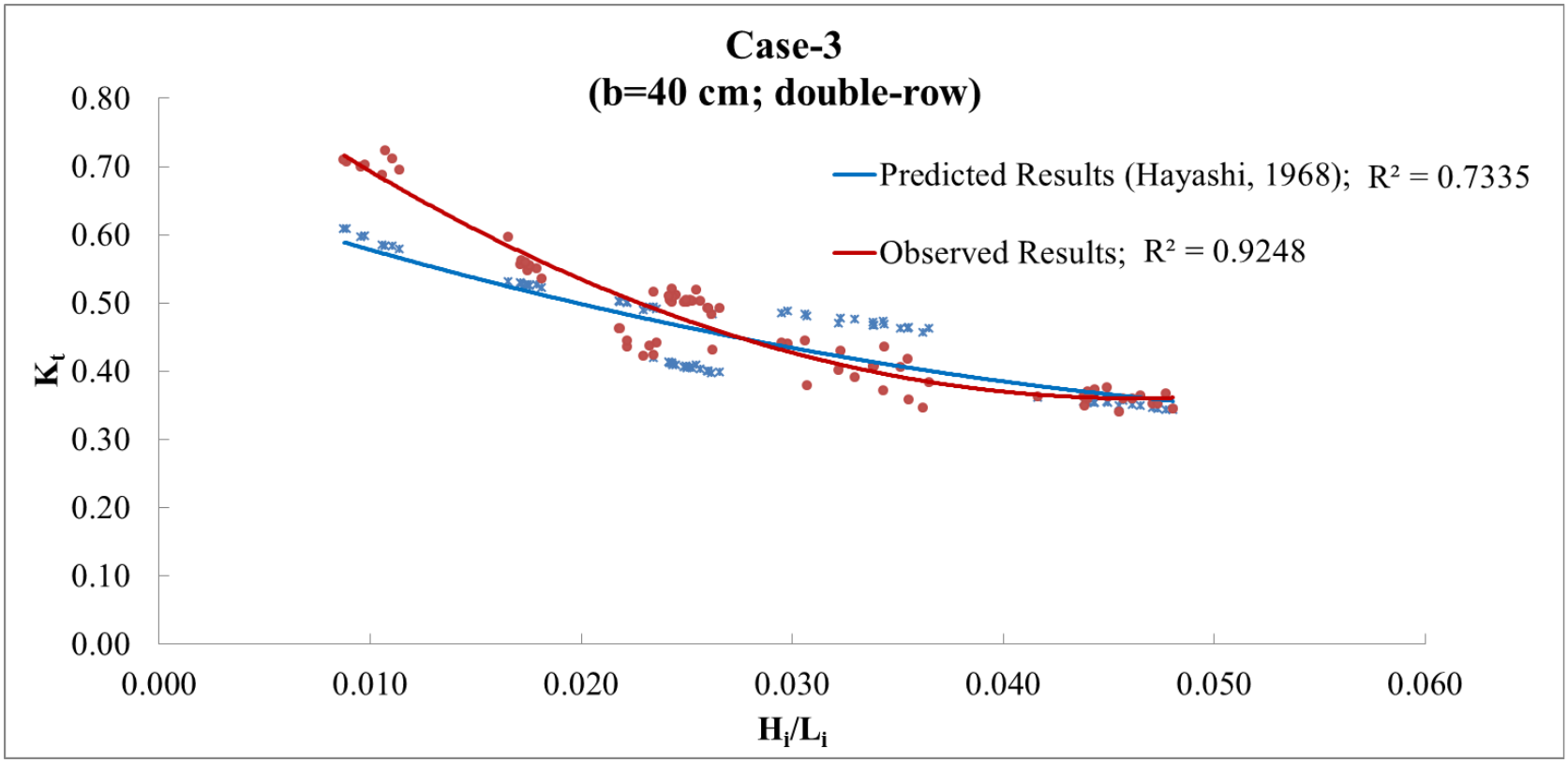

Figure 4.18: Observed and Predicted K_t values vs H_i/L_i (Case-3; b=40cm; double-row)

Theoretical curves for Case-1 and Case-3 are in good agreement with the experimental test results for incident wave steepness higher than 0.025. For wave steepness lower than 0.025 the trend for Case-8 (single row) continues. On the other hand, the theoretical curve for Case-2 is below with an acceptable range from the curve of observed experimental results. (10%-20%)

CHAPTER 5

CONCLUSION AND FUTURE RECOMMENDATION

In the present study, wave transmission through pile breakwaters were examined with model studies for different setup cases. Model studies were conducted with regular waves in the Coastal and Ocean Engineering Laboratory, Civil Engineering Department, Middle East Technical University. Aim of the studies is to understand the how the transmission through pile breakwaters changes with respect to:

- Incident wave approach angles (α),
- Spacing between piles (b),
- Incident wave steepness (H_i/L_i),
- Distances between rows (B)

In total, 390 laboratory experiments were carried out in three different flumes which are constructed in two basins with eight cases of setup. Considering present research, following conclusions can be derived:

- Transmission coefficient (K_t) decreases with increasing incident wave steepness (H_i/L_i). The influence of incident wave steepness (H_i/L_i) on wave transmission coefficient (K_t) reduces for the higher wave steepness ranges ($H_i/L_i>0.030$). Same trend of decreasing K_t with increasing H_i/L_i is also observed for the deep water wave steepness values (H_0/L_0).

- For lower wave steepness ($H_i/L_i<0.030$), the transmission coefficient values increase consistently with increasing pile spacing (b). However, in higher

wave steepness range (H_i/L_i>0.030), influence of pile spacing (b) on transmission coefficient reduces for larger pile spacing values.

- Within the same wave steepness range (0.01-0.025), for the cases with relative pile spacing of b/D=0.11 and b/D=0.17, decreasing incident wave approach angles (α=90° to α=45°) do not affect transmission coefficients significantly. However, for the relative pile spacing of b/D=0.22, decrease in transmission coefficients reaches up to 25 %. In other words, when the gap ratio is increased to a certain level, decreasing the wave approach angle would cause decrease in transmission coefficient in the same manner.

- Experimental studies are carried out for both single-row and double-row breakwaters. It is concluded that the double row breakwaters is more efficient to dissipate the wave energy and accordingly to decrease the wave transmission. Wave transmission rate through double-row pile breakwaters mainly depends on distance between pile rows (B).

- For the wave steepness range of 0.025<H_i/L_i<0.045, decreasing distance between rows results in increasing transmission coefficient (K_t) up to 21% for B=7m=6.7D, and 33% for B=0m (single-row) compared to B=12m. In other words, wave transmission through pile breakwater increases with decreasing distance between rows.

- Hayashi's (1968) solution for single row pile breakwaters is revised for double row pile breakwaters. For higher steepness ranges (H_i/L_i>0.03), experimental results for both single and double row pile breakwaters are in agreement with the theoretical results predicted using Hayashi's (1968) formula and the revised formula. However, for lower steepness ranges, the predicted results of the proposed formulas are not in good agreement with the experimental results.

Considering the experimental results and conclusions, following recommendations can shed light on the complex wave transmission phenomenon for pile breakwaters:

- Experiments can also be conducted with irregular waves to reflect the natural process reliably with wider range of wave characteristics.

- For the data analysis process, instead of selecting individual waves, the whole measured wave trains can be examined after a reflection analysis which is performed by means of spectral analysis (Goda, 2000).

- Experiments can be extended to cover wave approach angle (α) different than 90° and 45° with special emphasis on zero degree approach angle.

- In this study, three different spacing between piles (b) are examined. To understand the effect of pile spacing on wave transmission, additional model studies can be carried out by increasing the pile spacing range. Therefore, new charts can be plotted as pile spacing ratio to pile diameter (b/D) vs wave transmission coefficients (K_t).

- Effect of distance between rows (B) on wave transmission can be investigated further by utilizing different B values. Increased B range enables preparation of the new charts with relative distance between rows (B/L_i) vs transmission coefficients (K_t).

- Numerical solutions can be revised to focus on prediction of wave transmission coefficients in low ranges of wave steepness and influence of distance between rows (B).

- Data can be analysed with different curve fitting methodologies to increase coefficient of determination. Thus, interpretation of data may be done in a more efficient way considering the regions there are not data points measured.

REFERENCES

Ergin, A. (2009). *Coastal Engineering.* Ankara: METU Press

Goda, Y. (2000). Random seas and design of maritime structures. *Advanced series on ocean engineering*, **vol 15**, World Scientific, Singapore

Goda, Y. and Suzuki, Y. (1976). Estimation of incident and reflected waves in random wave experiments. *Proc. 15th Int. Conf. Coastal Engrg,* Hawaii

Hayashi, T., Hattori, M., Shirai, M. (1968). Closely spaced pile breakwater as a protection structure against beach erosion. *Coastal Engineering Proceedings, 1*(11)

Hayashi, T., Kano, T. (1966). Hydraulic research on the closely spaced pile breakwater. *Coastal Engineering Proceedings, 1*(10)

Herbich, J., Douglas, B. (1989). Wave transmission through a double-row pile breakwater. *Coastal Engineering Proceedings, 1*(21)

Herbich, J. B., Bretschneider, C. L. (1990). *Handbook of coastal and ocean engineering: Wave phenomena and coastal structures* Gulf Pub. Co; Butterworth-Heinemann, C/O Elsevier Science, Order Fulfillment, 11830 Westline Industrial Dr, Saint Louis, MO, 63146.

Hughes, S. A. (1993). *Physical models and laboratory techniques in coastal engineering*. Singapore; River Edge, NJ: World Scientific.

Isaacson, M., Premasiri, S., & Yang, G. (1998). Wave interactions with vertical slotted barrier. *Journal of Waterway, Port, Coastal and Ocean Engineering, 124*(3), 118-125.

Kakuno, S., & Liu, P. L. (1993). Scattering of water waves by vertical cylinders. *Journal of Waterway, Port, Coastal and Ocean Engineering,* (3), 302.

Koraim, A. S., Iskander, M. M., & Elsayed, W. R. (2014). Hydrodynamic performance of double rows of piles suspending horizontal c shaped bars. *Coastal Engineering, 84*(0), 81-96.

Kriebel, D., Bollmann, C. (2001). Wave transmission past vertical wave barriers. *Coastal Engineering Proceedings, 1*(25)

Kürüm, M. O., & Supervisor: Ergin, A. *An experimental study on the performance of box type floating breakwaters with screens [electronic resource]*.Ankara: METU; 2008.

Kyung-Duck Suh, Shin, S., & Cox, D. T. (2006). Hydrodynamic characteristics of pile-supported vertical wall breakwaters. *Journal of Waterway, Port, Coastal & Ocean Engineering, 132*(2), 83-96

Le Méhauté, B. (1972). Progressive wave absorber. *Journal of Hydraulic Research/Journal De Recherches Hydraulique, 10*(2), 153.

Lean, G. H. (1967). A simplified theory of permeable wave absorbers. *Journal of Hydraulic Research/Journal De Recherches Hydraulique, 5*(1), 15.

Mani, J. S., & Jayakumar, S. (1995). Wave transmission by suspended pipe breakwater. *Journal of Waterway, Port, Coastal & Ocean Engineering, 121*(6), 335.

Ouellet, Y., & Datta, I. (1986). Survey of wave absorbers. *Journal of Hydraulic Research, 24*(4), 265-280.

Rao, S., Rao, N. B. S., & Sathyanarayana, V. S. (1999). Laboratory investigation on wave transmission through two rows of perforated hollow piles. *Ocean Engineering, 26*(7), 675-699.

Suh, K., Ji, C., & Kim, B. H. (2011). Closed-form solutions for wave reflection and transmission by vertical slotted barrier. *Coastal Engineering, 58*(12), 1089-1096. doi:10.1016/j.coastaleng.2011.06.001

Sundar, V., & Subbarao, B. V. V. (2003). Hydrodynamic performance characteristics of quadrant front-face pile-supported breakwater. *Journal of Waterway, Port, Coastal and Ocean Engineering, 129*(1), 22-33. doi: 10.1061/(ASCE)0733-950X(2003)129:1(22)

Takahashi, S. (1996). *Design of vertical breakwaters* Port and Harbour Research Institute.

Truitt, C., Herbich, J. (1987). Transmission of random waves through pile breakwaters. *Coastal Engineering Proceedings, 1*(20)

USACE (2003). *Coastal engineering manual [CEM]* Engineer Manual 1110-2-1100, US Army Corps of Engineers, CHL-ERDC, WES, Vicksburg, MS

APPENDIX A

PRELIMINARY EXPERIMENTS FOR WAVE GAUGE AND ABSORPTION SYSTEM SETUP

The most appropriate setup for the wave gauge and absorption system was decided after several experiments conducted in Coastal and Ocean Engineering Laboratory, Middle East Technical University. The main concern of these experiments was to eliminate undesired reflection from the measured data. The preliminary wave gauge and absorption system setups are given in Figure A.1- Figure A.7.

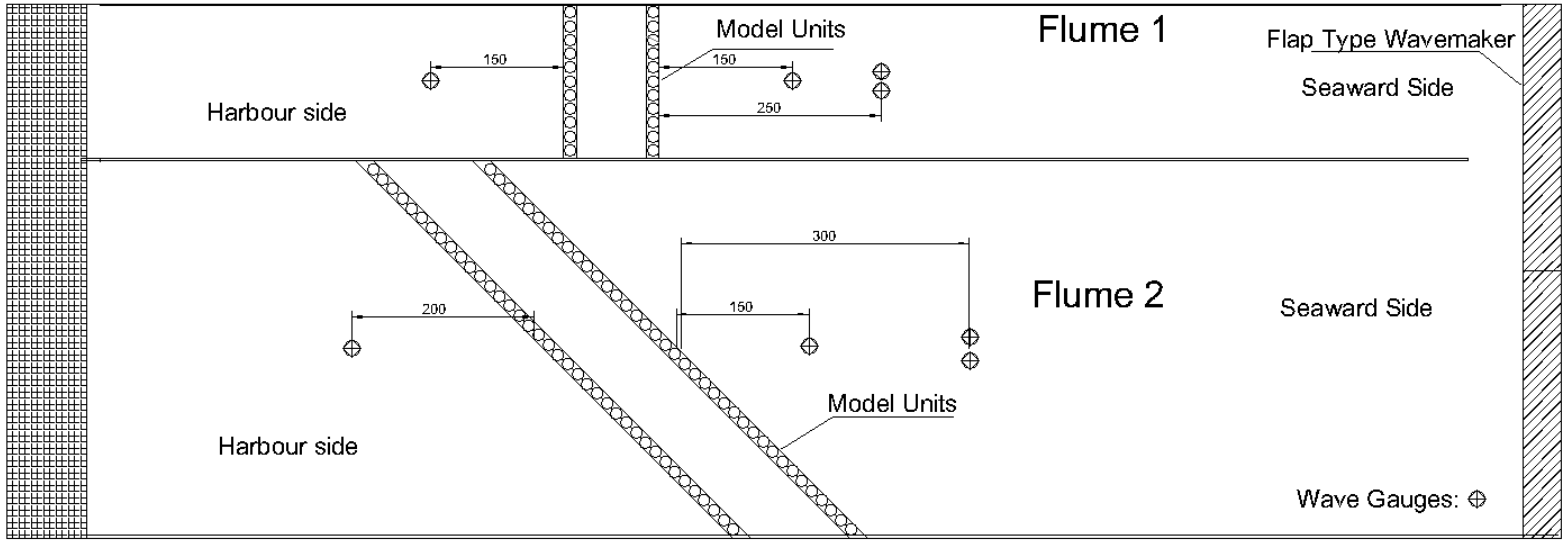

Figure A.1: Preliminary wave gauge and absorbtion system (1) of Basin-1

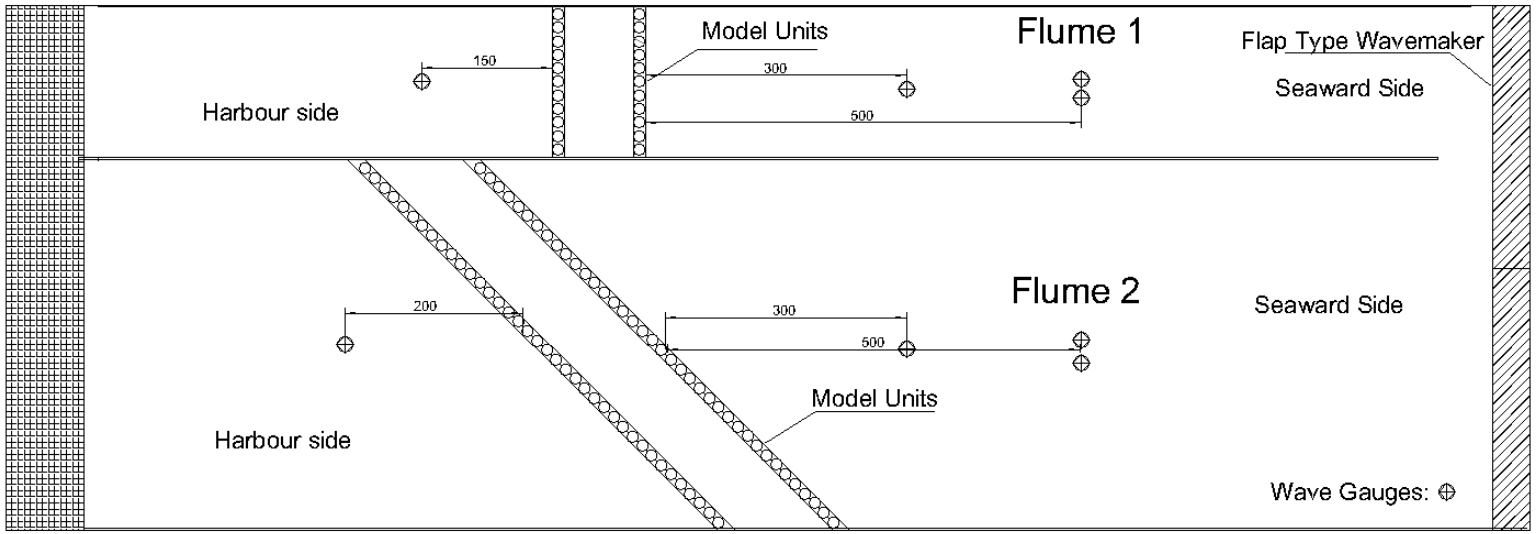

Figure A.2: Preliminary wave gauge and absorbtion system (2) of Basin-1

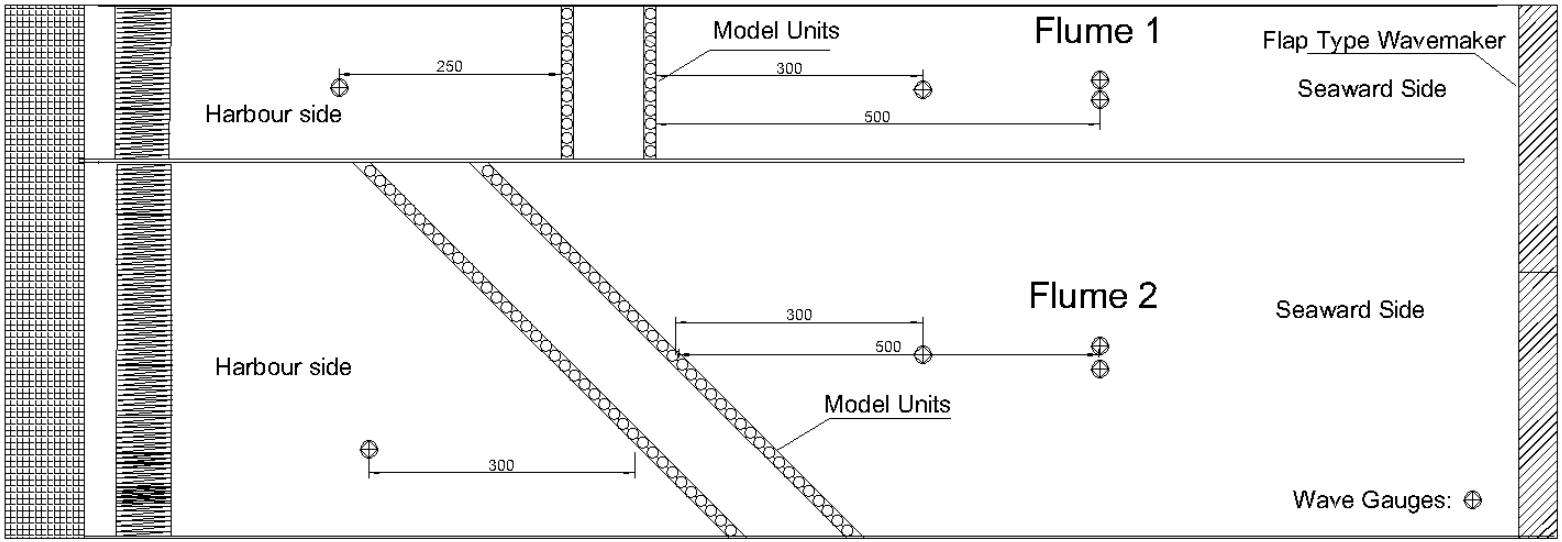

Figure A.3: Preliminary wave gauge and absorbtion system (3) of Basin-1

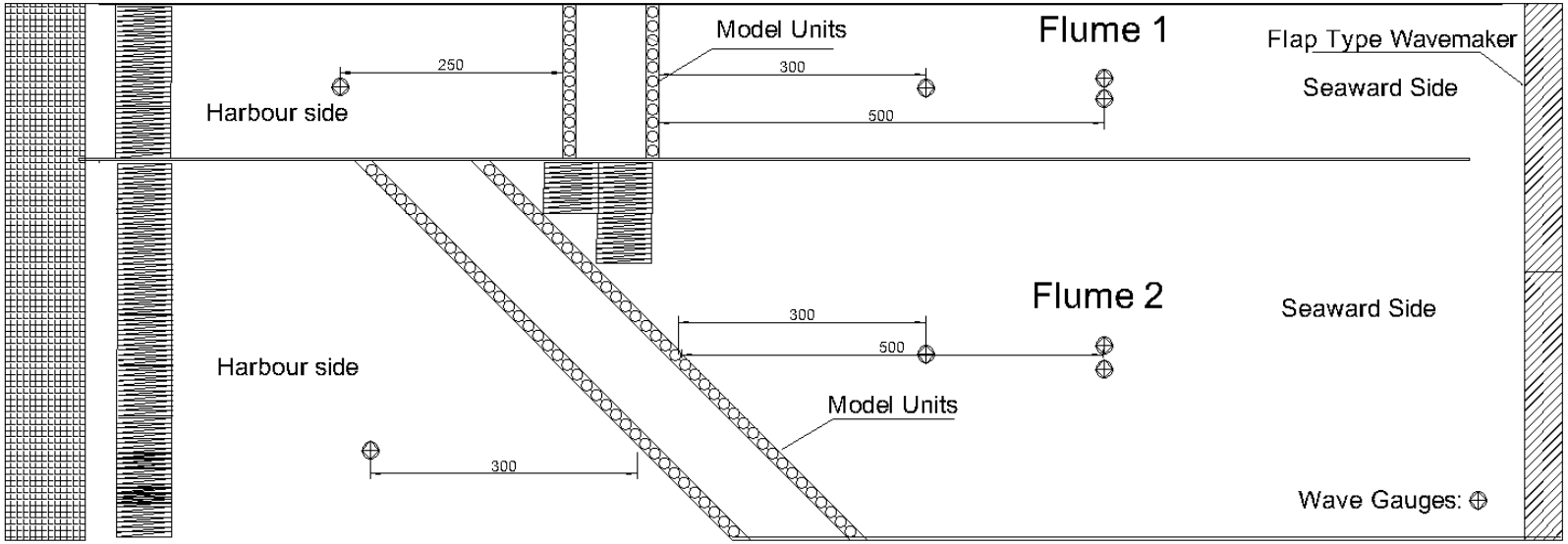

Figure A.4: Preliminary wave gauge and absorbtion system (4) of Basin-1

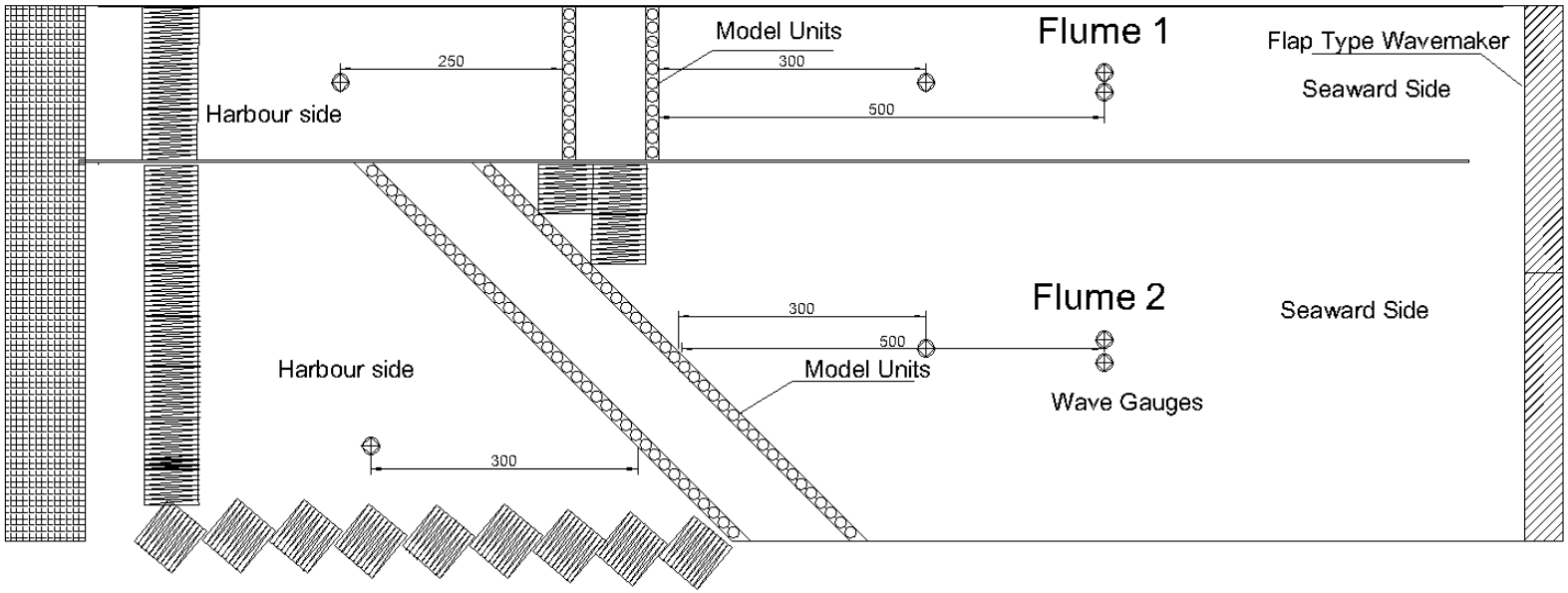

Figure A.5: Preliminary wave gauge and absorbtion system (5) of Basin-1

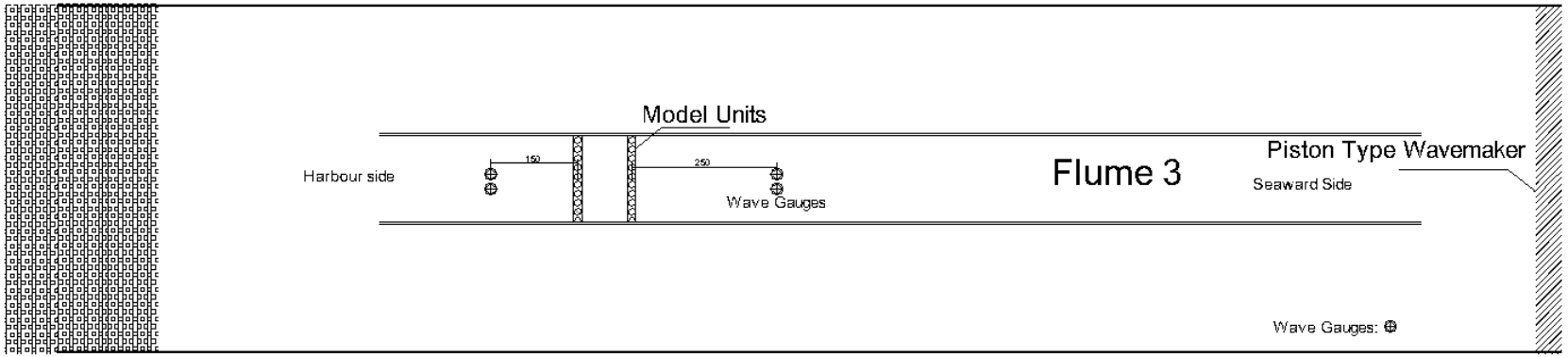

Figure A.6: Preliminary wave gauge and absorbtion system (1) of Basin-2

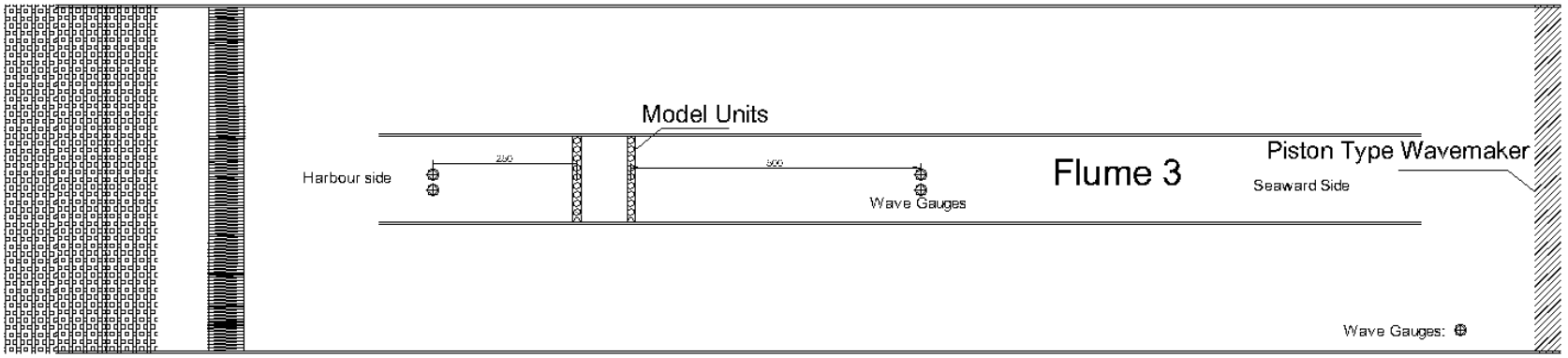

100

Figure A.7: Preliminary wave gauge and absorbtion system (2) of Basin-2

APPENDIX B

MEASURED AND CALCULATED DATA OF THE MODEL CASES

For each experiment, incident wave heights, wave periods and transmitted wave heights were measured. Wave lengths, wave steepness and transmission coefficients were calculated accordingly, and tabulated. (Table B.1- Table B.8)

Table B.1: Measured and calculated data of Case-1

CASE-1 (b=20cm, α=90°, B=12m)					
Measured			Calculated		
Wave Period (T_m) (sec)	Incident Wave Height (H_i) (m)	Transmitted Wave Height (H_t) (m)	Incident Wave Length (L_i) (m)	Incident Wave Steepness (H_i/L_i)	Transmission Coefficient (K_t)
7.5	1.4	0.4	62.0	0.023	0.28
7.5	1.4	0.4	62.4	0.022	0.29
8.2	1.2	0.4	69.2	0.017	0.37
8.2	1.1	0.4	69.4	0.017	0.37
9.9	0.9	0.4	85.8	0.010	0.48
9.9	0.9	0.4	85.8	0.010	0.47
7.5	1.4	0.4	61.7	0.022	0.30
7.5	1.4	0.4	62.3	0.022	0.28
8.3	1.2	0.4	70.3	0.016	0.37
8.3	1.2	0.4	69.9	0.016	0.37
9.9	0.8	0.4	86.1	0.010	0.48
10.0	0.8	0.4	87.3	0.010	0.47
7.4	1.4	0.5	61.2	0.022	0.35
7.5	1.4	0.5	61.9	0.022	0.34
8.4	1.2	0.5	71.8	0.016	0.42
8.5	1.1	0.5	72.3	0.015	0.48
9.5	0.8	0.5	82.3	0.010	0.56

Table B.1 (continued): Measured and calculated data of Case-1

Measured			Calculated		
Wave Period (T_m) (sec)	Incident Wave Height (H_i) (m)	Transmitted Wave Height (H_t) (m)	Incident Wave Length (L_i) (m)	Incident Wave Steepness (H_i/L_i)	Transmission Coefficient (K_t)
9.7	0.8	0.5	84.6	0.010	0.57
6.0	1.6	0.3	46.2	0.034	0.22
6.0	1.6	0.3	46.2	0.034	0.18
6.0	2.0	0.4	46.2	0.044	0.17
5.7	2.0	0.4	42.8	0.048	0.17
5.7	2.0	0.4	42.9	0.048	0.17
9.7	0.8	0.5	84.6	0.010	0.57
6.0	1.6	0.3	46.2	0.034	0.22
6.0	1.6	0.3	46.2	0.034	0.18
6.0	2.0	0.4	46.2	0.044	0.17
5.7	2.0	0.4	42.8	0.048	0.17
5.7	2.0	0.4	42.9	0.048	0.17
9.7	0.8	0.5	84.6	0.010	0.57
9.9	3.6	0.7	85.8	0.042	0.20
9.9	3.6	0.7	85.9	0.042	0.20
5.7	2.2	0.4	42.8	0.050	0.17
5.7	2.1	0.4	42.8	0.050	0.17
9.1	3.8	0.5	77.8	0.049	0.14
9.8	2.8	0.6	85.7	0.033	0.22
9.8	2.8	0.6	85.7	0.033	0.22
6.0	1.5	0.4	46.0	0.032	0.28
6.3	1.5	0.5	49.2	0.031	0.30
6.1	1.4	0.4	47.9	0.029	0.32
6.8	0.7	0.3	55.1	0.013	0.36
7.8	3.1	0.6	65.1	0.047	0.20
7.9	2.9	0.6	66.4	0.044	0.20
8.2	2.8	0.6	69.1	0.041	0.22
8.0	1.4	0.4	66.8	0.021	0.28
10.5	2.1	0.6	92.4	0.023	0.29
10.1	2.2	0.6	88.4	0.025	0.28
10.1	2.2	0.6	88.6	0.025	0.29
10.0	1.0	0.4	87.1	0.012	0.40
6.3	0.7	0.3	49.4	0.014	0.36
6.2	0.7	0.3	48.3	0.015	0.37
7.6	0.9	0.3	63.6	0.015	0.34
7.4	0.9	0.3	60.9	0.015	0.31
8.2	1.4	0.4	69.3	0.020	0.30
8.1	1.4	0.4	68.7	0.020	0.30
8.1	0.9	0.3	68.0	0.013	0.38

Table B.1 (continued): Measured and calculated data of Case-1

Measured			Calculated		
Wave Period (T_m) (sec)	Incident Wave Height (H_i) (m)	Transmitted Wave Height (H_t) (m)	Incident Wave Length (L_i) (m)	Incident Wave Steepness (H_i/L_i)	Transmission Coefficient (K_t)
8.1	0.8	0.3	68.3	0.012	0.38
10.1	1.0	0.4	88.6	0.012	0.42
10.1	0.7	0.4	88.2	0.008	0.49
10.0	0.8	0.4	87.0	0.009	0.48
6.1	1.4	0.4	47.6	0.030	0.28
7.8	2.8	0.6	64.9	0.044	0.20
8.1	2.9	0.6	68.4	0.043	0.21
10.7	2.2	0.6	93.6	0.023	0.29
7.3	1.3	0.3	60.5	0.021	0.27
8.0	1.0	0.3	67.4	0.015	0.35
10.2	0.8	0.4	88.7	0.009	0.47
6.0	1.5	0.5	46.1	0.033	0.30
6.2	1.5	0.5	48.3	0.030	0.32
6.1	1.6	0.5	47.1	0.034	0.30
8.0	3.1	0.7	67.0	0.046	0.22
8.2	2.8	0.6	69.1	0.041	0.22
7.6	3.0	0.6	63.5	0.047	0.20
9.9	2.2	0.6	86.4	0.025	0.29
10.2	2.1	0.7	88.9	0.024	0.33
10.1	2.1	0.7	88.3	0.024	0.33
6.0	1.6	0.4	46.8	0.035	0.25
6.3	1.5	0.4	49.4	0.030	0.29
6.2	1.4	0.4	48.6	0.029	0.29
7.8	2.9	0.6	65.4	0.044	0.21
8.0	3.0	0.6	67.4	0.044	0.20
7.7	2.9	0.6	64.5	0.045	0.19
7.9	3.0	0.6	65.8	0.045	0.19
10.0	2.1	0.6	87.4	0.024	0.29
10.2	2.2	0.6	89.2	0.024	0.29
10.2	2.1	0.6	89.3	0.024	0.30
6.2	1.5	0.5	48.5	0.031	0.32
6.0	1.5	0.4	46.7	0.031	0.29
6.1	1.5	0.4	47.2	0.031	0.29
8.0	3.0	0.6	66.9	0.045	0.21
7.7	3.0	0.7	64.5	0.047	0.24
7.9	3.0	0.6	66.0	0.045	0.22
10.0	2.1	0.6	87.0	0.025	0.28
10.3	2.1	0.7	90.2	0.023	0.31
10.3	2.1	0.6	90.0	0.023	0.30

Table B.1 (continued): Measured and calculated data of Case-1

Measured			Calculated		
Wave Period (T_m) (sec)	Incident Wave Height (H_i) (m)	Transmitted Wave Height (H_t) (m)	Incident Wave Length (L_i) (m)	Incident Wave Steepness (H_i/L_i)	Transmission Coefficient (K_t)
6.1	1.4	0.4	47.4	0.030	0.30
6.3	1.4	0.4	49.9	0.028	0.30
6.0	1.3	0.4	46.3	0.029	0.28
8.0	3.0	0.6	67.3	0.045	0.20
7.7	2.8	0.6	64.6	0.044	0.20
7.9	2.8	0.6	66.0	0.043	0.20
10.2	2.1	0.6	89.1	0.024	0.30
10.0	2.1	0.6	87.6	0.024	0.29
10.1	2.1	0.6	88.1	0.024	0.29
6.1	1.5	0.4	47.5	0.031	0.28
6.2	1.4	0.5	48.6	0.029	0.32
6.1	1.5	0.5	47.6	0.031	0.31
8.1	3.0	0.7	68.4	0.044	0.22
7.9	2.9	0.6	66.6	0.044	0.21
8.0	2.9	0.6	66.9	0.043	0.22
10.0	2.2	0.6	87.4	0.025	0.29
10.0	2.2	0.7	87.4	0.025	0.30
10.1	2.2	0.7	88.2	0.025	0.29
6.2	1.6	0.5	48.2	0.034	0.30
6.0	1.5	0.5	46.6	0.033	0.31
6.0	1.6	0.4	46.0	0.036	0.27
7.9	3.0	0.6	66.1	0.046	0.21
8.0	3.0	0.6	67.1	0.044	0.21
7.8	3.1	0.7	65.3	0.047	0.21
10.2	2.2	0.7	88.9	0.024	0.30
9.9	2.3	0.7	86.5	0.027	0.29
10.1	2.1	0.7	88.6	0.024	0.31
6.0	1.7	0.4	46.5	0.036	0.27
6.0	1.6	0.4	46.5	0.035	0.26
6.1	1.5	0.4	47.7	0.032	0.28
8.1	3.0	0.6	67.8	0.044	0.20
7.9	3.0	0.6	66.4	0.045	0.21
7.9	3.1	0.6	66.5	0.046	0.20
10.1	2.2	0.7	88.5	0.025	0.29
10.2	2.1	0.6	89.3	0.023	0.30
10.1	2.2	0.6	88.2	0.025	0.29

Table B.2: Measured and calculated data of Case-2

CASE-2 (b=30cm, α=90°, B=12m)					
Measured			**Calculated**		
Wave Period (T_m) (sec)	Incident Wave Height (H_i) (m)	Transmitted Wave Height (H_t) (m)	Incident Wave Length (L_i) (m)	Incident Wave Steepness (H_i/L_i)	Transmission Coefficient (K_t)
7.4	1.4	0.5	61.3	0.022	0.35
7.5	1.4	0.5	61.8	0.022	0.34
8.1	1.2	0.5	68.7	0.017	0.42
8.6	1.1	0.5	73.6	0.014	0.48
9.9	0.8	0.5	85.9	0.010	0.56
10.0	0.8	0.5	87.3	0.009	0.57
7.6	1.3	0.5	63.5	0.021	0.36
7.5	1.4	0.5	62.0	0.022	0.35
7.5	1.4	0.5	62.5	0.022	0.35
8.9	1.0	0.5	76.6	0.013	0.52
8.2	1.2	0.5	69.4	0.017	0.45
8.4	1.1	0.5	70.8	0.016	0.47
9.7	0.9	0.5	83.9	0.011	0.57
9.7	0.9	0.5	84.0	0.010	0.57
9.8	0.9	0.5	85.2	0.010	0.57
7.4	1.4	0.5	61.1	0.023	0.33
7.4	1.4	0.5	61.2	0.022	0.34
7.3	1.4	0.5	60.3	0.023	0.32
8.2	1.2	0.5	69.1	0.017	0.44
8.1	1.2	0.5	68.5	0.017	0.43
8.3	1.1	0.5	70.4	0.016	0.45
9.6	0.9	0.5	83.3	0.011	0.56
9.7	0.9	0.5	83.8	0.010	0.57
9.6	0.9	0.5	83.5	0.010	0.56
6.2	1.6	0.7	48.1	0.032	0.44
5.9	1.7	0.6	45.6	0.038	0.38
6.4	1.5	0.7	50.3	0.030	0.44
7.9	3.2	1.2	66.4	0.048	0.37
7.9	3.1	1.1	66.2	0.046	0.36
8.1	3.0	1.0	67.9	0.045	0.35
10.0	2.2	1.1	87.1	0.026	0.49
10.1	2.2	1.1	87.8	0.025	0.50
10.4	2.3	1.1	90.6	0.025	0.50
6.0	1.6	0.6	46.1	0.034	0.36
5.9	1.5	0.6	45.8	0.032	0.42
6.1	1.6	0.6	47.6	0.033	0.40
7.9	3.0	1.1	66.2	0.045	0.37
7.9	2.8	1.0	66.0	0.043	0.35

Table B.2 (continued): Measured and calculated data of Case-2

Measured			Calculated		
Wave Period (T_m) (sec)	Incident Wave Height (H_i) (m)	Transmitted Wave Height (H_t) (m)	Incident Wave Length (L_i) (m)	Incident Wave Steepness (H_i/L_i)	Transmission Coefficient (K_t)
8.1	2.9	1.1	68.6	0.042	0.37
10.2	2.2	1.1	89.3	0.025	0.50
10.0	2.3	1.1	87.5	0.026	0.48
10.1	2.2	1.1	88.3	0.025	0.50
6.1	1.7	0.6	47.9	0.035	0.37
6.0	1.6	0.6	46.1	0.034	0.37
6.1	1.5	0.6	47.4	0.031	0.43
6.2	1.5	0.6	49.1	0.030	0.43
6.1	1.4	0.6	47.9	0.030	0.39
7.8	2.9	1.0	65.6	0.044	0.35
7.7	2.8	1.0	64.4	0.044	0.36
7.9	2.8	1.1	66.3	0.043	0.37
10.0	2.2	1.1	86.9	0.025	0.51
10.1	2.1	1.1	88.6	0.023	0.51
10.0	2.1	1.1	87.0	0.025	0.50
6.1	1.5	0.6	47.1	0.032	0.41
6.2	1.3	0.6	48.7	0.028	0.43
6.0	1.5	0.6	46.9	0.031	0.41
7.7	2.8	1.0	63.9	0.044	0.35
8.1	2.8	1.1	68.5	0.042	0.37
7.9	2.9	1.0	66.3	0.043	0.35
10.1	2.1	1.1	88.0	0.024	0.51
10.1	2.1	1.1	88.4	0.023	0.53
10.1	2.1	1.1	88.5	0.024	0.52
6.3	1.5	0.5	50.0	0.030	0.36
5.9	1.5	0.6	45.3	0.033	0.39
6.3	1.4	0.6	49.2	0.029	0.43
8.0	2.9	1.0	66.8	0.044	0.35
8.0	2.9	1.0	67.0	0.044	0.34
8.1	2.9	1.1	68.1	0.043	0.36
10.2	2.2	1.1	88.8	0.024	0.52
10.2	2.2	1.1	89.6	0.024	0.52
10.2	2.1	1.1	89.2	0.024	0.52

Table B.3: Measured and calculated data of Case-3

CASE-3 (b=40cm, α=90°, B=12m)					
Measured			**Calculated**		
Wave Period (T_m) (sec)	Incident Wave Height (H_i) (m)	Transmitted Wave Height (H_t) (m)	Incident Wave Length (L_i) (m)	Incident Wave Steepness (H_i/L_i)	Transmission Coefficient (K_t)
7.6	1.4	0.6	63.0	0.023	0.42
7.4	1.4	0.6	61.2	0.022	0.43
7.3	1.4	0.6	60.2	0.023	0.42
8.2	1.2	0.7	68.8	0.017	0.56
8.1	1.2	0.7	68.7	0.017	0.55
8.2	1.2	0.7	69.2	0.017	0.56
10.3	0.8	0.6	89.8	0.009	0.71
10.4	0.8	0.6	91.1	0.009	0.71
10.1	0.8	0.6	88.1	0.010	0.70
7.5	1.4	0.6	61.9	0.022	0.44
7.5	1.3	0.6	61.8	0.022	0.46
7.3	1.4	0.6	60.6	0.024	0.44
8.0	1.2	0.7	67.3	0.018	0.55
8.0	1.2	0.7	67.5	0.018	0.54
8.4	1.2	0.7	70.8	0.017	0.60
9.5	0.9	0.6	81.8	0.011	0.71
9.4	0.9	0.6	81.1	0.011	0.69
9.7	0.9	0.7	84.6	0.011	0.72
7.5	1.4	0.6	62.2	0.022	0.46
7.4	1.4	0.6	60.8	0.023	0.44
8.1	1.2	0.7	68.6	0.018	0.55
8.2	1.2	0.7	68.9	0.017	0.56
9.7	0.9	0.6	84.6	0.011	0.69
9.9	0.8	0.6	86.5	0.010	0.70
6.1	1.5	0.7	47.4	0.032	0.43
6.0	1.7	0.7	47.0	0.035	0.41
6.1	1.6	0.7	47.7	0.034	0.41
8.0	3.0	1.1	67.6	0.044	0.37
7.8	2.9	1.1	65.3	0.045	0.38
8.1	2.8	1.0	68.0	0.042	0.36
7.9	3.1	1.1	65.8	0.047	0.35
10.1	2.3	1.1	88.3	0.026	0.50
10.2	2.2	1.1	89.1	0.024	0.51
10.1	2.1	1.1	88.3	0.024	0.52
5.9	1.7	0.6	45.3	0.036	0.38
6.3	1.6	0.6	49.4	0.032	0.40
6.0	1.6	0.6	46.8	0.034	0.41
7.9	3.1	1.1	65.8	0.047	0.35

Table B.3 (continued): Measured and calculated data of Case-3

Measured			Calculated		
Wave Period (T_m) (sec)	Incident Wave Height (H_i) (m)	Transmitted Wave Height (H_t) (m)	Incident Wave Length (L_i) (m)	Incident Wave Steepness (H_i/L_i)	Transmission Coefficient (K_t)
7.8	3.0	1.1	65.5	0.047	0.36
8.0	2.9	1.0	67.0	0.044	0.35
10.2	2.2	1.1	88.7	0.025	0.50
10.3	2.2	1.1	89.8	0.025	0.50
10.1	2.3	1.1	88.0	0.026	0.49
6.0	1.6	0.7	46.5	0.035	0.42
6.1	1.6	0.7	47.7	0.034	0.41
5.9	1.6	0.6	45.8	0.034	0.37
7.9	3.2	1.2	66.0	0.048	0.37
7.8	3.1	1.1	65.4	0.048	0.34
8.0	2.9	1.1	67.2	0.044	0.36
10.1	2.2	1.1	88.4	0.025	0.50
10.2	2.2	1.1	89.0	0.024	0.50
10.2	2.2	1.1	89.5	0.025	0.50
6.2	1.5	0.7	48.6	0.031	0.44
6.0	1.5	0.6	46.7	0.033	0.39
7.0	1.5	0.6	56.7	0.026	0.43
7.9	3.0	1.1	66.2	0.045	0.36
7.9	3.0	1.0	66.7	0.046	0.34
8.0	3.0	1.1	67.6	0.044	0.36
10.0	2.3	1.1	87.3	0.027	0.49
10.2	2.3	1.1	88.8	0.026	0.48
10.1	2.3	1.1	88.2	0.026	0.49
6.2	1.5	0.6	48.8	0.030	0.44
6.3	1.5	0.7	50.0	0.030	0.44
6.0	1.7	0.6	46.9	0.036	0.35
8.0	3.0	1.1	67.0	0.044	0.37
7.9	2.9	1.1	66.6	0.044	0.36
7.7	2.9	0.7	64.1	0.046	0.36
10.1	2.1	1.1	88.3	0.024	0.50
10.3	2.2	1.1	90.1	0.024	0.51
10.1	2.1	1.1	88.1	0.023	0.52
6.0	1.6	0.6	46.1	0.036	0.36
6.2	1.5	0.6	49.1	0.031	0.38
6.0	1.6	0.7	46.7	0.034	0.44
7.8	2.9	1.0	65.1	0.044	0.36
7.9	3.0	1.1	66.7	0.044	0.37
7.8	3.0	1.1	65.6	0.046	0.36
10.1	2.1	1.1	88.3	0.024	0.51

Table B.4: Measured and calculated data of Case-4

CASE-4 (b=20cm, α=45°, B=12m)					
Measured			**Calculated**		
Wave Period (T_m) (sec)	Incident Wave Height (H_i) (m)	Transmitted Wave Height (H_t) (m)	Incident Wave Length (L_i) (m)	Incident Wave Steepness (H_i/L_i)	Transmission Coefficient (K_t)
7.5	1.1	0.4	62.0	0.023	0.38
7.5	1.1	0.3	62.4	0.022	0.28
8.2	0.9	0.3	69.2	0.017	0.35
8.2	0.9	0.3	69.4	0.017	0.34
9.9	0.7	0.3	85.8	0.010	0.44
9.9	0.7	0.3	85.8	0.010	0.42
7.5	1.1	0.3	61.7	0.022	0.27
7.5	1.1	0.3	62.3	0.022	0.27
8.3	0.9	0.3	70.3	0.016	0.35
8.3	0.9	0.3	69.9	0.016	0.35
9.9	0.7	0.3	86.1	0.010	0.44
10.0	0.7	0.3	87.3	0.010	0.44
7.4	1.1	0.4	61.2	0.022	0.35
7.5	1.1	0.4	61.9	0.022	0.36
8.4	0.9	0.4	71.8	0.016	0.45
8.5	0.8	0.4	72.3	0.015	0.50
9.5	0.7	0.4	82.3	0.010	0.57
9.7	0.7	0.4	84.6	0.010	0.58

Table B.5: Measured and calculated data of Case-5

CASE-5 (b=30cm, α=45°, B=12m)					
Measured			**Calculated**		
Wave Period (T_m) (sec)	Incident Wave Height (H_i) (m)	Transmitted Wave Height (H_t) (m)	Incident Wave Length (L_i) (m)	Incident Wave Steepness (H_i/L_i)	Transmission Coefficient (K_t)
7.5	1.1	0.4	61.8	0.022	0.36
8.1	0.9	0.4	68.7	0.017	0.45
8.6	0.8	0.4	73.6	0.014	0.50
9.9	0.7	0.4	85.9	0.010	0.57
10.0	0.7	0.4	87.3	0.009	0.58
7.6	1.0	0.4	63.5	0.021	0.36
7.5	1.1	0.4	62.0	0.022	0.34
7.5	1.1	0.4	62.5	0.022	0.34
8.9	0.8	0.4	76.6	0.013	0.51
8.2	0.9	0.4	69.4	0.017	0.44
8.4	0.9	0.4	70.8	0.016	0.47
9.7	0.7	0.4	84.0	0.010	0.52
9.8	0.7	0.4	85.2	0.010	0.51
7.4	1.1	0.3	61.1	0.023	0.32
7.4	1.1	0.4	61.2	0.022	0.33
7.3	1.1	0.3	60.3	0.023	0.31
8.2	0.9	0.4	69.1	0.017	0.41
8.1	0.9	0.4	68.5	0.017	0.42
8.3	0.9	0.4	70.4	0.016	0.45
9.6	0.7	0.4	83.3	0.011	0.55
9.7	0.7	0.4	83.8	0.010	0.53
9.6	0.7	0.4	83.5	0.010	0.55

Table B.6: Measured and calculated data of Case-6

CASE-6 (b=40cm, α=45°, B=12m)					
Measured			**Calculated**		
Wave Period (T_m) (sec)	Incident Wave Height (H_i) (m)	Transmitted Wave Height (H_t) (m)	Incident Wave Length (L_i) (m)	Incident Wave Steepness (H_i/L_i)	Transmission Coefficient (K_t)
7.6	1.1	0.4	63.0	0.023	0.35
7.4	1.1	0.4	61.2	0.022	0.35
7.3	1.1	0.4	60.2	0.023	0.34
8.2	0.9	0.4	68.8	0.017	0.47
8.1	1.0	0.4	68.7	0.017	0.45
8.2	0.9	0.4	69.2	0.017	0.47
10.3	0.7	0.4	89.8	0.009	0.59
10.4	0.7	0.4	91.1	0.009	0.57
10.1	0.7	0.4	88.1	0.010	0.57
7.5	1.1	0.4	61.9	0.022	0.36
7.5	1.1	0.4	61.8	0.022	0.38
7.3	1.1	0.4	60.6	0.024	0.35
8.0	0.9	0.4	67.3	0.018	0.45
8.0	0.9	0.4	67.5	0.018	0.45
8.4	0.9	0.4	70.8	0.017	0.46
9.5	0.7	0.4	81.8	0.011	0.58
9.4	0.7	0.4	81.1	0.011	0.58
7.5	1.1	0.4	62.2	0.022	0.41
7.4	1.1	0.4	60.8	0.023	0.35
8.1	1.0	0.4	68.6	0.018	0.46
8.2	0.9	0.4	68.9	0.017	0.46
9.7	0.7	0.4	84.6	0.011	0.57
9.9	0.7	0.4	86.5	0.010	0.57

Table B.7: Measured and calculated data of Case-7

CASE-7 (b=30cm, α=90°, B=7m)					
Measured			**Calculated**		
Wave Period (T_m) (sec)	Incident Wave Height (H_i) (m)	Transmitted Wave Height (H_t) (m)	Incident Wave Length (L_i) (m)	Incident Wave Steepness (H_i/L_i)	Transmission Coefficient (K_t)
6.1	1.6	0.7	47.2	0.033	0.46
6.2	1.4	0.7	49.1	0.028	0.51
6.1	1.5	0.7	47.3	0.032	0.47
8.1	2.9	1.3	68.0	0.042	0.44
8.1	2.9	1.3	68.3	0.042	0.44
8.1	2.9	1.3	67.8	0.042	0.44
10.1	2.3	1.3	87.9	0.026	0.56
10.0	2.3	1.3	87.6	0.026	0.57
10.1	2.2	1.3	88.4	0.025	0.57
6.2	1.4	0.7	48.1	0.030	0.48
6.1	1.4	0.7	48.0	0.029	0.50
6.2	1.4	0.7	48.9	0.028	0.50
8.1	2.9	1.3	67.8	0.043	0.44
8.2	2.7	1.2	69.4	0.039	0.45
8.1	2.9	1.3	67.8	0.043	0.44
10.2	2.2	1.3	89.1	0.024	0.58
10.1	2.2	1.3	88.3	0.025	0.58
10.1	2.2	1.3	88.2	0.025	0.57
6.1	1.5	0.7	47.2	0.032	0.46
6.1	1.5	0.7	47.1	0.032	0.44
6.1	1.5	0.7	47.1	0.032	0.46
6.1	1.5	0.7	47.1	0.032	0.45
8.1	2.8	1.2	68.1	0.041	0.42
8.0	2.9	1.2	67.7	0.042	0.42
8.1	2.8	1.2	68.2	0.042	0.41
8.0	2.8	1.2	67.7	0.042	0.41
10.1	2.3	1.2	88.0	0.026	0.52
10.1	2.2	1.2	88.3	0.025	0.52
10.1	2.2	1.2	88.2	0.025	0.54
10.1	2.2	1.2	88.2	0.025	0.52
6.1	1.5	0.7	47.5	0.031	0.48
6.0	1.5	0.7	47.0	0.031	0.47
6.1	1.4	0.7	47.3	0.031	0.47
6.1	1.5	0.7	47.0	0.032	0.46
6.1	1.4	0.6	47.2	0.031	0.45
8.1	2.8	1.2	68.0	0.042	0.41
8.1	2.8	1.1	68.1	0.042	0.40
8.1	2.8	1.1	68.0	0.042	0.40

Table B.7 (continued): Measured and calculated data of Case-7

Measured			Calculated		
Wave Period (T_m) (sec)	Incident Wave Height (H_i) (m)	Transmitted Wave Height (H_t) (m)	Incident Wave Length (L_i) (m)	Incident Wave Steepness (H_i/L_i)	Transmission Coefficient (K_t)
8.1	2.8	1.1	68.7	0.041	0.41
8.0	2.8	1.2	67.7	0.042	0.42
10.1	2.2	1.2	88.2	0.025	0.52
10.1	2.3	1.2	88.0	0.026	0.51
10.1	2.2	1.2	88.0	0.026	0.52
10.2	2.3	1.2	88.7	0.026	0.52
10.1	2.2	1.2	88.2	0.025	0.52

Table B.8: Measured and calculated data of Case-8

CASE-8 (b=30cm, α=90°, B=0m;single-row)					
Measured			Calculated		
Wave Period (T_m) (sec)	Incident Wave Height (H_i) (m)	Transmitted Wave Height (H_t) (m)	Incident Wave Length (L_i) (m)	Incident Wave Steepness (H_i/L_i)	Transmission Coefficient (K_t)
6.1	1.5	0.8	47.3	0.031	0.51
6.3	1.3	0.8	49.3	0.027	0.58
6.1	1.4	0.7	47.8	0.030	0.53
10.0	2.2	1.5	87.4	0.026	0.68
10.1	2.2	1.6	88.0	0.025	0.71
10.1	2.3	1.5	87.8	0.026	0.66
10.1	2.1	1.5	88.5	0.024	0.71
6.1	1.4	0.7	47.6	0.030	0.51
6.1	1.4	0.8	47.1	0.030	0.52
6.1	1.5	0.8	47.2	0.031	0.55
6.1	1.5	0.8	47.4	0.031	0.52
6.1	1.4	0.8	47.6	0.030	0.53
6.1	1.4	0.8	47.6	0.030	0.52
6.1	1.5	0.8	47.4	0.031	0.52
6.1	1.5	0.8	47.2	0.031	0.53
10.1	2.2	1.5	88.2	0.025	0.68
10.0	2.2	1.5	87.3	0.025	0.68
10.1	2.2	1.5	88.0	0.025	0.69
10.0	2.2	1.5	87.3	0.025	0.68
6.2	1.4	0.8	48.2	0.029	0.54
6.2	1.4	0.7	48.2	0.029	0.53
6.0	1.5	0.8	46.3	0.032	0.53

Table B.8 (continued): Measured and calculated data of Case-8

Measured			Calculated		
Wave Period (T_m) (sec)	Incident Wave Height (H_i) (m)	Transmitted Wave Height (H_t) (m)	Incident Wave Length (L_i) (m)	Incident Wave Steepness (H_i/L_i)	Transmission Coefficient (K_t)
6.1	1.4	0.8	48.0	0.029	0.56
6.2	1.4	0.7	48.1	0.029	0.52
6.1	2.2	1.1	48.0	0.046	0.48
6.1	2.3	1.1	47.6	0.048	0.50
6.1	2.3	1.1	47.6	0.048	0.49
6.1	2.2	1.1	47.9	0.045	0.50
6.2	1.6	0.9	48.2	0.033	0.55
6.1	1.7	0.9	47.1	0.036	0.52
6.1	1.7	0.9	47.4	0.035	0.52
6.1	1.6	0.8	48.0	0.033	0.54
6.1	1.9	1.0	47.4	0.040	0.50
6.1	1.9	1.0	47.0	0.040	0.51
6.1	1.9	1.0	47.5	0.039	0.51
6.1	1.9	0.9	47.3	0.040	0.50
6.1	1.9	1.0	47.4	0.040	0.51
6.1	1.9	0.9	47.5	0.039	0.51
6.1	2.3	1.1	47.3	0.048	0.49
6.1	2.2	1.1	47.5	0.047	0.49
6.1	1.7	0.9	47.5	0.037	0.52
6.1	1.7	0.9	47.2	0.036	0.51
6.1	1.6	0.8	47.4	0.035	0.52
6.1	1.7	0.8	47.2	0.036	0.50
6.1	1.6	0.8	47.3	0.035	0.51
8.1	2.3	1.2	68.0	0.033	0.55
8.3	2.1	1.2	69.9	0.030	0.58
8.1	2.2	1.2	67.9	0.033	0.54
8.1	2.2	1.2	68.3	0.033	0.56
8.1	2.3	1.3	68.4	0.033	0.55
6.1	1.9	0.9	47.0	0.041	0.49
6.0	1.9	0.9	46.9	0.041	0.48
6.1	1.9	1.0	47.7	0.040	0.51
6.0	2.3	1.1	46.9	0.049	0.47
6.1	2.3	1.1	47.0	0.049	0.47
6.1	2.3	1.0	47.0	0.048	0.46
6.1	1.7	0.8	47.1	0.036	0.50
6.1	1.7	0.9	47.1	0.036	0.50
6.0	1.7	0.8	46.4	0.037	0.49
6.1	1.5	0.8	47.2	0.031	0.53
6.1	1.5	0.8	47.1	0.032	0.52
6.1	1.5	0.8	47.2	0.032	0.51
8.1	2.3	1.2	68.1	0.034	0.51
8.2	2.3	1.3	69.3	0.033	0.55

APPENDIX C

SCATTERING OF DATA IN SIMILAR EXPERIMENTAL STUDIES

The studies of Rao et al. (1999) are given in Figure C.1 and Figure C.2 to show the scattering of data in similar experimental studies.

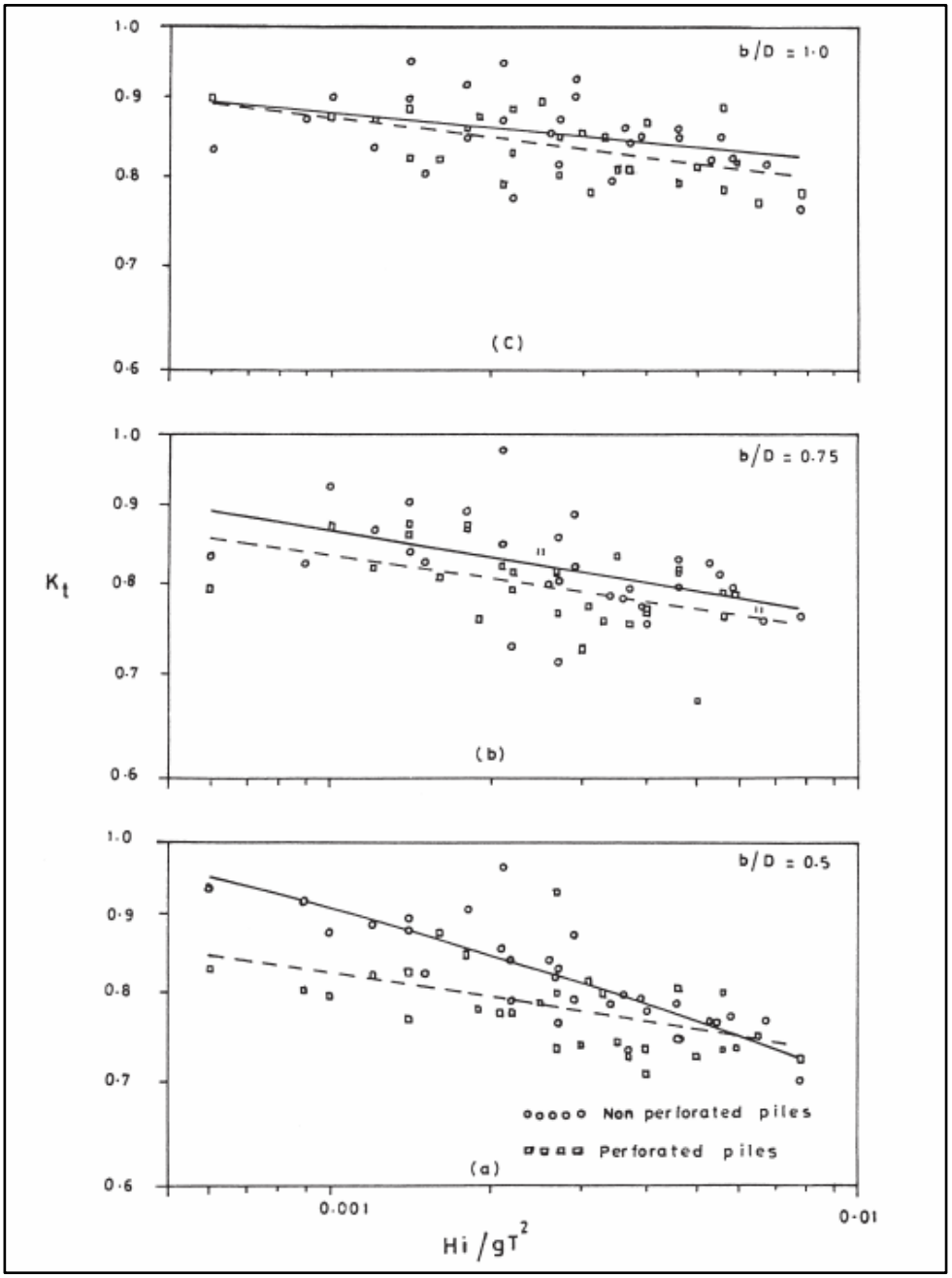

Figure C.1: Rao et al. (1999)'s research on double-row pile breakwater (K_t vs H_i/gT^2)

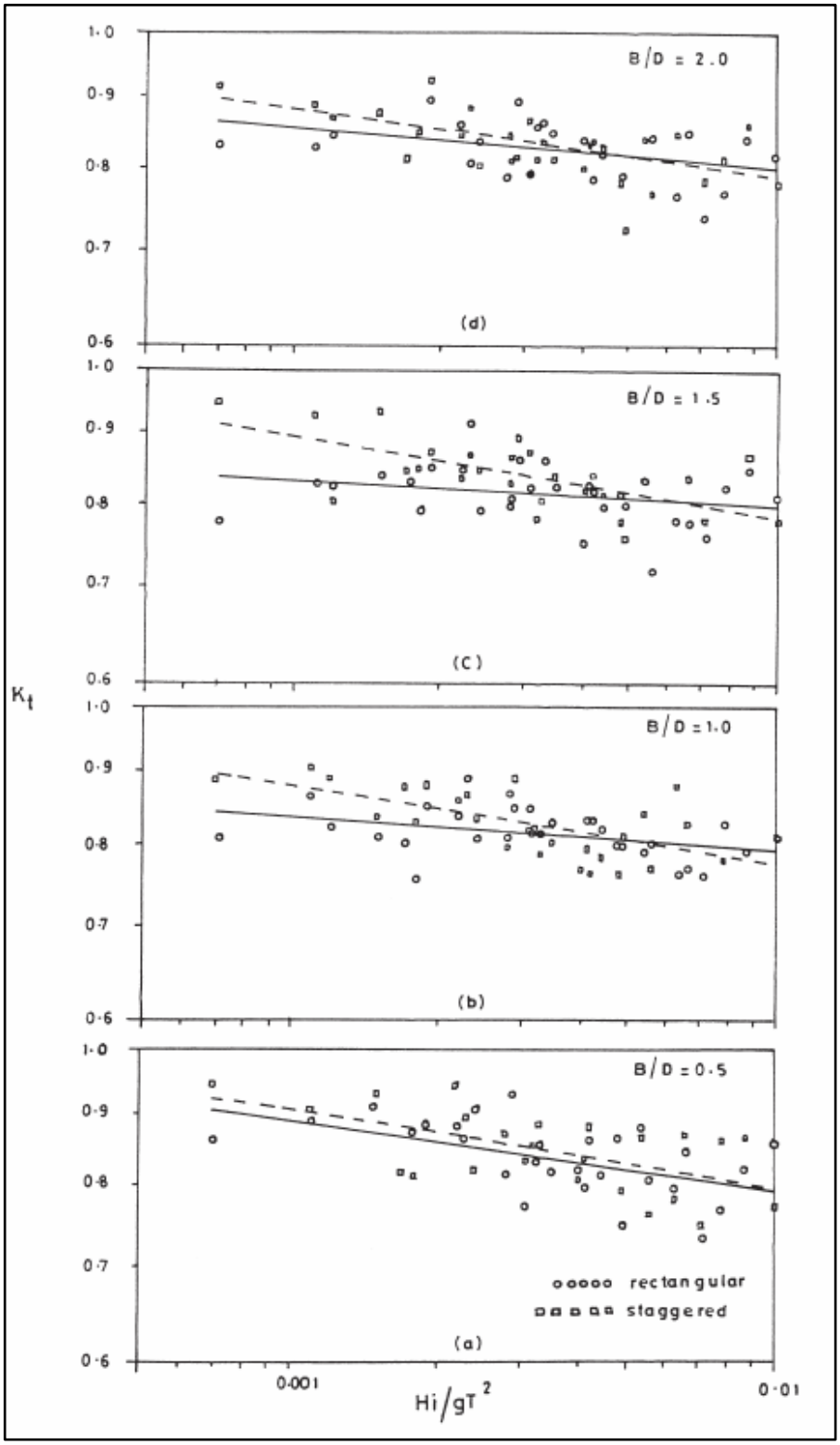

Figure C.2: Rao et al. (1999)'s research on double-row perforated pile breakwater (K_t vs H_i/gT^2)

APPENDIX D

RESULTS FOR CASE-1, CASE-2 AND CASE-3 WITH DEEP WATER WAVE STEEPNESS

The results of Case-1, 2 and 3 were tabulated and plotted as transmission coefficient (K_t) vs deep water wave steepness (H_0/L_0). (Table D.1) (Figure D.1- Figure D.3)

Table D.1: Deep water wave steepness and corresponding transmission coefficients for Case-1, 2 and 3

	Case-1 b=20cm	**Case-2 b=30cm**	**Case-3 b=40cm**
(H_0/L_0)	**K_t**	**K_t**	**K_t**
0.010	0.37	0.50	0.59
0.015	0.32	0.44	0.50
0.020	0.28	0.40	0.43
0.025	0.25	0.38	0.39
0.030	0.23	0.37	0.37
0.035	0.21	0.38	0.38
0.040	0.21	0.41	0.42
0.045	0.21	0.45	0.49
0.050	0.22	0.51	0.58

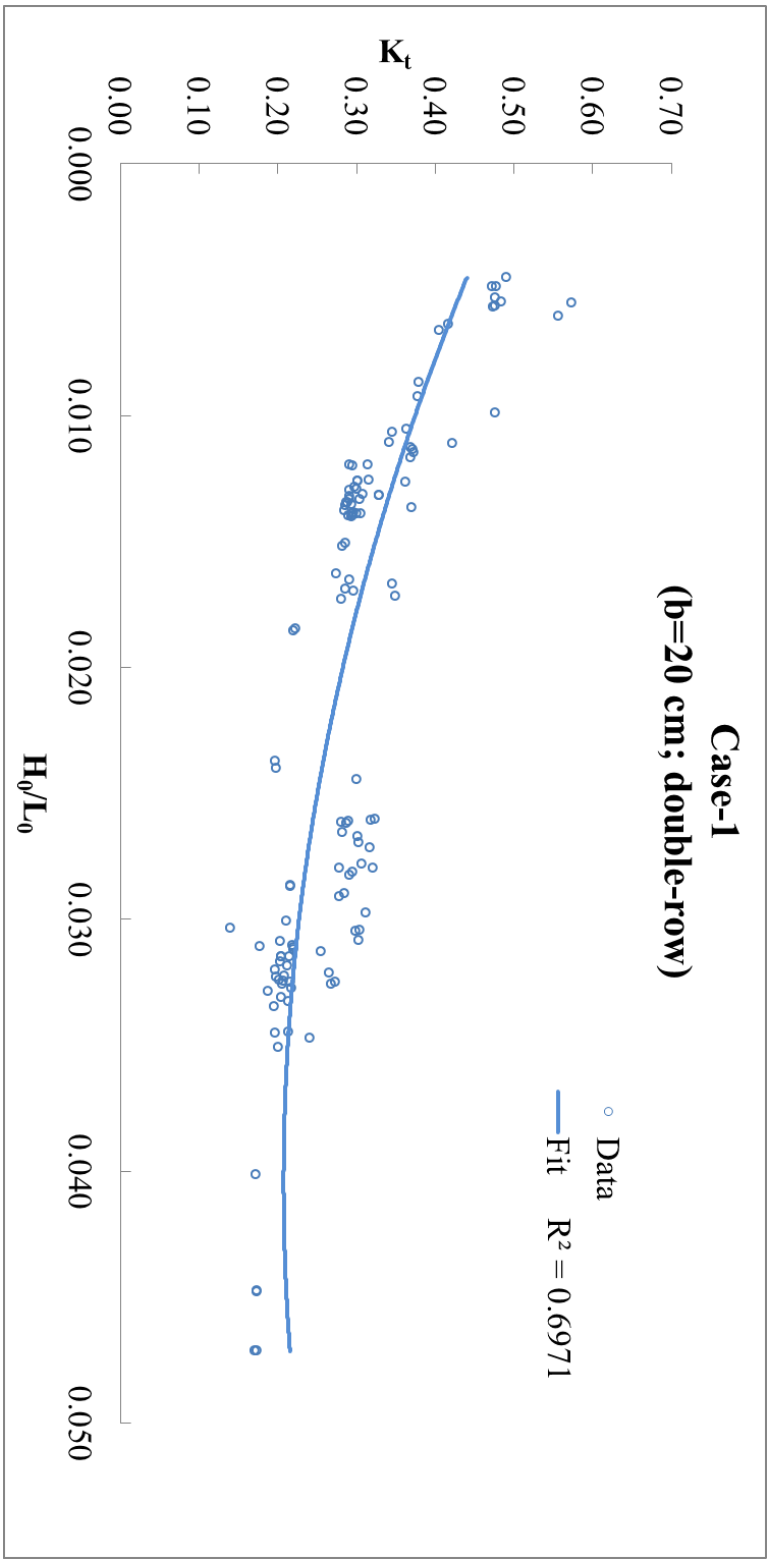

Figure D.1: K_t vs H_0/L_0 for Case-1

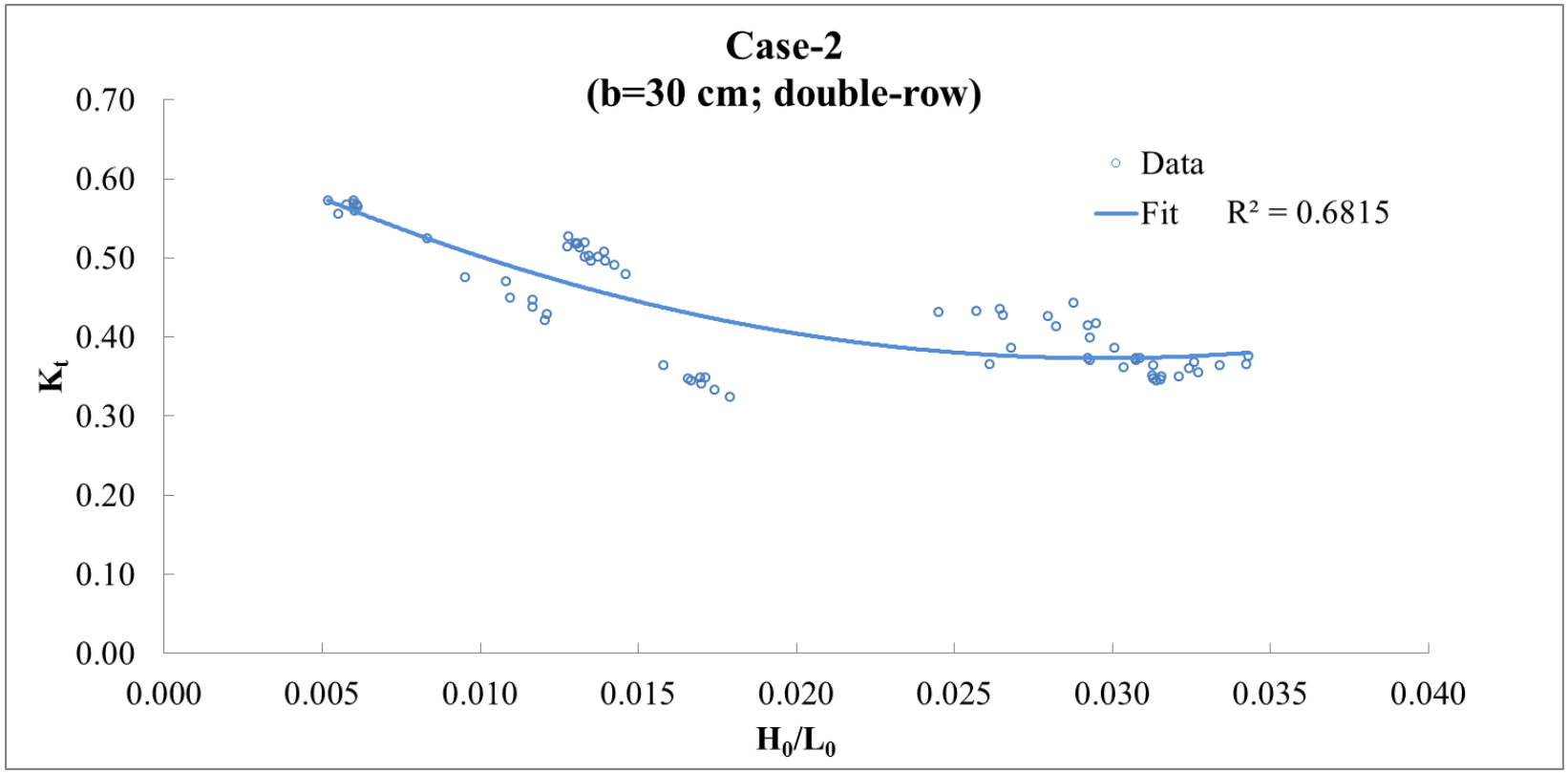

Figure D.2: K_t vs H_0/L_0 for Case-2

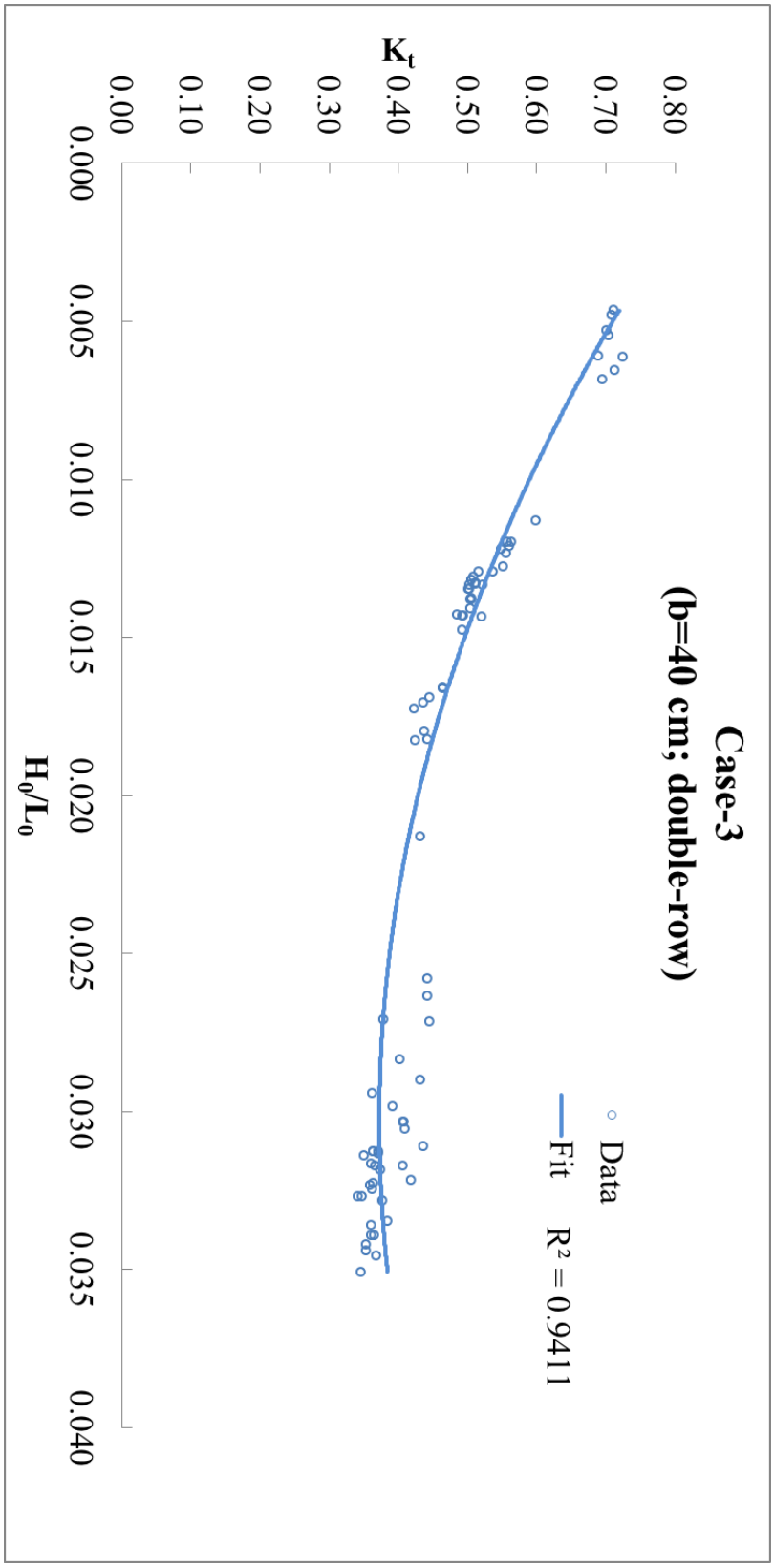

Figure D.3: K_t vs H_0/L_0 for Case-3